INDIRECT METHOD OF THE BIOSENSOR BASED ON FLOW INJECTION ANALYSIS FOR DETERMINATION OF MERCURY

PIYANART SUEBSANOH

A THESIS SUBMITTED IN PARTIAL FULFILLMENT OF THE REQUIREMENTS FOR THE DEGREE OF MASTER OF SCIENCE

MAJOR IN CHEMISTRY

FACULTY OF SCIENCE

UBON RATCHATHANI UNIVERSITY

ACADEMIC YEAR 2015

UBON RATCHATHANI UNIVERSITY

THESIS APPROVAL

MASTER OF SCIENCE

IN CHEMISTRY FACULTY OF SCIENCE

TITLE INDIRECT METHOD OF THE BIOSENSOR BASED ON FLOW INJECTION ANALYSIS FOR DETERMINATION OF MERCURY

AUTHOR MISS PIYANART SUEBSANOH

EXAMINATION COMMITTEE

ASST. PROF. DR. SANCHAI PRAYOONPOKARACH	CHAIRPERSON
ASST. PROF. DR. ANCHALEE SAMPHAO	MEMBER
ASST. PROF. DR. SUWAT PABCHANDA	MEMBER

ADVISOR .....

(ASST. PROF. DR. ANCHALEE SAMPHAO)

....

(ASSOC. PROF. DR. UTITH INPRASIT)
DEAN, FACULTY OF SCIENCE

(ASSOC. PROF. DR. ARIYAPORN PONGRAT)
VICE PRESIDENT
FOR ACADEMIC AFFAIRS

ACADEMIC YEAR 2015

ACKNOWLEDGEMENTS

I would like to thank my advisor, Asst. Prof. Dr. Anchalee Samphao, whose dedication, guidance and impressive understanding of the chemical sciences has helped my development as a chemist. Her enthusiasm for chemistry has been an important driving force to help me overcome the frustrations and failures encountered in this research. I would not be able to complete this work without her support. Moreover, I would like to thank Prof. Kurt Kalcher from University of Graz, Austria for helps, valuable suggestions and comments during my study. I wish to thank Asst. Prof. Dr. Sanchai Prayoonpokarach from Suranaree University of Technology, Nakhon Ratchasima, Thailand for being a chair of my thesis defense and invaluable discussions. I would also thank Asst. Prof. Dr. Suwat Pabchanda who has personally suggested and supported me for serving as the thesis committee. Thanks to the Center of Excellence for Innovation in Chemistry (PERCH-CIC) and Faculty of science, Ubon Ratchathani University for financial support.

I would like to thank the research group of Asst. Prof. Dr. Anchalee Samphao for their support and friendship over the years. I am also thankful to all my friends for being here whenever I needed. Thanks to Chemistry and Microbiology departments in providing instruments for characterization and staffs for some advices to this project.

Finally, my deepest and most sincere appreciation goes to my family for their constant encouragement, unconditional support and endless love.

Piyanart

Piyanart Suebsanoh

Researcher

บทคัดย่อ

ชื่อเรื่อง	: การตรวจวัดทางอ้อมของไบโอเซนเซอร์ในระบบการไหลอัตโนมัติเพื่อวิเคราะห์ปริมาณปรอท
โดย	: ปิยนาถ สืบเสนาะ
ชื่อปริญญา	: วิทยาศาสตรมหาบัณฑิต
สาขาวิชา	: เคมี
อาจารย์ที่ปรึกษา	: ผู้ช่วยศาสตราจารย์ ดร. อัญชลี สำเภา
คำสำคัญ	: ปรอท, กลูโคสออกซิเดส, ไบโอเซนเซอร์, ระบบการไหลแบบอัตโนมัติ, การยับยั้งเอนไซม์

งานวิจัยนี้ พัฒนาไบโอเซนเซอร์ในระบบการไหลอัตโนมัติ เพื่อตรวจวัดปริมาณปรอทโดยอาศัยหลักการยับยั้งการทำงานของเอนไซม์ซึ่งเป็นวิธีวิเคราะห์ที่เรียกว่าการตรวจวัดทางอ้อม เตรียมไบโอเซนเซอร์โดยตรึงเอนไซม์กลูโคสออกซิเดสในสารละลายนาฟิออนบนผิวหน้าขั้วไฟฟ้าพิมพ์สกรีนคาร์บอนที่ปรับปรุงด้วยแมงกานีสไดออกไซด์ 5 เปอร์เซ็นต์โดยน้ำหนักเพื่อทำหน้าที่เป็นขั้วไฟฟ้าใช้งานและติดตั้งเข้ากับอิเล็กโทรเคมิคอลเซลล์ที่ใช้เป็นส่วนตรวจวัดทางไฟฟ้าของระบบการไหลอัตโนมัติ

จากนั้นทำการศึกษาสภาวะที่เหมาะสมต่อการทำงานของไบโอเซนเซอร์ในระบบการไหลอัตโนมัติที่ได้พัฒนาขึ้น ให้ผลการทดลอง ดังนี้ ศักย์กระตุ้นสารตัวกลางทางไฟฟ้าที่ +0.46 โวลต์เทียบกับขั้วไฟฟ้าอ้างอิงซิลเวอร์/ซิลเวอร์คลอไรด์, สารละลายอิเล็กโทรไลต์เกื้อหนุน 0.1 โมลต่อลิตร ฟอสเฟตบัฟเฟอร์ ที่พีเอช 7.0, ปริมาณเอนไซม์กลูโคสออกซิเดสที่ตรึงบนผิวหน้าขั้วไฟฟ้า 80 ยูนิตต่อตารางเซนติเมตร, ความเข้มข้นกลูโคส 200 มิลลิกรัมต่อลิตร, ปริมาตรของการฉีดสารตัวอย่างเข้าไปในระบบการไหล 250 ไมโครลิตร และ อัตราการไหลของสารละลายตัวพาที่ 1.2 มิลลิลิตรต่อนาที

ประเมินความถูกต้องโดยศึกษาการตอบสนองของปรอทต่อไบโอเซนเซอร์ พบว่าให้ช่วงความเป็นเส้นตรงของการตรวจวัดปริมาณปรอทคือ 100 - 1000 ไมโครกรัมต่อลิตร โดยแสดงสมการเส้นตรง $y = 0.0407x - 0.5760$ และ $r^2 = 0.9975$ ขีดจำกัดต่ำสุดของการตรวจพบและตรวจวัดคือ 29 และ 96 ไมโครกรัมต่อลิตร ตามลำดับ ความเที่ยงของการวิเคราะห์ (วิเคราะห์ 10 ครั้ง) และความเที่ยงของการเตรียมไบโอเซนเซอร์ (ขั้วไฟฟ้า 3 ขั้ว) ให้ค่าส่วนเบี่ยงเบนมาตรฐานสัมพัทธ์ร้อยละ 3.68 และ 4.12 ตามลำดับ ไบโอเซนเซอร์ที่ใช้งานไปแล้วสามารถนำกลับมาใช้ใหม่ โดยชะล้างผิวหน้าขั้วไฟฟ้าด้วยสารละลายเอทิลีนไดเอมีนเตตระอะซิติกแอซิดความเข้มข้น 0.05 โมลต่อลิตร ทำการทดลองด้วยการไหลผ่านผิวหน้าขั้วไฟฟ้าเป็นเวลา 2 นาที พบว่าขั้วไฟฟ้าให้ร้อยละของการนำกลับมาใช้ใหม่ร้อยละ 100 หลังการใช้งานสามารถเก็บขั้วไฟฟ้าที่อุณหภูมิ 4 องศาเซลเซียส และยังมีความเสถียรมากกว่า 21 วัน โดยค่ากระแสที่ลดลงเมื่อเทียบกับกระแสเริ่มต้นยังคงเหลือถึงร้อยละ 62

นอกจากนี้งานวิจัยได้ศึกษาตัวรบกวนการตรวจวัดปรอทด้วยไบโอเซนเซอร์ที่พัฒนาขึ้น พบว่า ตะกั่ว แคดเมียม และ ทองแดง รบกวนการวิเคราะห์ที่ระดับความเข้มข้น 10 มิลลิกรัมต่อลิตร แต่ไม่รบกวนที่ระดับความเข้มข้น 1.0 มิลลิกรัมต่อลิตร

ยิ่งไปกว่านั้น งานวิจัยนี้ได้ศึกษาจลนพลศาสตร์ของเอนไซม์กลูโคสออกซิเดสที่ถูกตรึงบนผิวหน้าขั้วไฟฟ้า พบว่าให้ค่า Michaelis-Menten constant (K_m) และกระแสสูงสุด (I_{max}) คือ 5.80 มิลลิโมลต่อลิตร และ 4.41 ไมโครแอมแปร์ ตามลำดับ บ่งบอกให้ทราบว่าเอนไซม์ที่ตรึงอยู่บนผิวหน้าขั้วไฟฟ้ายังคงให้ประสิทธิภาพของการเร่งปฏิกิริยาเท่ากับเอนไซม์อิสระ จากนั้นทำการศึกษาจลนพลศาสตร์ของการยับยั้งเอนไซม์ พบว่าปรอทยับยั้งการทำงานของเอนไซม์กลูโคสออกซิเดสเป็นชนิดแบบไม่แข่งขัน

ไบโอเซนเซอร์ที่พัฒนาขึ้นถูกประเมินความถูกต้องโดยนำไปตรวจวัดปริมาณปรอทในสารตัวอย่างที่มีการรับรอง (DORM-2) ซึ่งระบุความเข้มข้นของปรอท 4.64 ± 0.26 มิลลิกรัมต่อกิโลกรัม ผลการตรวจวัดพบปริมาณปรอทให้ค่า 4.55 ± 0.07 มิลลิกรัมต่อกิโลกรัม ซึ่งสอดคล้องกับค่ามาตรฐานที่มีการรับรอง โดยแสดงร้อยละการได้กลับคืนถึงร้อยละ 98 ยิ่งไปกว่านั้น ไบโอเซนเซอร์ที่พัฒนาขึ้นนำไปประยุกต์ใช้ในการหาปริมาณปรอทในตัวอย่างจริงเปรียบเทียบกับเทคนิคมาตรฐานโคลเวเพอร์อะตอมมิกแอพซอร์พชั่นสเปกโทรเมทรี ผลการทดลองจากสองเทคนิคนำมาทดสอบด้วยสถิติค่า t พบว่า t จากการคำนวณของทุกตัวอย่าง มีค่าน้อยกว่า t ในตาราง ที่ระดับร้อยละของความเชื่อมั่น 95 สามารถสรุปผลการวิเคราะห์จากทั้งสองวิธีให้ค่าที่ไม่แตกต่างกันอย่างมีนัยสำคัญ

ABSTRACT

TITLE : INDIRECT METHOD OF THE BIOSENSOR BASED ON FLOW INJECTION ANALYSIS FOR DETERMINATION OF MERCURY
AUTHOR : PIYANART SUEBSANOH
DEGREE : MASTER OF SCIENCE
MAJOR : CHEMISTRY
ADVISOR : ASST. PROF. ANCHALEE SAMPHAO, Ph.D.
KEYWORDS : MERCURY, GLUCOSE OXIDASE, BIOSENSOR, FLOW INJECTION ANALYSIS, ENZYMATIC INHIBITION

In this research a biosensor based on flow injection analysis (FIA) for indirect determination of mercury (Hg (II)) by enzymatic inhibition has been developed. Glucose oxidase in Nafion solution immobilized on a screen-printed carbon electrode (GOx/SPCE) bulk modified with manganese dioxide 5 % (m) as a working electrode ($GOx/MnO_2/SPCE$) assembled with an electrochemical cell as a detector based on FIA was experimentally studied.

The optimum conditions of the biosensor based on FIA, an operating potential of +0.46 V versus Ag/AgCl, supporting electrolyte of 0.1 $mol.L^{-1}$ phosphate buffer solution at pH 7.0, enzyme loading of 80 $U.cm^{-2}$, glucose loading of 200 $mg.L^{-1}$ with 250 µL injection volume and flow rate of 1.2 $mL.min^{-1}$, were continually studied.

The accuracy of the biosensor responded to mercury was evaluated in terms of a linear range of 100 - 1000 $\mu g.L^{-1}$ with the linear equation of $y = 0.0407x - 0.5760$ and $r^2 = 0.9975$. The limit of detection and limit of quantification were of 29 $\mu g.L^{-1}$ and 96 $\mu g.L^{-1}$, respectively. The repeatability and reproducibility were of 3.68% (10 measurements) and 4.12% (3 sensors), respectively. After inhibition, the biosensor surface was regenerated by flowing through 0.05 $mol.L^{-1}$ EDTA for 2 min and percentage of regeneration was at 100%. The storage stability of the biosensor had been investigated after the electrodes were stored in dry condition at 4 °C in a refrigerator and its stability yielded more than 21 days with relative current percentage of 62%.

Moreover, interferences of an inhibition-based enzyme catalytic process were investigated; the results presented only Pb (II), Cd (II) and Cu (II) having a significant effect at high concentration of 10 $mg.L^{-1}$ but no effect at low concentration of 1 $mg.L^{-1}$.

Furthermore, the kinetic catalytic reaction of GOx was studied. The apparent Michaelis-Menten (K_m) constant and I_{max} could be calculated to be 5.80 $mmol.L^{-1}$ and 4.41 μA, respectively. The immobilized glucose oxidase indicated acts as the free enzyme. Besides, the kinetic inhibition of GOx was investigated. The result was found and concluded that GOx was inhibited by mercury as a noncompetitive inhibition type.

The biosensor based FIA was evaluated to detect mercury in a certified reference material (DORM-2) with certified values of 4.64 ± 0.26 $mg.Kg^{-1}$ mercury. As the results, the proposed biosensor presented mercury at 4.55 ± 0.07 $mg.Kg^{-1}$ with good recovery of 98%.

Moreover, the practical biosensor was successfully demonstrated in determination of mercury in real samples, and the samples were detected by cold vapor generation atomic absorption spectrometry as the reference method. The results from both methods were calculated using paired t-test. The t-value is significantly smaller than the tabulated critical value indicating that it is not significant statistical different between these results at a confidence interval for 95% probability.

CONTENTS

CONTENTS (CONTINUED)

CONTENTS (CONTINUED)

LIST OF TABLES

LIST OF TABLES (CONTINUED)

LIST OF TABLES (CONTINUED)

LIST OF FIGURES

LIST OF FIGURES (CONTINUED)

LIST OF FIGURES (CONTINUED)

LIST OF FIGURES (CONTINUED)

LIST OF FIGURES (CONTINUED)

LIST OF FIGURES (CONTINUED)

LIST OF FIGURES (CONTINUED)

LIST OF FIGURES (CONTINUED)

LIST OF ABBREVIATIONS

ABBREVIATIONS	FULL WORD
AAS	Atomic absorption spectrometry
AChE	Acetyl choline esterase
AE	Auxiliary electrode
Ag/AgCl	Silver/Silver chloride reference electrode
aq	Aqueous
AR	Analysis reagent
Arg	Arginine
Asn	Asparagine
ATCh	Acetyl thio choline
BSA	Bovine serum albumin
C	Concentration of solution
C_0	Initial current
C_1	Current after stored
CE	Counter electrode
cm	Centimeter
cm^2	Square centimeter
$cm^2.s^{-1}$	Square centimeter per second
CNT	Carbon nanotube
CPO	Chlorpyrifosoxon
CV	Cyclic voltammetry
CVAAS	Cold vapor atomic absorption spectrometry
D	Diffusion coefficient
DI	Deionized water
dmAChE	Drosophila melanogaster acetyl choline esterase
DNA	Deoxyribonucleic acid
DORM-2	Dogfish muscle certified reference material
E	Enzyme

LIST OF ABBREVIATIONS (CONTINUED)

ABBREVIATIONS	FULL WORD
EC	Electrochemical cell
EDTA	Ethylenediaminetetraacetic acid
eeAChE	Electric eel acetyl choline esterase
E-Inh	Enzyme-inhibitor complex
E_{pa}	Anodic peak potential
E_{pc}	Cathodic peak potential
E-S	Enzyme-substrate complex
E-S-Inh	Tertary complex containing enzyme-substrate inhibitor
FAD	Flavine adenine dinucleotide
FIA	Flow injection analysis
FIAS-AAS	Flow injection analysis system atomic absorption spectrometry
FTIR	Fourier transform infrared spectrometry
g	Gram
GA	Glutaraldehyde
GC	Glassy carbon
GOx	Glucose oxidase
GOx/MnO_2/SPCE	Glucose oxidase immobilized with screen printed carbon electrode modified with manganese dioxide
H	Peak height
h	hour
HGAAS	Hydride generation atomic absorption spectometry
His	Histidine
HPR	Herseradish peroxidase
I	Peak height given by biosensor after inhibition
I_0	Peak height before inhibition
I_1	Peak height before inhibition

LIST OF ABBREVIATIONS (CONTINUED)

ABBREVIATIONS	FULL WORD
I_2	Peak height after regeneration
I_{max}	Maximum current
I_{pa}	Anodic current
I_{pc}	Cathodic current
I_{ss}	Steady-state current
ICP-AES	Inductively coupled plasma atomic emission spectrometry
ICP-MS	Inductively coupled plasma mass spectrometry
k_1	Rate constant of forward reaction 1
k_{-1}	Rate constant of reverse reaction 1
K_2	Rate constant of forward reaction 2
K_I and K_i	Equilibrium dissociation constants of the E-S-Inh complex the E-Inh complex
k_{cat}	Single first-order rate constant
K_m	Michaelis-Menten constant
kV	Kilovolt
KU	Kilo unit
LOD	Limit of detection
LOQ	Limit of quantification
$L.\mu g^{-1}$	Liter per microgram
mg	Milligram
$mg.Kg^{-1}$	Milligram per kilogram
$mg.L^{-1}$	Milligram per liter
min	Minute
mL	Milliliter
$mL.min^{-1}$	Milliliter per minute
mm	Millimeter

LIST OF ABBREVIATIONS (CONTINUED)

ABBREVIATIONS	FULL WORD
mm^2	Square millimeter
$mmol.L^{-1}$	Millimole per liter
MnO_2/SPCE	Screen printed carbon electrode modified with manganese dioxide
$mol.L^{-1}$	Mole per liter
mV	Millivolt
$mV.s^{-1}$	Millivolt per second
n	Number of measurements
nA	Nanoampare
ND	None detection
$ng.mL^{-1}$	Nanogram per milliliter
nm	Nanometer
P	Product
2-PAM	2-pyridinealdoxime methiodine
PDDA	Poly(diallyldimethylammonium chloride)
Phe	Phenylalanine
$pmol.L^{-1}$	Pico mole per liter
PVP	Poly(vinyl pyridine)
QCM	Quartz crystal microbalance
R	Recorder
r^2	Correlation coefficient
RE	Reference electrode material
S	Substrate
s	Second
s^{-1}	Per second
SAW	Surface acoustic wave
SD	Standard deviation

LIST OF ABBREVIATIONS (CONTINUED)

ABBREVIATIONS	FULL WORD
SEM	Scanning electron microscope
SPR	Surface plasmon resonance
T	Residence time
t	Time
t_0	Peak height measurement
t_b	Peak width at the baseline
Trp	Tryptophan
Tyr	Tyrosine
$U.cm^{-2}$	Unit per square centimeter
V	Volt
V_1	Volume after dilution
V_2	Volume before dilution
v/v	Volume by volume
V_{max}	Maximum velocity
W	Waste
WE	Working electrode
w/v	Weight by volume
w/w	Weight by weight
°C	Degree celsius
µA	Microampare
$\mu g.L^{-1}$	Microgram per liter
µL	Microliter
$\mu mol.L^{-1}$	Micromole per liter
v	Rate of product formation of an enzyme catalyzed reaction
δ	Thickness of the diffusion layer

CHAPTER 1
INTRODUCTION

1.1 Importance and source of research

Mercury is currently industrially used in production of batteries, switches, and bulbs. It is also used as an antifouling agent in paints, as a fungicide in agriculture, and as a catalyst in plastic production. Medicinally, it is used as a germicidal and bactericidal agent in the making of amalgam dental fillings. One of the most common is water pollution, caused by dumping of industrial waste into waterways. As a result, contaminated by mercury in aquatic animals when human consumes, it is cumulative in the body by food cycle. Mercury in any form is poisonous, with mercury toxicity most commonly affecting the neurological, gastrointestinal and renal organ systems. Moreover, mercury is attracted to thiol groups and bind to proteins on membranes or to enzymes in living system. Hence, they were disrupted through damage and possible mutation to the genes. Poisoning can result from mercury vapor inhalation, ingestion, injection, and absorption through the skin [1].

Determination of mercury is usually performed with various techniques such as cold vapor atomic absorption spectrometry (CVAAS) [2-3], hydride generation atomic absorption spectrometry (HGAAS) [4-5], inductively coupled plasma atomic emission spectrometry (ICP-AES) [6] and inductively coupled plasma mass spectrometry (ICP-MS) [7-8] which require sample pretreatment, expensive instrumentation and skilled operators. These spectroscopic techniques are not suitable for the task of on-site testing and monitoring [9].

Alternative attention to determine mercury ions is currently interested to the study of biosensors in environmental analysis owing to some advantages, such as rapidly expanding its field of application, good sensitivity and low cost over the traditional techniques. Biosensors have become an active area of research to detect various chemicals monitoring of components, the significant applications of enzyme inhibition biosensors includes the determination of heavy metals [10]. Most of the biosensors for detecting metal ions are designed on the inhibition of the enzyme activities.

Biosensors based on the principle of enzyme inhibition have been applied for a wide range of significant analytes such as pesticide [11-12], heavy metals [13-15] and glycol alkaloids [16-17]. The choice of enzyme/analyte system is based on the fact that these toxic analytes inhibit normal enzyme function. In general, the development of these biosensing systems relies on a quantitative measurement of the enzyme activity before and after exposure to a target analyte. Typically the percentage of inhibited enzyme that results after exposure to the inhibitor is quantitatively related to the inhibitor concentration [18-19]. Consequently, the residual enzyme activity is inversely related to the inhibitor concentration.

Normally, enzyme inhibition-based biosensors measured in batch system but this method has disadvantages such as the measuring chamber is large, the contact time between the enzyme and the inhibitor is long and the dilution of the analyte is high [20-21]. To avoid the disadvantages of batch system, flow injection analysis (FIA) system was studied for determination of metal ions by enzyme inhibition-based biosensor [22-24]. Due to the basic set-up of the FIA system itself, it offers several important advantages compared to batch systems.

FIA is an automated method in which a sample is injected into a continuous flow of a carrier solution that mixes with other continuously flowing solutions before reaching a detector. The FIA based biosensor presented some desirable characteristics, such as simplicity, low consumption of reagents, high sample throughput, good sensitivity and selectivity, possibility of on-line sample pretreatment, and easy automation.

Therefore, this research focused on the developed methods for mercuric ion determination by catalytic glucose oxidase inhibition. The enzyme immobilized on a screen printed carbon electrode modified with MnO_2 was carried out. This electrode assembled with an electrochemical cell coupled with flow injection analysis was studied for determination of mercury.

1.2 Objective

To determine mercury by inhibition of glucose oxidase immobilized on a screen printed carbon electrode modified with MnO_2 based on flow injection analysis

1.3 Scope of research

Various scopes to develop and validate the biosensor based on flow injection to detect mercury are as follows;

1.3.1 development of biosensor by immobilized glucose oxidase (GOx) on surface of screen-printed carbon electrode modified with manganese dioxide ($GOx/MnO_2/SPCE$),

1.3.2 development of the biosensor based on flow injection analysis (FIA),

1.3.3 investigation of parameters affecting the inhibition of GOx based-biosensor in FIA system using chronoamperometry as follows;,

1.3.3.1 operating potential (vary operating potentials at +0.40, +0.42, +0.44, +0.46 +0.48 and +0.50 V versus Ag/AgCl),

1.3.3.2 buffer pH solution (vary pH of carrier solutions at 5.0, 5.5, 6.0, 6.5, 7.0, 7.5 and 8.0),

1.3.3.3 enzyme loading (vary GOx concentrations at 40, 80, 120 and 160 $U.cm^{-2}$),

1.3.3.4 substrate concentration (vary glucose concentrations at 50, 100, 200, 400, 600, 800 and 1000 $mg.L^{-1}$),

1.3.3.5 injection volume (vary injection volumes at 20, 50, 100, 250 and 500 μL),

1.3.3.6 flow rate (vary flow rates at 0.6, 0.8, 1.0, 1.2, 1.4 and 1.6 $mL.min^{-1}$),

1.3.4 investigation of the inhibition of GOx based on FIA,

1.3.5 validation methods of $GOx/MnO_2/SPCE$ based on FIA for the indirect determination of mercury (linear range, limit of detection, limit of quantification, repeatability, reproducibility, regeneration, interferences, the storage stability and accuracy),

1.3.6 determination of Michaelis-Menten constant (K_m) of GOx evaluated using amperometry,

1.3.7 studies of kinetic reaction and inhibition of GOx immobilized on $MnO_2/SPCE$ by mercury,

1.3.8 study of the surface morphology and electrochemical reaction of GOx/MnO_2/SPCE by scanning electron microscopy and cyclic voltammetry, respectively,

1.3.9 applications of GOx/MnO_2/SPCE based on FIA for the determination of mercury in certified reference material (DORM-2) and real samples (water sample, spiked water, seafoods and spiked seafoods),

1.3.10 comparison of the results from both the proposed biosensor based on FIA and the standard method (cold vapor generation atomic absorption spectrometry).

CHAPTER 2
THEORETICALS AND LITERATURE REVIEWS

The purpose of this chapter is to summarize principle of a biosensor, flow injection analysis and methods for detection. A brief literature reviews is also presented to understand development, characterizations and applications of biosensor.

2.1 Biosensor

A biosensor can be considered as a combination of a bioreceptor, biological components (e.g. tissue, organelles, enzymes, antibodies, etc.) and a transducer as a detection method (e.g. optical, piezoelectric, electrochemical, etc.) depicted in Figure 2.1. When specific target compounds interact with the biological recognition element, a signal is produced at a transducer, corresponding to the concentration of the substance [25].

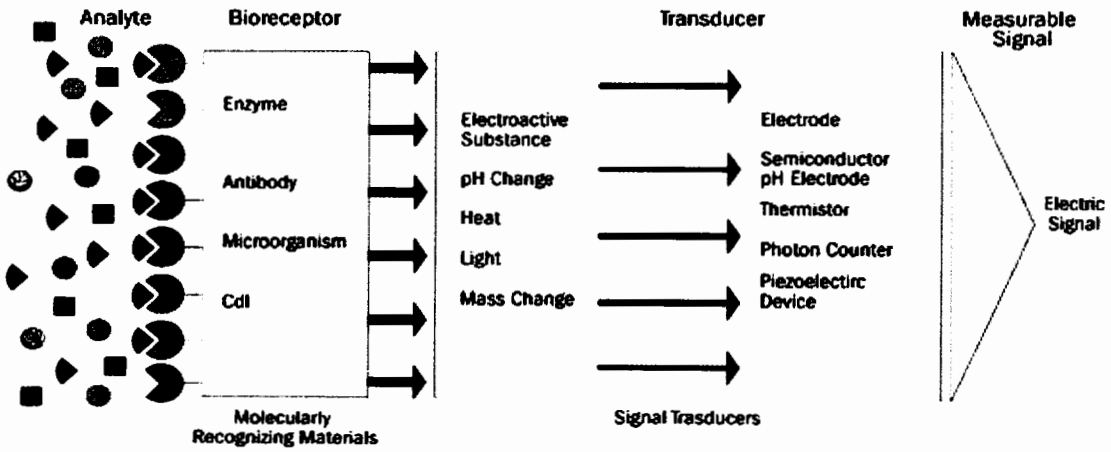

Figure 2.1 General model of a biosensor differentiating between molecular recognition, transduction and data processing [26]

As demonstrated above, a biosensor consists of a bioreceptor and a transducer. A detailed list of different possible bioreceptors and transducers is shown in Figure 2.2.

Different combinations of bioreceptors and transducers constitute several types of biosensors to suit a wide-ranging applications [27].

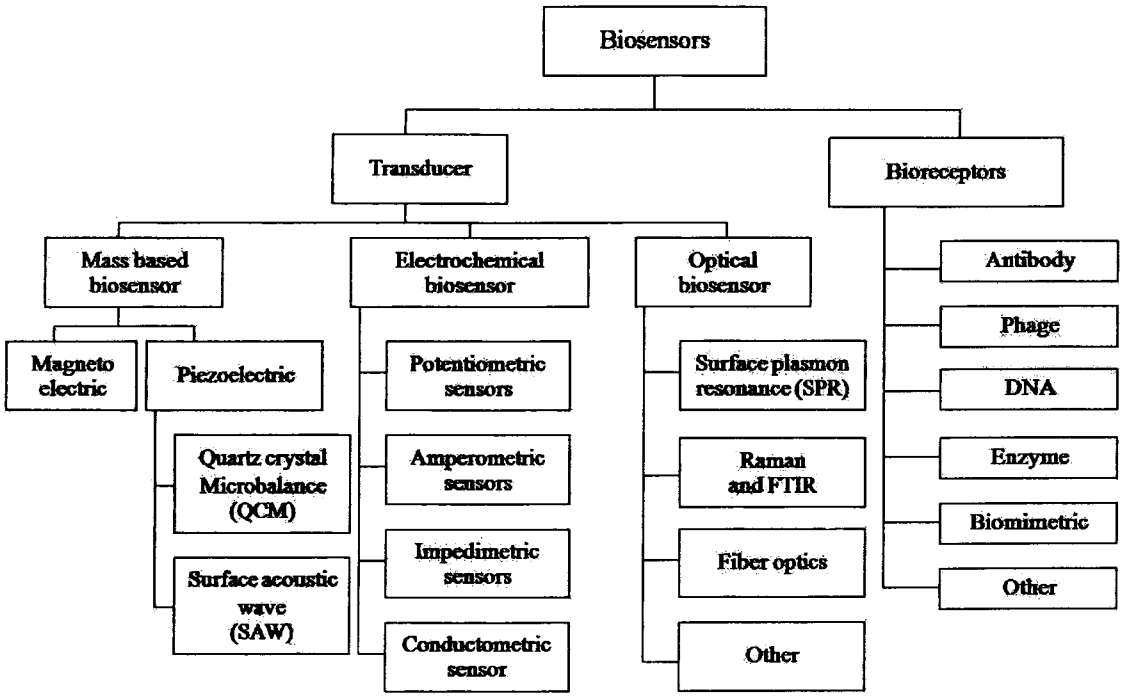

Figure 2.2 Classification of transducers and bioreceptors used in various biosensors (modified from Mohanty et al. [27])

2.1.1 Transducer

A transducer is an analytical device which provides and output quantity having a given relationship to the input quantity [28]. Biosensor can be classified according to transduction methods which they utilize. Classification to the transducing elements, biosensors can be classified as: optical, piezoelectric (mass detection methods), thermo metric and electrochemical detection [29].

In this research our biosensor is classified by amperometric detection which is explained in section 2.12.2. The bioreceptor, which is used in our biosensor, is enzyme for specific interaction with its target analyte resulting from biochemical reaction consequently transformed through the transducer for measurable signal. The principle of bioreceptor is described in the next section.

2.1.2 Bioreceptor

Bioreceptors are a key to specificity for biosensor technologies. They are responsible for binding the analyte of interest to the sensor for the measurement [30]. Bioreceptor can be classified as: antibody, nucleic acids, cells and enzymes. In this research enzyme as a bioreceptor was selected to react with an analyte.

Enzymes receptor

In enzyme receptor, the biological element is the enzyme which reacts selectively with its substrate [31]. It is well known that the response of a biosensor to the addition of a substrate is determined by the concentration of the product of the enzymatic reaction on the surface of the sensor. The reaction is controlled by the rate of two simultaneous processes, i.e. the enzymatic conversion of the substrate and the diffusion of the product from the enzyme layer. Enzymes are classified into six broad groups of activity as shown in Table 2.1.

Within this there are further subdivisions depending upon the detailed reaction type, co substrate, and substrate resulting in a unique number for each enzyme and this is written as EC a.b.c.d. with the following meaning; "EC" is Enzyme Commission, "a" show to which of six main classes that were shown in Table 2.1; "b" indicates the subclass, "c" is the sub-subclass and d is the serial number of the enzyme in its sub-subclass. Thus the enzyme glucose oxidase, widely used in glucose sensors, is EC 1.1.3.4. This defines it as oxidoreductase acting on the CH-OH group of electron donors with dioxygen as the electron acceptor and having the specific substrate β-D-glucose. There is now a general framework of enzyme catalysis into which specific cases can be fitted and which accounts for both the kinetic and chemical mechanisms that enzyme adopt [32-33].

Table 2.1 Enzyme categories and their biochemical properties and functions which are used for selective detection of their competent substrates as analytes by biosensor. [34]

Main class	Group	Biochemical properties
1	Oxidoreductases	Catalyze redox reaction by adding or removing hydrogen atoms, oxygen atoms or electrons from one substrate to another (e.g. glucose oxidase, alcohol dehydrogenases)
2	Transferases	Transfer functional groups between donors (e.g. dextransucrase, glucokinase)
3	Hydrolases	Add H_2O across a bond, hydrolyzing hydrogen (e.g. invertase, lipase)
4	Lyases	Add small molecules, for example H_2O, NH_3 or CO_2 to double bonds or remove these elements to produce double bonds (e.g. furmarase)
5	Isomerases	Carry out many kinds of isomerization, for example L to D isomerization (e.g. alanine racemase, robulosepthsphate 3-epimerase)
6	Ligases	Catalyze reactions in which two chemicals are joined or ligated with the use of energy from ATP, that is, ATP linked bond formation (e.g. glutamine synthelase, pyruvate carboxylase)

The theory explaining the catalytic action of enzymes was proposed that the substrate and enzyme formed some intermediate substance which is known as the enzyme substrate complex [35]. The reaction can be represented in equation 2.1.

$$E + S \rightleftharpoons ES \longrightarrow E + P \qquad (2.1)$$

Where E is Enzyme
S is Substrate
E-S is Enzyme substrate complex
P is Product

Basic mechanism (equation 2.1) by which general enzyme catalyzes chemical reaction begins with the binding of the substrate (or substrates) to the active site on the enzyme. The active site is a specific region of the enzyme combining with the substrate. The binding of the substrate to the enzyme causes changes in the distribution of electrons in the chemical bonds of the substrate and ultimately causes the reactions that lead to formation of products. Products are released from the enzyme surface to regenerate the enzyme for another reaction cycle.

Mechanism of enzyme catalyzed that active sites in the induced enzyme are schematically shown with rounded contours in Figure 2.3. Binding of the first substrate (gold) induces a physical conformational shift (angular contours in the protein that facilitates binding of the second substrate (blue), with far lower energy than otherwise required. When catalysis is completed, the product is released, and the enzyme returns to its uninduced state. The induced fit model has been compared to a hand-in-glove model, wherein it may be difficult to insert the first finger into the proper place, but once done, the other fingers go in easily because the glove is now properly aligned [36].

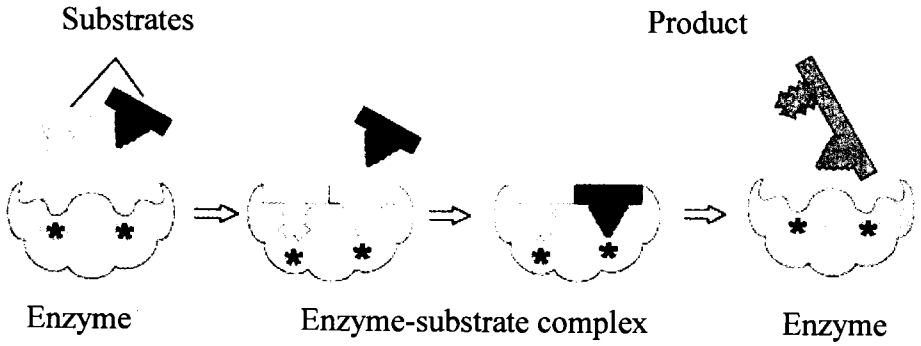

Figure 2.3 Induced-fit model of enzyme catalysis [36]

In this research, enzyme in the type of oxidoreductase chosen for fabrication of the biosensor to detect mercury was studied. Therefore, to know factors affecting the enzyme-based sensor is needed. Parameters affecting enzyme sensor response are shown in the next topic.

2.2 Parameters generally affecting the performance of enzymatic biosensors

The stability of an enzyme sensor depends on a number of physical and chemical parameters. Many factors such as pH, temperature, concentration of enzyme, substrate concentration and interference are as follows.

2.2.1 Influence of pH

Effect of pH on the response comes from two possibilities. Firstly, enzymatic activity is a function of pH and, secondly, pH may affect dissociation equilibrium of the product, and only one form will be detectable by the transducer. The loss of activity due to the pH can be compensated by increasing the enzyme concentration. The conversion of substrate can be maintained at its maximal level and the enzyme sensor will have very little dependence on pH. The pH-dependence curve is then broader and flatter than that of the same enzyme in solution.

2.2.2 Enzyme amount

Enzymes are catalysts, not consumed by the reaction, and the precise amount (or concentration) is not crucial for the operation of a biosensor. However, there are limiting factors. Provided that there is sufficient enzyme present so that this process is not rate limiting. However, if there is too much enzyme or the quality of the enzyme preparation is poor, so that considerable material is needed to provide sufficient units of enzyme activity, the excess of material can affect the rates of mass transport (principally diffusion) to the transducer [25].

2.2.3 Substrate concentrations

Changing of the substrate concentrations affects the rate of reaction of an enzyme catalyzed reaction. If the amount of the enzyme is kept constant and the substrate concentration is then gradually increased, the reaction velocity will increase until it reaches a maximum. After this point, increases in substrate concentration will not increase the velocity.

In this research, the biosensor was fabricated by immobilizing glucose oxidase on the surface of a screen printed electrode. Thus, immobilized enzyme method is described in the next section.

2.3 Methods of immobilization

The regular enzyme immobilization methods are as follows [37].

2.3.1 Adsorption

It is a simplest and involves minimal preparation. Many substances adsorb enzymes on their surfaces, e.g. alumina, charcoal, clay, cellulose, kaolin, silica gel, glass and collagen. No reagents are required, there is no clean-up step and there is less disruption to the enzymes. However, the bonding is weak and this method is only suitable for exploratory work over a short time-span.

Adsorption can roughly be divided into two classes: physical adsorption (physisorption) and chemical adsorption (chemisorption). Physisorption is usually weak and occurs via the formation of van der Waals bonds, occasionally with hydrogen bonds or charge-transfer forces. Chemisorption is much stronger and involves the formation of covalent bonds. Adsorbed biomaterial is very susceptible to changes in pH, temperature, ionic strength and the substrate. However, these methods are satisfactory for short-term investigations. A schematic diagram of adsorbed immobilization is presented in Figure 2.4.

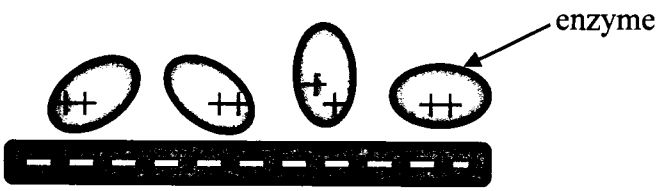

Figure 2.4 Schematic diagram of adsorbed immobilization [38]

2.3.2 Microencapsulation

It is a process in which tiny particles are produced to give small capsules. A microcapsule is a small sphere with a uniform around it. The capsules used are as follows: cellulose acetate (dialysis membrane), polycarbonate, a synthetic polytetrafluoroethylene (Teflon) and a synthetic polymer, which is selectively

permeable to gases such as oxygen. Other materials sometimes used are Nafion and polyurethane.

The biomaterial or enzyme is held inside the membrane. A schematic diagram of microencapsulated immobilization is presented in Figure 2.5. This method is adaptable, limits contamination and biodegradation, has no interfere with the reliability of the enzyme. This enzyme immobilization is stable towards changes in temperature, pH, ionic strength and chemical composition.

Figure 2.5 Schematic diagram of microencapsulated immobilization [39]

2.3.3 Entrapment

Enzyme or biomaterial is mixed with monomer solution, which is then polymerized to a gel, trapping the biomaterial. Unfortunately, this can cause barriers to the diffusion of substrate, thus slowing the reaction. It can also result in loss of bioactivity through pores in the gel. This can be counter acted by cross-linking. The most commonly used gel is poly acrylamide, although starch gels and nylon have been used. Conducting polymers such as polypyrroles are particularly useful with electrodes. The problems are the following: (i) large barriers are created, inhibiting the diffusion of the substrate, which slows the reaction and hence the response time of the sensor. (ii) There is loss of enzyme activity through the pores in the gel. This problem may be overcome by cross-linking, with, e.g., glutaraldehyde. A schematic diagram of entrapment method of immobilization is presented in Figure 2.6.

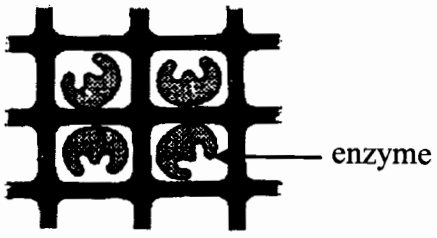

Figure 2.6 Schematic diagram of entrapment immobilization [39]

2.3.4 Cross-linking

In this method, enzyme or biomaterial is chemically bonded to solid supports or to another supporting material such as a gel. Bifuntional reagents such as glutaraldehyde are used. There is some diffusion limitation due to damage to the biomaterial. In addition, the mechanical strength is poor. It is a useful method to stabilized adsorbed biomaterials. A schematic diagram of entrapment method of immobilization is presented in Figure 2.7.

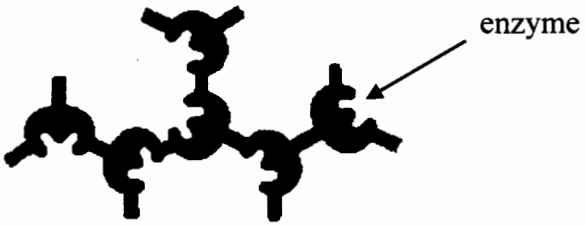

Figure 2.7 Schematic diagram of cross-linking immobilization [40]

2.3.5 Covalent bonding

This method involves a carefully designed bond between a functional group in the biomaterial to the support matrix. Nucleophilic groups in the amino acids of the biomaterials, which are not essential for the catalytic action, are suitable. Some functional groups, which are not essential for the catalytic activity of an enzyme, can be covalently bonded to the support matrix (transducer or membrane). This method uses nucleophilic groups for coupling such as $-NH_2$, -COOH, -OH, C_6H_4OH, -SH and imidazole. Reactions need to be performed under mild conditions such as low temperature, low ionic strength and pH in the physiological range.

The advantage is that the enzyme will not be released during use. In order to protect the active site, the reaction is often carried out in the presence of the substrate. A schematic diagram of covalent bonding immobilization is presented in Figure 2.8.

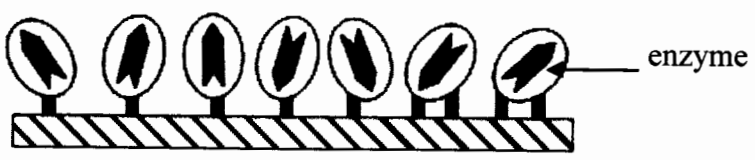

Figure 2.8 Schematic diagram of covalent bonding immobilization [41]

In this research, enzyme glucose oxidase immobilized via microencapsulation method by Nafion was studied because encapsulated immobilization has largely been driven by the benefits with respect to enhanced stability, repeated use, facile separation from reaction mixtures, and the prevention of enzyme contamination in products [42]. To understand mechanism of enzyme glucose oxidase, the next section is explained enzyme glucose oxidase.

2.4 Enzyme glucose oxidase (GOx)

The glucose oxidase enzyme (β-D-glucose: oxygen 1-oxidoreductase, GOx) is a dimeric glycoprotein consisting of two identical polypeptide chain subunits that are covalently linked together via disulfide bonds (-S-S-). Figure 2.9 depicts the flavine adenine dinucucleotide (FAD) moiety and the key conserved active site residues of a GOx. Active-site residues of GOx are Tyr-73, Phe-418, Trp-430, Arg-516, Asn-518, His-520 and His-563. Arg-516 is the most critical amino acid for the efficient binding of β-D-glucose.

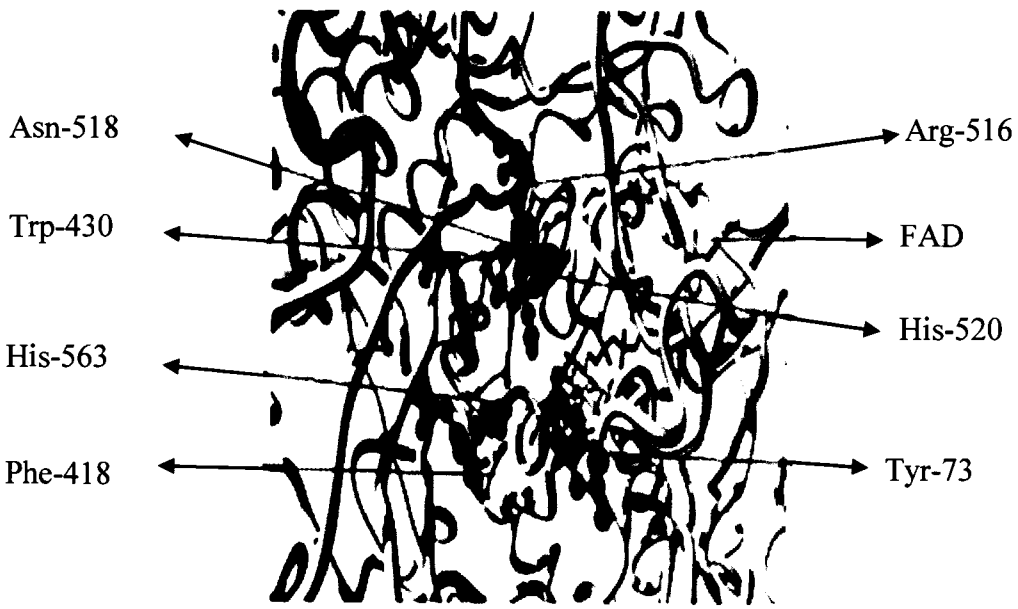

Figure 2.9 Glucose oxidase from P. amagasakiense showing the FAD moiety [43]

GOx is a flavoprotein which catalyzes the oxidation of β-D-glucose to D-glucono-δ-lactone and H_2O_2 using molecular oxygen as an electron transfer. This

reaction can be divided in to a reductive and an oxidative step (Figure 2.10). In the reductive half reaction, GOx catalyzes the oxidation of β-D-glucose to D-glucono-δ-lactone, which is non-enzymatically hydrolyzed to gluconic acid. Subsequently the FAD ring of GOx is reduced to $FADH_2$. In the oxidative half reaction, the reduced GOx is reoxidized by oxygen to yield H_2O_2. The H_2O_2 is cleaved by catalase to produce water and oxygen.

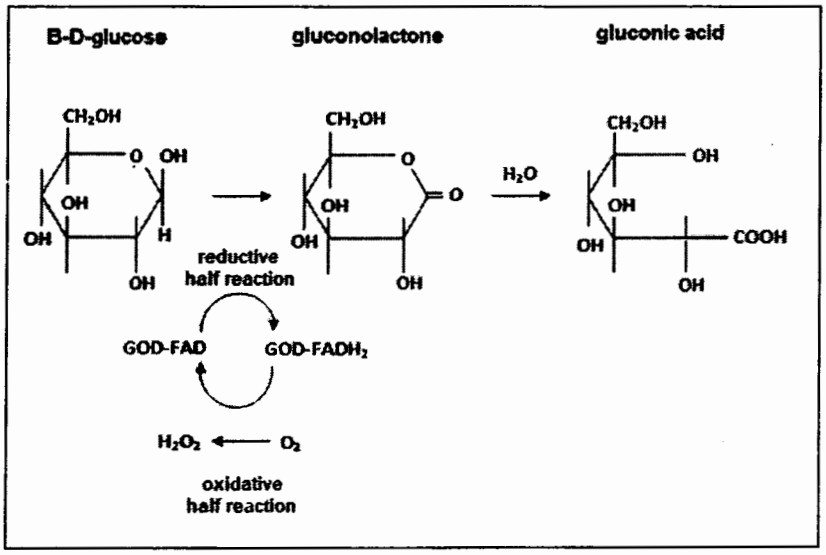

Figure 2.10 Representation of GOx reaction [43]

In this research, we developed the biosensor for determination of mercury by inhibition of GOx. The enzyme kinetics is necessary studied. Therefore, the next section is discussed about enzyme kinetics.

2.5 Enzyme kinetics

The majority of chemical transformations inside cells are catalyzed by enzymes. Enzymes accelerate the rate of chemical reactions (both forward and backward) without being consumed in the process and tend to be very selective, with an individual enzyme accelerating only a specific reaction. The model for enzyme action, first suggested by Brown and Henri but later established more thoroughly Michaelis and Menten, suggests the binding of free enzyme to the substrate forming an enzyme-substrate complex and the mechanism is often written as equation 2.2.

$$E + S \underset{}{\overset{K_m}{\rightleftharpoons}} ES \xrightarrow{k_{cat}} E + P \qquad (2.2)$$

Where the K_m is the substrate concentration that provides a reaction velocity that is half of the maximal velocity obtained under saturating substrate conditions. The K_m value is often referred to in the literature as the *Michaelis constant*. In addition, k_{cat} is single first-order rate constant.

Equation 2.2 predicts that the reaction velocity will be proportional to the concentration of the ES complex as equation 2.3.

$$v = \frac{V_{max}[S]}{K_m + [S]} \qquad (2.3)$$

Where v is rate of product formation of an enzyme catalyzed reaction, V_{max} is the maximum velocity of enzyme catalyzed reaction and [S] is concentration of substrate.

To understand the enzyme kinetics, the key parameters of the Michaelis-Menten equation is obtained in the following section.

K_m ($mol.L^{-1}$)

The K_m for a given enzyme is constant, that provides an indication of the binding strength of that enzyme to its substrate. A high K_m indicates the enzyme binds the substrate weakly. Conversely, a low K_m indicates a higher affinity for the substrate.

k_{cat} (s^{-1})

The k_{cat}, also thought of as the turnover number of the enzyme, is a measure of the maximum catalytic production of the product under saturating substrate conditions per unit time per unit enzyme. The larger the values of k_{cat}, the more rapidly catalytic events occur.

V_{max}

The V_{max} is the maximum velocity that an enzyme could achieve. The measurement is theoretical because at a given time, it would require all enzyme molecules to be tightly bound to their substrates.

The graphical evaluation of nonlinear plots to obtain Michaelis-Menten parameters relies on accurate curve fitting as shown in Figure 2.11 (a).

Moreover, the problems associated with evaluating enzyme kinetics using a nonlinear plot can be avoided by using one of the three common linearization methods to obtain estimates for K_m and V_{max} by Lineweaver-Burk equation as shown in equation 2.4 and graphical determination of K_m and V_{max} by Lineweaver-Burk double reciprocal plot as shown in Figure 2.11 (b).

$$\frac{1}{v} = \left(\frac{K_m}{V_{max}}\right)\left(\frac{1}{[S]}\right) + \left(\frac{1}{V_{max}}\right) \tag{2.4}$$

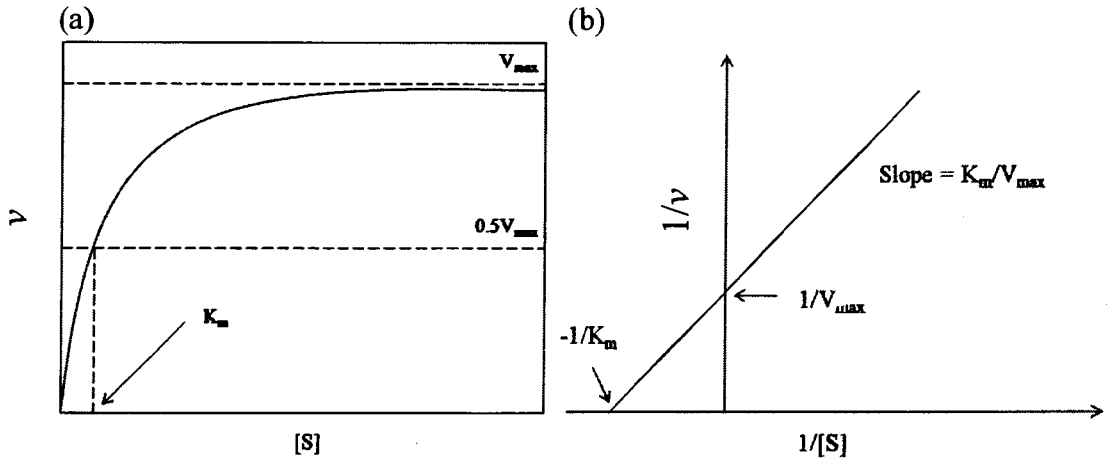

Figure 2.11 (a) Change in velocity (v) with the concentration of substrate ([S]) for the reaction shown by equation 2.3 catalyzed by enzymes. (b) Linear representations of the Lineweaver-Burk double reciprocal plot for the reaction shown by equation 2.4. (modified from Copeland [35])

In this thesis, the developed amperometric biosensor for indirect determination of mercury that the enzyme kinetics followed by characteristic of typical Michaelis-Menten kinetics was studied. The apparent K_m which depicts the enzyme-substrate kinetics of biosensor can be calculated from the Lineweaver-Burk equation 2.5.

$$\frac{1}{I_{SS}} = \left(\frac{K_m}{I_{max}}\right)\left(\frac{1}{[S]}\right) + \frac{1}{I_{max}} \tag{2.5}$$

Where I_{ss} is the steady-state current and I_{max} is the maximum current measured under substrate saturation. The enzymes kinetic in amperometric technique have been extensively used to determine the enzyme activity like glucose oxidase [44-46].

In this research, we developed the biosensor for determination of mercury by inhibition of GOx. Therefore, enzyme inhibition system is explained in the next section.

2.6 Enzyme inhibition systems

The enzyme-inhibitor reaction is habitually complicated; the inhibition of the enzyme can be either reversible or irreversible.

2.6.1 Reversible inhibition

This inhibition is characterized by a high rate of association and dissociation of inhibitors with the enzyme. Consequently, the biosensor based on reversible inhibition can be repetitively regenerated and thus termed as multiple use biosensors. However, the biosensor response may vary considerably with each assay because some of the enzyme activity lost after every inhibition-regeneration step.

The inhibition process of the immobilized enzyme can be described by the following equation 2.6.

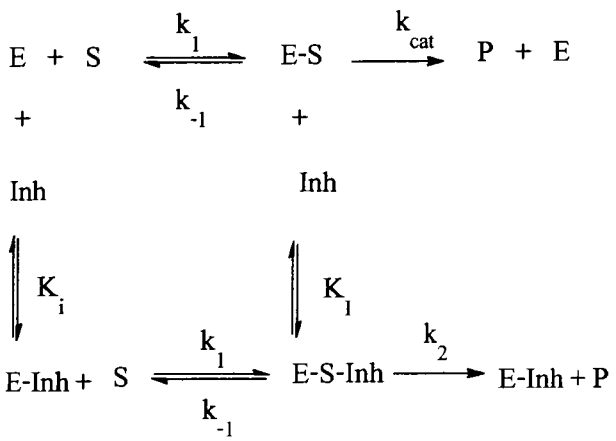

(2.6)

Where: E is immobilized enzyme;

S is free substrate;

P is product;

E-S is enzyme-substrate complex;

E-Inh is enzyme-inhibitor complex;

E-S-Inh is ternary complex containing enzyme-substrate inhibitor;

K_I and K_i are equilibrium dissociation constants of the E-S-Inh complex the E-Inh complex

Based on the mechanism to inhibit the enzyme activity, the inhibitors may further be classified into competitive, noncompetitive, and uncompetitive inhibitors. Table 2.2 shows the characteristic behavior of each type of inhibitor. For an enzyme-catalyzed reaction, the effect of different types of the inhibitor on the velocity versus substrate concentration curve is shown in Figure 2.12.

Table 2.2 Type of enzyme inhibitors [47]

Inhibitor type	**Binding site on enzyme**	**Kinetic effect**
competitive inhibitor	-Inhibitor competitively binds to substrate binding site of enzyme i.e., active site, due to its close resemblance to substrate structure. -Inhibition can be reversed by increasing the concentration of substrate to a level where it out-competes inhibitor.	No change in V_{max} but K_m increased
noncompetitive inhibitor	-Inhibitor binds to a site on enzyme which is totally different from active site. -This inhibition cannot be reversed by increasing the substrate concentration, as the binding sites are different for both, inhibitor and substrate.	No change in K_m But V_{max} decreased
uncompetitive inhibitor	-Inhibitor binds only to the E-S complexes. -This E-S-Inh cannot form product due to conformational changes in enzyme.	Both V_{max} and K_m decreased

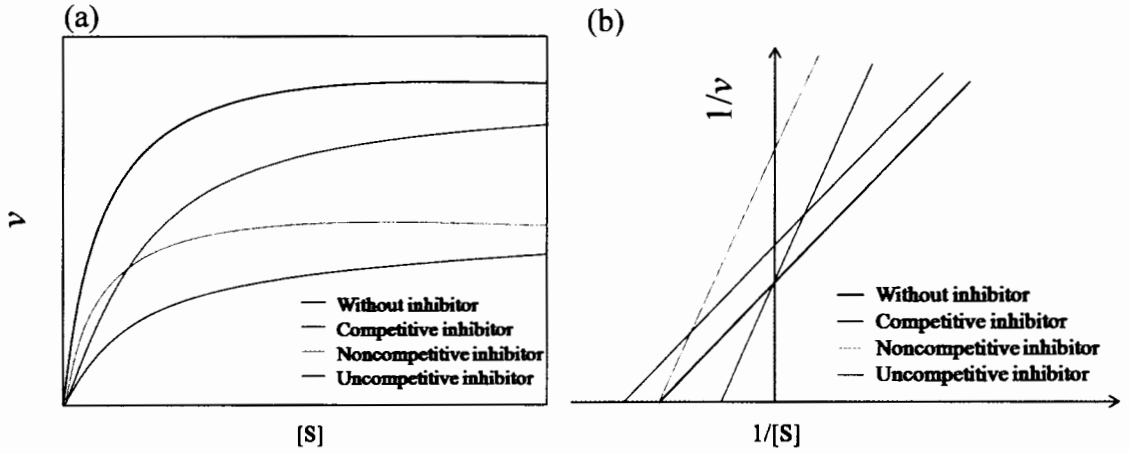

Figure 2.12 Dependence of reaction velocity on the substrate concentration that graph is shown the velocity in the absence and presence of different types of inhibitors; (a) Michaelis-Menten equation (b) Linewaever-Burk double reciprocal plot. (modified from Copeland [35])

2.6.2 Irreversible inhibition

For irreversible inhibitors, the enzyme-inhibitor interaction results in the formation of a covalent bond between the enzyme active center and the inhibitor. It directed the formation of a highly reactive inhibitor product that binds to the enzyme irreversibly and thus inhibits its activity. The term irreversible means that the decomposition of the enzyme-inhibitor complex results in the destruction of enzyme, e.g. its hydrolysis and oxidation [19].

In this section, we discussed the enzyme kinetics and kinetic inhibition. Therefore, next section is discussed about enzyme inhibition system.

2.7 Inhibited reaction of glucose oxidase with mercury

To understand mechanism of GOx based inhibition by mercury is necessary to investigate structure of GOx consisting of various amino acids (discussed in section 2.4) and cysteine (Figure 2.13).

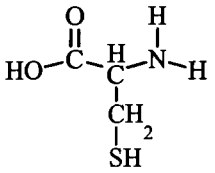

Figure 2.13 Chemical structure of cysteine

In general, in the case of metal cation the interaction mechanism is not completely known, but the action revealed by different metals on the activity of oxidases is usually by binding of the metal salts to the thiol groups of the proteins [48-50]. The mechanism is shown in Figure 2.14. When the enzyme is inhibited with mercuric ion, its catalytic reaction is not occurred.

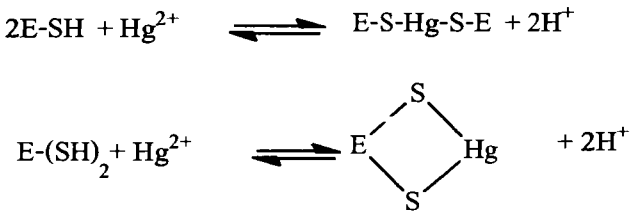

Figure 2.14 The mechanism inhibition GOx with mercury [49-50]

In this proposed research, after mercury exposure to GOx, the activity of GOx was inhibited. To perform multiple measurements, the regeneration of GOx is described in next section.

2.8 Regeneration of GOx

For the regeneration of enzyme activity, several reagents or combination of reagents have been used; including the metal-chelating agent (ethylene diaminetetraacetic acid, EDTA) or thiols [51], cysteine [52] or a mixture of EDTA with dithiothreitol [53] were studied. EDTA is a chelating agent as the chemical structure shown in Figure 2.15 that reacts with the metal ion leading to the formation of a stable complex. In this way removing the inhibitor and regenerating enzyme activity, EDTA was used for reactivation of GOx after the inhibition produced by the mercuric cation (Hg^{2+}).

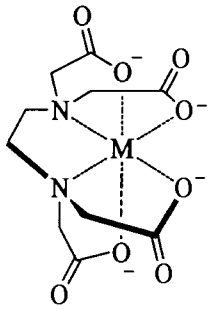

Figure 2.15 The metal-chealating agent of ethylenediaminetetraacetic acid [54]

After inhibition of GOx by mercuric ion, the biosensor was regenerated by using EDTA which the regeneration of the electrode surface could be satisfied. Moreover, immobilized GOx on surface of a screen-printed carbon electrode is important role to be investigated. Thus, the properties of screen printed electrode materials will be useful to study so that it is described in the next section.

2.9 Screen printed electrode materials

Heterogeneous carbon materials have been used as biosensors because of its availability in a variety of forms, low cost, broad exploitable potential window, low background current, chemical inertness, ease of chemical modification and suitability for various applications. Among the various carbon-based electrodes available for the development of biosensors, screen-printed carbon electrodes (SPCE) has got widespread popularity due to its ease of preparation and modification and mass production of highly reproducible electrodes. Therefore, SPCE was chosen for fabrication of biosensor in this research.

The SPCEs in this research were adopted as electrochemical transducer to evaluate the enzymatic activity. Screen printed electrodes were produced by printing carbon ink onto a plastic support (polyester or polycarbonate) and worked as a working electrode (Figure 2.16 (A)). Its surface could be easily controlled and designed by a printing machine depicted in Figure 2.16 (B). Moreover, the inks were used for printing the layers consist of polymer binders in organic solvents. The inks used for working electrode could be modified or added with some modifiers in order to change the characteristics of the carbon electrodes.

For this purpose, the amperometric transducer has been used. The analyte detected on SPCE's surface is H_2O_2 produced from glucose oxidase. However, it oxidation or reduction at bare electrode of the high over voltage was required. These phenomena can be controlled by deliberately attaching chemical reagents to the electrode surface.

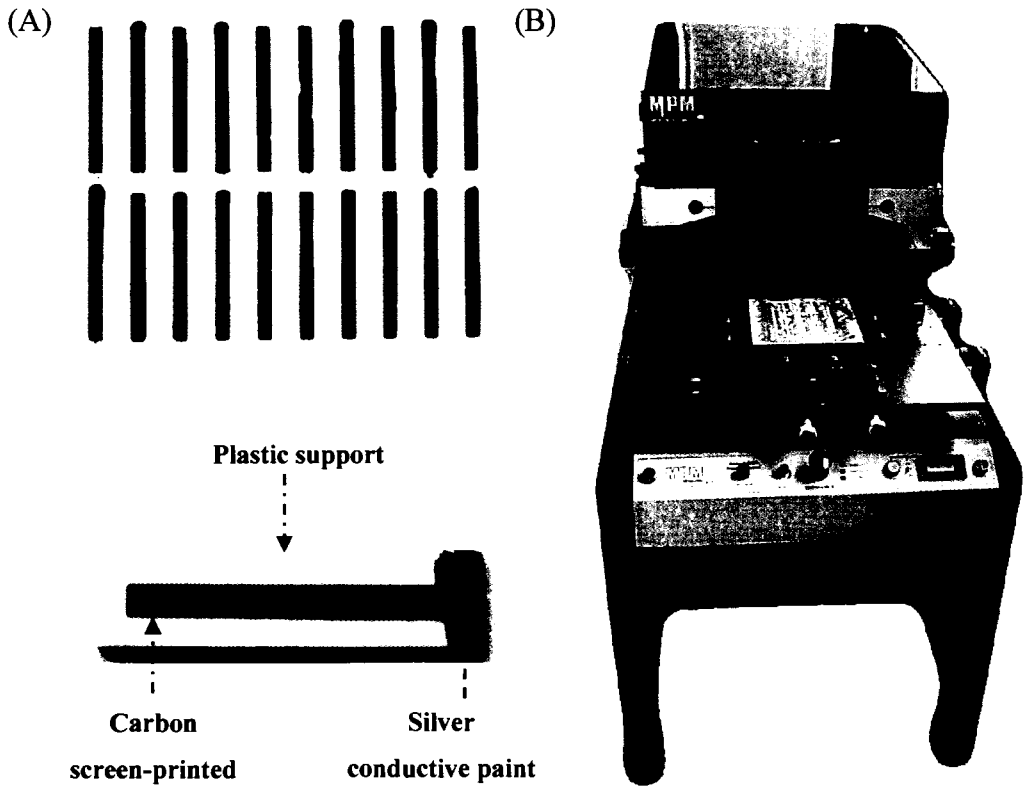

Figure 2.16 Screen printed carbon electrode (A) and screen printing machine (B) [55]

In this research, the screen-printed carbon electrodes which they were prepared by printing carbon ink modified manganese dioxide as a mediator on an alumina substrate was investigated (followed Turkusic et al. [56]). Electrocatalytic reaction of manganese dioxide modified with screen-printed carbon electrode is discussed in the next section.

2.10 Manganese dioxide modified on electrode

Manganese dioxide (MnO_2), a very usual transition metal oxide, has attracted considerable attention in various fields such as electrocatalytic oxygen reduction and electrochemical capacitors. It is low cost, low toxicity, large abundance, and good electrochemical activity. When MnO_2 modified on SPCE as the biosensor, it is catalytic reduction of H_2O_2 produced from catalytic enzyme reaction. Mechanism of MnO_2 catalyzed to H_2O_2 is presented in Figure 2.17.

Glucose is enzymatically oxidized with molecular oxygen forming gluconolactone and H_2O_2 as an intermediate (I). The latter reacts chemically with MnO_2 producing manganese species at lower oxidation states (II), which can be electrochemically reoxidized to MnO_2 (III). The oxidative current flow is directly related to the glucose concentration. Besides this rapid electrochemical process, a kinetically slower chemical reoxidation of MnO/Mn_2O_3 with H_2O_2 (corresponding to a catalytic decomposition of hydrogen peroxide) is possible. From this reaction, the potential range of 400 - 500 mV is applied towards H_2O_2 [55].

In this research the biosensor modified with 5% (m) MnO_2 as a mediator prepared by modify with heterogeneous carbon ink printed on ceramic support in order that the reduction of over potential is occurred. Besides, a biosensor coupled with flow injection analysis system offers possibility to improve sensitivity, precision, and fast response. Such an approach is desirable for the real time analysis and repetitive measurements. Consequently, the flow injection analysis based biosensor was studied to indirect determination of mercury. The flow injection analysis is explained in the next section.

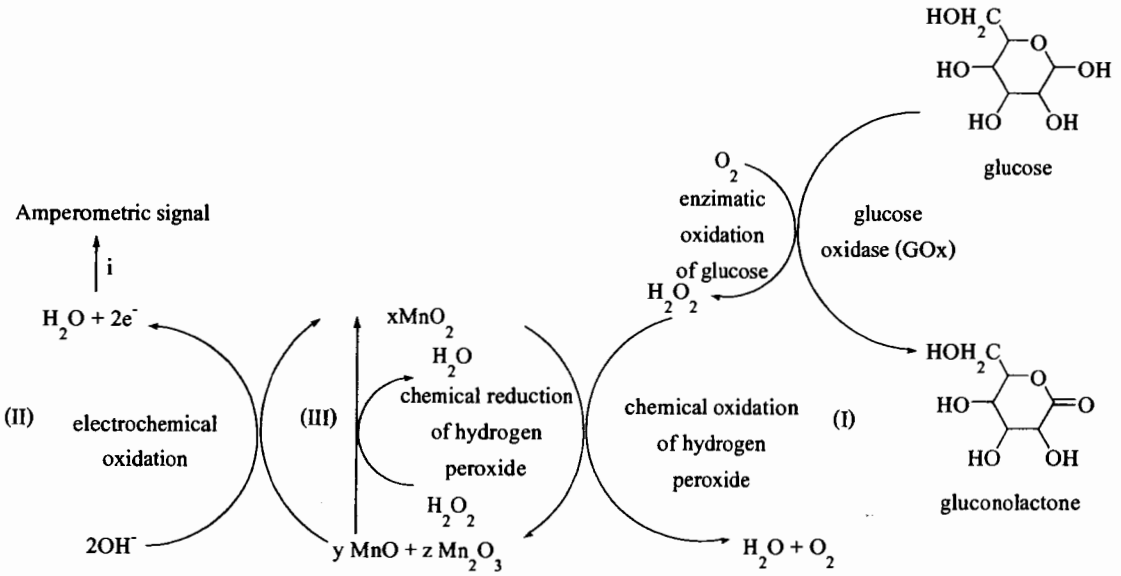

Figure 2.17 Reaction mechanism of glucose measurement with the biosensor and action of MnO_2 catalyzed glucose oxidase at the surface of the biosensor [56]

2.11 Flow injection analysis

Flow injection analysis (FIA) is based on the injection of liquid sample into a continuous moving carrier steam of a suitable liquid. FIA is a simple, rapid and versatile technique that is now firmly established, with widespread application in quantitative chemical analysis. The designation of FIA was proposed in 1975 by Ruzicka and Hansen [57]. The inclusion of the term injection in the name of this technique occurred because the technique originally entailed using a syringe to inject a sample through a septum into a reagent flow.

The simplest flow injection analyzer which is depicted in Figure 2.18 (a) consists of a pump which is used to propel the carrier stream through a narrow tube, an injection port, through which a well-defined volume of a sample solution "S" is injected into the carrier stream in a reproducible manner; and a micro reactor in which the sample zone disperses and reacts with the components of the carrier stream, forming a species which is sensed by a flow through detector and recorded. A typical recorder output has the form of a peak (Figure 2.18 (b)), the height "H", width "W", or area "A" of which is related to the concentration of the analyte. The time span between the sample injection "S" and the peak maximum, which yields the analytical

readout as peak height "H", is the residence time t during which the chemical reaction takes place.

In this research the enzymatic inhibition based on the biosensor as a transducer coupled with FIA for mercury detection was studied. Voltammetric technique was used for the signal recorded and its principle is explained in the next section.

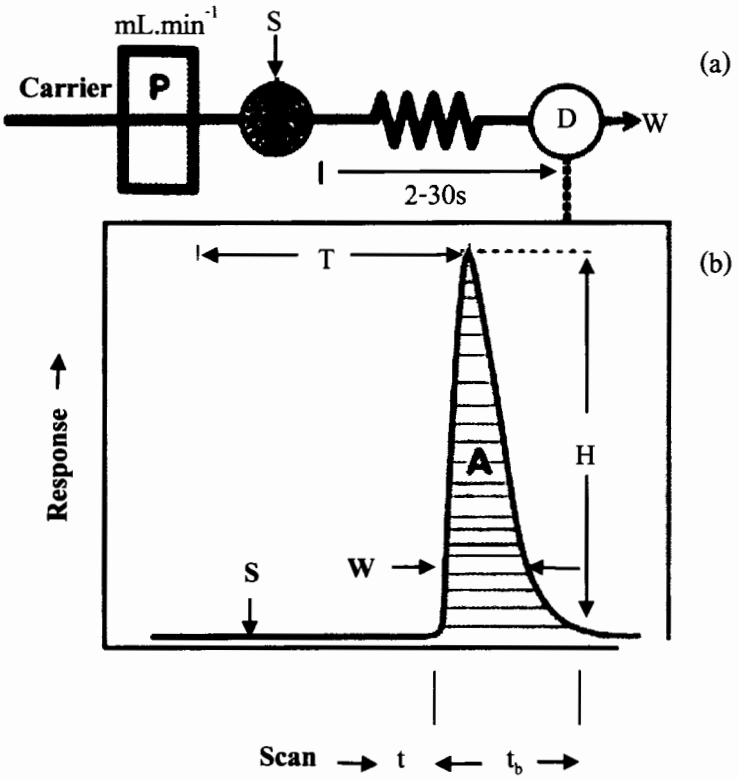

Figure 2.18 (a) The simplest single line FIA manifold utilizing a carrier stream of reagent; S is the injection port, D is the detector, and W is the waste. (b) The analog output has the form of a peak, the recording starting at S (time of injection to). H is the peak height, W is the peak width at a selected level, and A is the peak area. T is the residence time corresponding t_o the peak height measurement, and t_b is the peak width at the baseline [57].

2.12 Voltammetry

2.12.1 Cyclic voltammetry

Cyclic Voltammetry (CV) is an electrochemical technique which measures current that develops in an electrochemical cell under conditions where

voltage is in excess of that predicted by the Nernst equation. CV is performed by cycling the potential of a working electrode, and measuring the resulting current.

The potential of the working electrode is measured against a reference electrode which maintains a constant potential, and the resulting applied potential produces an excitation signal. In the forward scan of Figure 2.19, the potential first scans negatively, starting from a greater potential (a) and ending at a lower potential (d). The potential extreme (d) is call the switching potential, and is the point where the voltage is sufficient to have caused an oxidation or reduction of an analyte. The reverse scan occurs from (d) to (g), and is where the potential scans positively. This figure shows a typical reduction occurring from (a) to (d) and an oxidation occurring from (d) to (g). It is important to note that some analytes undergo oxidation first, in which case the potential would first scan positively. This cycle can be repeated, and the scan rate can be varied. The slope of the excitation signal gives the scan rate used.

Figure 2.20 shows a cyclic voltammogram resulting from a single electron reduction and oxidation. Consider the following reversible reaction in equation 2.7.

$$M^+ + e^- \rightleftharpoons M \qquad (2.7)$$

Where M is redox species

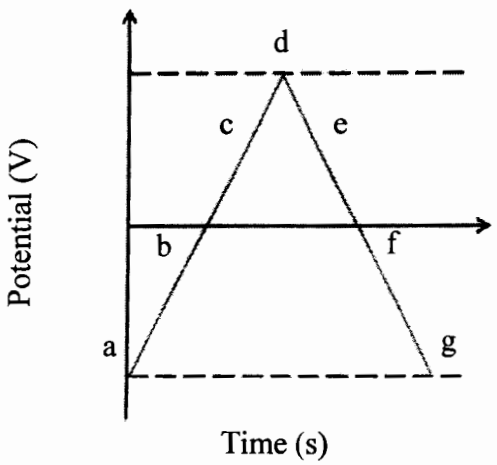

Figure 2.19 The waveform of the potential applied during a typical cycle voltammetry measuring the current at the working electrode during the potential scans [58]

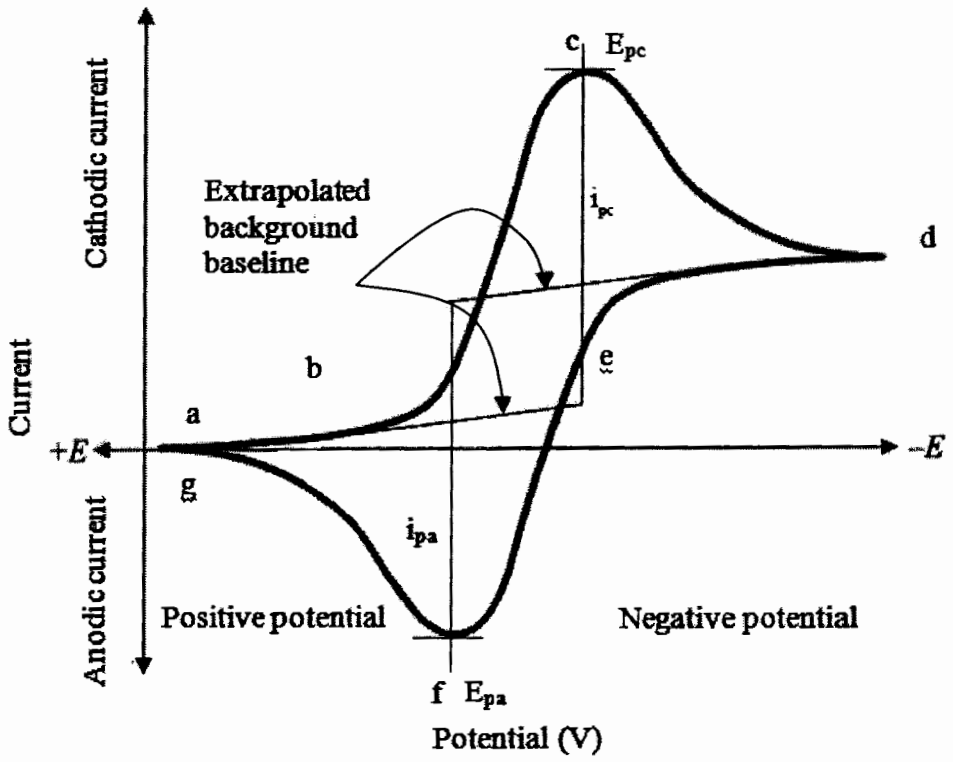

Figure 2.20 Voltammogram of a Single electron oxidation-reduction [58]

The reduction process occurs from (a) the initial potential to (d) the switching potential. In this region, the potential is scanned negatively to cause a reduction. The resulting current is called cathodic current (i_{pc}). The corresponding peak potential occurs at (c), and is called the cathodic peak potential (E_{pc}). The E_{pc} is reached when all of the substrate at the surface of the electrode has been reduced. After the switching potential has been reached (d), the potential scans positively from (d) to (g). This results in anodic current (i_{pa}) and oxidation to occur. The peak potential at (f) is called the anodic peak potential (E_{pa}), and is reached when all of the substrate at the surface of the electrode has been oxidized. In principle, the cyclic voltammogram is used to characterize potential oxidation or reduction of analyte.

2.12.2 Amperometry

Amperometry is an electrochemical technique for measurement of the current that a fixed potential is applied on a working electrode [59]. A heterogeneous electron transfer reaction, i.e., the oxidation and reduction of electro active substance, take place on the working electrode as Figure 2.21. The reaction considered as a set of equilibrium involved in the diffusion of the reactant to the electrode, the reaction at the

electrode, and the diffusion of the product away from the electrode surface into the bulk of the solution.

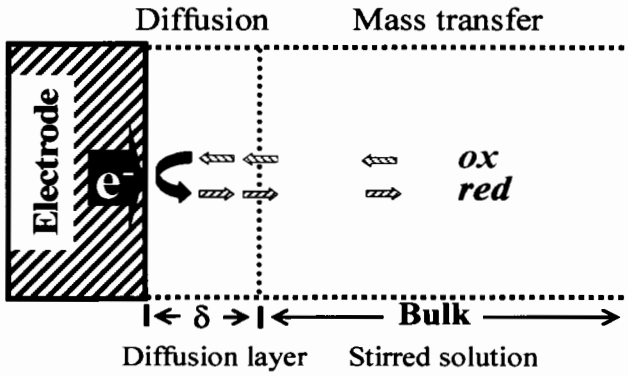

Figure 2.21 Schematic diagram of electrode reaction processes involved in stirred solution. Arrows indicated the direction of oxidizing species (ox) moving into the electrode and reduced to reducing species (red) which move out to the bulk solution. The δ is thickness of the diffusion layer.

Amperometric measurements are usually performed in the three electrode set-up where the potential of the working electrode is maintained by a potentiostat and is relative to a reference electrode (usually Ag/AgCl or saturated calomel electrode) and the current flowing between working and a counter (auxiliary) electrode is measured as presented in Figure 2.22. The current has become effectively independent of time indicated by the equation (2.8)

$$I = nFAC\sqrt{\frac{D}{\pi t}} \tag{2.8}$$

Where I is current (A)

n is number of electrons

A is area of electrode (cm^2)

C is concentration of solution ($mol.L^{-1}$)

D is diffusion coefficient ($cm^2.s^{-1}$)

t is time (s)

The general set-up system based on FIA was discussed and used for the experimental explained in chapter 3.

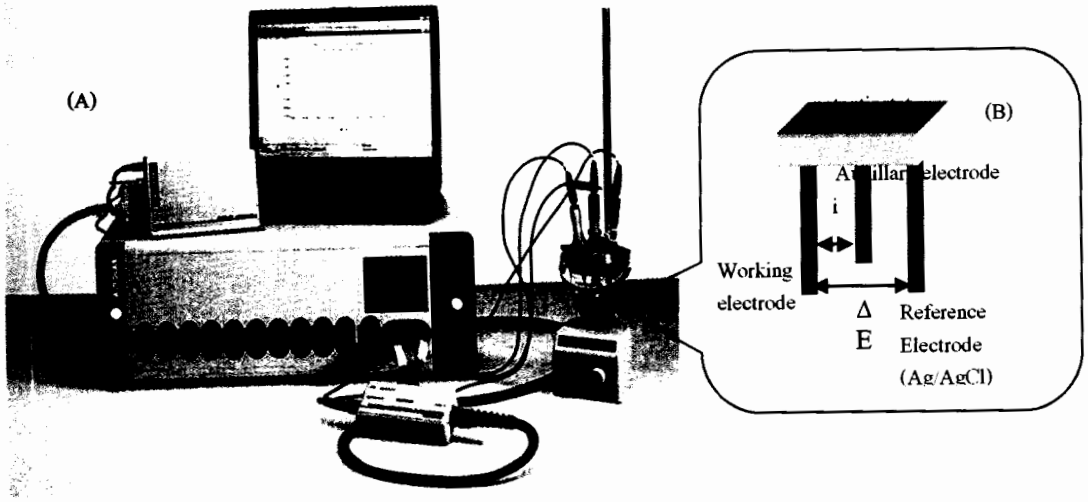

Figure 2.22 (A); Potentiostat/galvanostat and (B); diagram of electrochemical cell

The GOx/MnO_2/SPCE based on FIA was developed for indirect methond of mercury. The indirect determination of mercury according to decreasing of the enzymatic reaction is presented. Its measurement based on FIA is described in the next section.

2.13 Biosensor based enzymatic inhibition using flow injection analysis

The determination of an inhibitor of an enzymatic reaction requires the presence of a substrate. There are two possibilities: the inhibitor could be injected into a carrier stream containing the substrate; or the substrate could be injected into a carrier stream containing the inhibitor. The first method only applies when the inhibition reaction is rapid and has the disadvantage of high consumption of substrate. The second method, injection of the substrate, is more widely used because inhibition reactions are often slow, especially those involving irreversible inhibitors. This method facilitates the incubation of the enzyme in the presence of its inhibitor and its reactivation by a regenerating agent. This system is particularly useful for monitoring water pollution because the toxic chemicals or polluting compounds that act as enzyme inhibitors are often found in flowing liquids. Furthermore, the low consumption of substrate makes

the method economically feasible and very convenient. The detection involves immobilization of the enzyme either on a membrane fixed to the electrode or in a reactor placed just upstream of the transducer. They were applied to the measurement of organophosphate insecticides and carbamates based on FIA [60-62].

The system also presents the possibility of performing successive calibration, measurement and rinsing steps. The system is calibrated by first passing a carrier liquid with no inhibitor through the detection cell to obtain a reference peak corresponding to the maximal response of the biosensor. A series of solutions with different inhibitor concentrations are then used to obtain the corresponding percentage inhibitions (% inhibition). Percentage inhibition is given by equation 2.9.

$$\% \text{ Inhibition} = \left(\frac{I_0 - I}{I_0}\right) \times 100 \qquad (2.9)$$

Where "I_0" is the reference peak height given by biosensor before inhibition, and "I" is the peak height after inhibition. Once the enzyme sensor has been in contact with the inhibitor, it is rinsed with a solution containing a reactivating agent. In principle, the injection of substrate should give the reference peak again as the peak after reactivation (Figure 2.23). The biosensors based FIA have been extensively used to determine the environmental pollutants like organophosphorus pesticides [63-65].

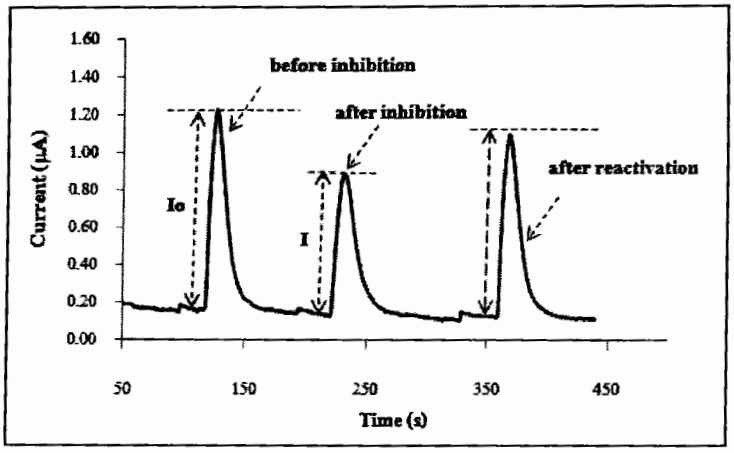

Figure 2.23 Typical flow injection peaks during inhibitor determination (modified form Canh [26])

In the measurement, the inhibitor reduces the signal of the biosensor by reducing the enzymatic activity on the transducer. It is determined by fixing the substrate concentration and varying the inhibitor concentration. A calibration curve is then plotted as a function of inhibitor concentration versus percentage inhibition as depicted in Figure 2.24.

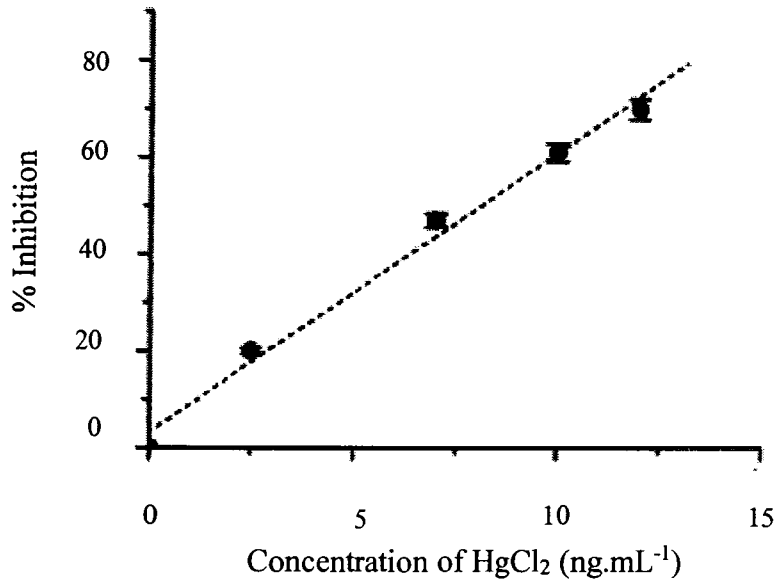

Figure 2.24 Calibration curve for mercury based on the inhibition degree of glucose-oxidase [66]

The determination of mercury by our proposed method is significantly confident so that all samples were determined and compared with cold vapor atomic absorption spectrometry as a reference technique presented in the next section.

2.14 Cold vapor atomic absorption spectrometry (CVAAS)

Cold vapor atomic absorption spectrometry (CVAAS) is an analytical technique that measures the concentrations of mercury.

The cold-vapor technique is an atomization method limited to only the determination of mercury, due to its being only metallic element to have a large enough vapor pressure at ambient temperature. The method initiates by converting mercury into Hg (II) by oxidation from nitric or sulfuric acids, followed by a reduction of Hg (II) with $SnCl_2$ (the mechanism of reaction followed in equation 2.10). The

mercury is then swept into a long-pass absorption tube by bubbling a stream of inert gas through the reaction mixture. The concentration is determined by measuring the absorbance of this gas at 253.7 nm.

$$Hg^{2+}(aq) + Sn^{2+}(aq) \longrightarrow Hg^{0}(g) + Sn^{4+}(aq) \qquad (2.10)$$

Besides, this research was done which it was summarized and developed from many reviews as follows.

2.15 Literature reviews

The literature reviews were divided into three main parts which are reviewing about screen-printed carbon electrode modified with manganese dioxide, indirect determination of biosensor based on batch analysis and indirect determination of biosensor based on FIA.

2.15.1 Screen-printed carbon electrode modified with manganese dioxide

In 2001, Turkusic et al. [55] developed a simple biosensor by bulk-modification of carbon ink with manganese dioxide as a mediator and GOx as a biocomponent was investigated for its ability to serve as amperometric detector for glucose in hydrodynamic as well as in FIA mode. The sensor could be operated at a potential of +0.48 V versus Ag/AgCl under experimental conditions (0.1 $mol.L^{-1}$ phosphate buffer, pH 7.5) and exhibited excellent reproducibility and stability. Factors influencing the amperometric response such as injection volume, flow rate and applied working potential were studied in detail. The screen-printed electrode exhibited a linear amperometric increase with the concentration of D-glucose from 2 - 2500 $mg.L^{-1}$ and provided a 3S detection limit of 0.085 $mg.L^{-1}$. Due to its remarkable stability this sensor could be operated continuously for more than four weeks or more than 1000 sample injections. No change of signal height could be observed within an operation period of 12 h. The sensor was exploited for FIA-amperometric determination of glucose in beer and wine samples.

In 2004, Beyene et al. [67] summarized the development of sensors and biosensors based on heterogeneous carbon electrodes modified with manganese

dioxide. A comparison was made between the performances of sensors produced by film and bulk modification of carbon paste electrode and screen-printed carbon electrode and application of these electrodes as sensors for hydrogen peroxide. Modified electrodes are appreciated for their main advantages as reduction of the H_2O_2 overvoltage and hence diminishing interferences from other species by promotion of electron transfer reactions. As the results, the sensor could be operated at a potential of +0.44 to 0.48 V versus Ag/AgCl.

In 2005, Turkusic et al. [56] studied the determination of bonded glucose in different compounds, such as cellobiose, saccharose, 4-nitrophenyl-β-D-glucopyranoside, as well as in beer samples by immobilized glucose on to a screen-printed carbon electrode modified with manganese dioxide using FIA. Bonded glucose was released with glucosidase in solution, and the free glucose was detected with the modified screen-printed electrode. The release of glucose by the aid of glucosidase from cellobiose, saccharose and 4-nitrophenyl-β-D-glucopyranoside in solution showed that stoichiometric quantities of free glucose could be monitored in all three cases. The optimum conditions in FIA system were shown about flow rate of 0.2 $mL.min^{-1}$, injection volume of 0.25 mL and operation potential at +0.48 V versus Ag/AgCl. The under optimum conditions were detected of glucose in free form. As the results linear range from 11 - 13,900 $\mu mol.L^{-1}$ and the limit of detection of 1 $\mu mol.L^{-1}$ were obtained. A concentration of 100 $\mu mol.L^{-1}$ yields a relative standard deviation of approximately 7 % with five injections. These values correspond to the same concentrations of bonded glucose supposed that it is liberated quantitatively (incubation for 2 h with glucose oxidase). Bonded glucose could be determined in beer samples using the same assay. The results corresponded very well with the reference procedure.

2.15.2 Indirect determination of biosensor based on batch analysis

It is the most common recognition system in which an enzyme, either mono or multi enzyme, is immobilized in a thin layer at the transducer surface by differ immobilization techniques. This immobilized enzyme consumed substrate or analyte along with a co-substrate (if any) and yield product(s). The biosensor response is then achieved by either measuring the co-substrate consumption or product yield. This is called direct determination of analytes [47]. Alternatively, indirect

determination refers to the assessing of substance or inhibitors that specifically interact with immobilized enzyme and inhibits its biocatalytic properties. Such inhibitors bind either to the enzyme or enzyme-substrate complex and further interfere with the enzymatic reactions.

Table 2.3 summarizes the characteristics of various biosensors for heavy metal ion sensing, produced by immobilized enzymes with different kinds of transducers. For the inhibitive determination of trace mercury, a large number of enzymes have been used: urease [15, 68-71], glucose oxidase [72], herseradish peroxidase [13], alcohol oxidase [73] and glycerol 3-phosphate oxidase [74], and invertase [22]. Some studies have also focused on the analysis of different organic forms of mercury: phenyl mercury [75] using urease, methyl mercury and phenyl mercury using invertase [52].

Table 2.3 Enzyme inhibition-based biosensors for heavy metals

Inhibitors	Enzymes	Immobilization matrix	Techniques	Sample	Linear range/LOD	Nature of inhibition	Reference
Hg^{2+}, Hg^{+}, methyl mercury, mercury-glutathione complex	Herseradish peroxidase (HRP)	Entrapment in β-cyclodextrin polymer	Amperometric	-	LOD = 0.1, 0.1, 1.7 $\mu g.L^{-1}$	Reversible in less than 8 s,irreversible in 1-8 min	Han et al. [13]
Hg^{2+}	GOx	Immobilized in a polyvinylpyridine (PVP) in presence of 2-aminoethanethiol	Amperometric		1 – 100 $\mu g.L^{-1}$ LOD = 0.2 $\mu g.L^{-1}$	Reversible	Alexander and Rechnitz [14]
Hg^{2+}, Ag^{+}, Cu^{2+}, Cd^{2+}, Pb^{2+}, Cr^{3+}, Fe^{3+}, Co^{2+}, Ni^{2+}, Zn^{2+}, Mn^{2+}	GOx	Immobilized in electrosynthesized poly-o-phenylenediamine	Amperometric	-	5 - 180, 0.05 - 0.40, 10 - 100, 100 - 250, 20 - 150, 36 - 253, 55 - 400, 35 - 440	-	Guascito et al. [20]
Hg^{2+}	GOx	Cross-linked with GA	Amperometric		0.49 – 783.21 $\mu g.L^{-1}$ and 783.21 $\mu g.L^{-1}$ – 25.55 $mg.L^{-1}$	-	Liu et al. [21]
$HgCl_2$, $Hg(NO_3)_2$, Hg_2Cl_2, methyl mercury, phenyl mercury	Invertase GOx	Cross-linkage with glutaraldehyde and deposition on laponite modified electrode	Amperometric	-	I_{50} = 0.27, 0.032, 0.27, 0.34, 0.12 $mg.L^{-1}$	Irreversible	Mohammadi et al. [52]
Hg^{2+}	GOx	Cross-linking with glutaraldehyde and bovine serum albumin	Amperometric	Spiked water	2.5 – 1.2 $\mu g.L^{-1}$ LOD = 1 $\mu g.L^{-1}$	-	Mohammadi, et al. [66]

Table 2.3 Enzyme inhibition-based biosensors for heavy metals (Continued)

Inhibitors	Enzymes	Immobilization matrix	Techniques	Sample	Linear range/LOD	Nature of inhibition	Reference
Hg^{2+}, Ag^{+}, Cu^{2+}, Ni^{2+}	Urease	Immobilization in ultrabind membrane	Optical fiber biosensor	-	1 x 10^{-9} to 1 x 10^{-5} mol.L^{-1}, 1 x 10^{-8} to 1 x 10^{-5} mol.L^{-1}, 1 x 10^{-7} to 1 x 10^{-5} mol.L^{-1}, 1 x 10^{-6} to 1 x 10^{-5} mol.L^{-1}, 2 x 10^{-5} to 1 x 10^{-3} mol.L^{-1}, 2 x 10^{-5} to 1 x 10^{-3} mol.L^{-1}, 1 x 10^{-4} to 1 x 10^{-3} mol.L^{-1},	Irreversible	Kuswandi [69]
$Hg(NO_3)_2$, $HgCl_2$, $Hg_2(NO_3)_2$, phenyl mercury	Urease	Entrapment in sol-gel film	Potentiometric	Water samples	0.05 - 1.0/0.2, 0.05 - 1.0/0.2, 0.05 - 1.0/0.1, 0.1 - 5.0/0.5 µmol.L^{-1}	-	Doong and Tsai, [75]
Hg^{2+},Cu^{2+}, Cd^{2+}	Urease	Entrapment in sol-gel matrix	Optical	Tap, river water	LOD = 10 nmol.L^{-1}, 50 µmol.L^{-1}, 500 µmol.L^{-1}	-	Tsai and Doong, [76]
Hg^{2+}, Cu^{2+}	GOx	Electropolymerisation in PPD	Amperometric	-	2.5 µmol.L^{-1} to 0.2 mmol.L^{-1} 2.5 µmol.L^{-1} to 0.2 mmol.L^{-1}	Reversible	Malitesta et al. [77]
Cd^{2+}	Urease	Self-assembled monolayer	Optical (SPR)	-	0-10 mg.L^{-1} (dynamic range)	-	May May et al. [78]
Ag^{+}, Ni^{2+}, Cu^{2+}	Urease	Deposition onto electrode area and covering with 4-vinyl pyridine and Nafion	Potentiometric pH-SFET	-	LOD = 3.5 x 10^{-8}, 7 x 10^{-5}, 2 x 10^{-6} mol.L^{-1}	Irreversible	Soldatkin et al. [79]

Table 2.3 Enzyme inhibition-based biosensors for heavy metals (Continued)

Inhibitors	Enzymes	Immobilization matrix	Techniques	Sample	Linear range/LOD	Nature of inhibition	Reference
Cu^{2+}	Acetyl choline esterase	Cross-linking with glutaraldehyde vapor	Amperometric	-	0.05 – 4.0 mmol.L^{-1}	Reversible	Evtugyn et al. [80]
Chromium (VI)	GOx	Cross-linking with GA and covering with aniline membrane	Amperometric	Soil samples	0.49 μg.L^{-1} to 8.05 mg.L^{-1} LOD = 0.49 μg.L^{-1}	-	Zeng, et al. [81]
Ag^{+}, Hg^{2+}, Cu^{2+}	Urease	Immobilized into Nafion film on the surface of an ion sensitive field effect transistor (ISFET)	Ion sensitive field effect transistor (ISFET)	Fish product	I_{50} = 0.2 μmol.L^{-1}, 1.5 μmol.L^{-1}, 5 μmol.L^{-1} LOD = 0.1 μmol.L^{-1}, 1 μmol.L^{-1}, 3 μmol.L^{-1}	-	Volotovsky et al. [82]
Cd^{2+}, Cu^{2+}, Pb^{2+}, Zn^{2+}	GOx	Cross-linking with GA and BSA	Amperometric	Wine	LOD = 1 μg.L^{-1}, 6 μg.L^{-1}, 3 μg.L^{-1}	Reversible	Ghica et al. [83]
Hg^{2+}		Entrapment	Amperometric		I_{50} = 2.8×10^{-4} mol.L^{-1}	-	Cosnier et al. [84]
Hg^{2+}	GOx	Entrapment with Nafion	Amperometric		2.0 – 32.5 mg.L^{-1}mg.L^{-1} LOD = 0.5 mg.L^{-1}	-	Samphao. et al. [85]

2.15.3 Indirect determination of biosensor based on FIA

In 1999, Bertocchi et al. [86] developed an enzymatic amperometric sensor for determination of mercury (II) in pharmaceuticals, based on inhibition of invertase and glucose sensor. For immobilization of GOx, a total of 10 μL of the GOx solution was then placed onto 1 cm^2 immobilon membrane and allowed to dry at room temperature for 2 h. Unreacted sites onto the membrane were blocked by soaking with 0.1 $mol.L^{-1}$ glycine for 10 min. Before use, the membrane was washed with 1 $mol.L^{-1}$ KCl to eliminate noncovalently bound enzyme. The biosensor was assembled by placing the following membranes on the jacket provided with the electrode. The electrode was inserted into the platinum surface was contacted with the cellulose acetate membrane. Analytical parameters for measurements in batch and flow injection analysis were optimized and the results were compared with atomic absorption spectroscopy (AAS).

The amperometric procedure for determination of mercury (II) based on invertase inhibition and glucose sensor has been improved and transferred into a FIA system shown in Figure 2.25. Good sensitivity and reproducibility have been obtained in the 10 - 60 $ng.mL^{-1}$ range of mercury (II).

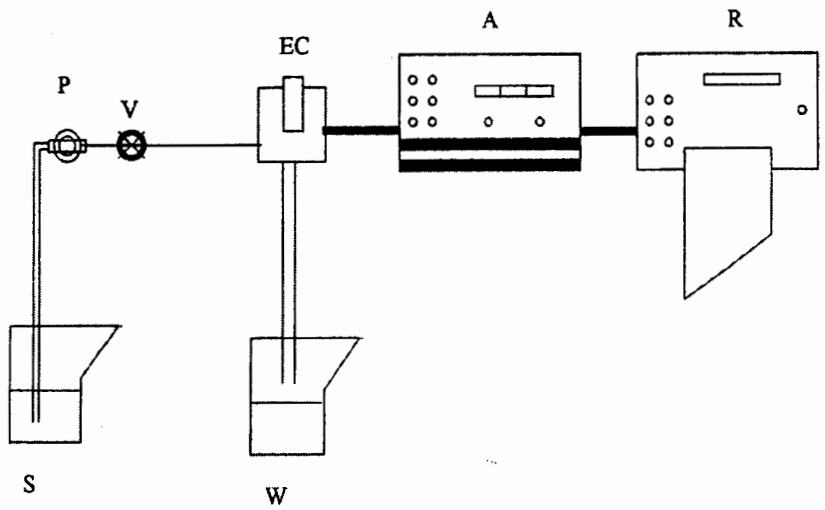

Figure 2.25 Scheme of the FIA system apparatus: A = amperometer; EC = electrochemical cell; P = peristaltic pump; R = recorder; S = sucrose; V = valve; W = waste [86]

In 2002, Jeanty et al. [87] studied a biosensor for determination of the organophosphorus pesticide (paraoxon, chlorpyrifosoxon, and malaoxon). They developed the biosensor based on inhibition of acetylcholinesterase (AChE) and amperometric detection in a FI system. The biosensor was prepared from electric eel (eeAChE) and Drosophila melanogaster (dmAChE) and immobilized on the surface of platinum electrode within a layer of poly (vinyl alcohol) bearing styrylpyridinium groups. Figure 2.26 shows signal from inhibition process of the biosensor to all pesticides.

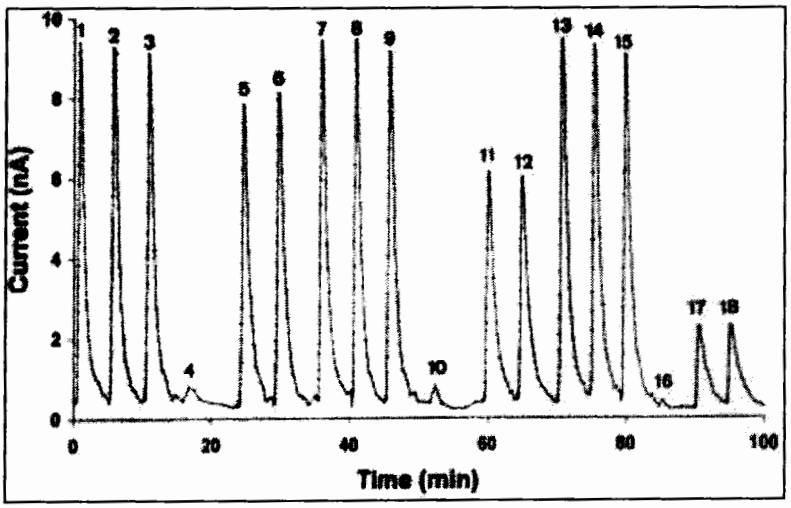

Figure 2.26 Example of flow-injection signal recorded for determination of chlorpyrifosoxon (CPO) based on inhibition of the activity of dmAChE in the biosensor used. [87]

In 2006, Liu and Lin [63] was studied a highly sensitive flow injection amperometric biosensor for organophosphate pesticides and nerve agents based on self-assembled acetylcholinesterase (AChE) on a carbon nanotube (CNT)-modified glassy carbon (GC) electrode AChE immobilized on the negatively charged CNT surface by alternatively assembling a cationic poly(diallyldimethylammonium chloride) (PDDA) layer and an AChE layer. The electrocatalytic activity of CNT leads to a greatly improved electrochemical detection of the enzymatically generated thiocholine product at low oxidation overvoltage (+150 mV), higher sensitivity, and stability. The developed PDDA/AChE/PDDA/CNT/GC biosensor integrated into a flow injection system was used to monitor organophosphate pesticides. The sensor performance, including inhibition time and regeneration conditions, was optimized with respect to operating conditions. Figure 2.27 shows the typical current versus time plot during the inhibition and regeneration process of the biosensor. Under the optimal conditions, the biosensor was used to measure as low as 0.4 $pmol.L^{-1}$ paraoxon with 6 min for inhibition time. The biosensor had excellent operational lifetime stability with no decrease in the activity of enzymes for more than 20 repeated measurements over a 1-week period. The developed biosensor system is an ideal tool for online monitoring of organophosphate pesticides and nerve agents.

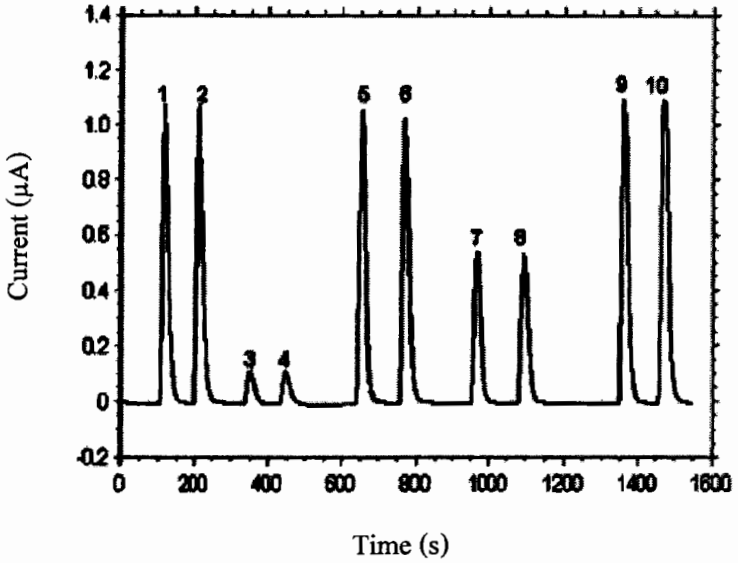

Figure 2.27 Typical amperometric responses of biosensor during the flow injection analysis of paraoxon. Note that the current versus time record was paused during the inhibition and regeneration. Flow rate, 0.25 mL.min^{-1}; working potential, 150 mV. [63]

In 2011, Marinov et al. [60] focused on the application of the flow-injection system for detection and quantification of three organophosphorus pesticides paraoxon ethyl, monocrotophos and dichlorvos in unary solutions and in binary mixtures. The flow-injection system configuration is presented in Figure 2.28. The optimal operating conditions were determined: flow rate of 0.5 mL.min^{-1}, substrate concentration of 100 μmol.L^{-1}, and incubation and reactivation time at 10 min. The sensitivity of the constructed biosensor was calculated to be 0.083 μA μmol.L^{-1} cm^{-2}. The detection limits 0.87×10^{-11} mol.L^{-1} for paraoxon, 1.08×10^{-11} mol.L^{-1} for monocrotophos and 1.22×10^{-10} mol.L^{-1} for dichlorvos. The bimolecular inhibition constants k_i were calculated by performing amperometric measurements of the residual enzyme activity after incubation for 10 min in a series of samples with varying pesticide concentrations (from 2 - 100 μmol.L^{-1}). The highest inhibition potency observed for paraoxon (2.3×10^{5} (mol.L^{-1})$^{-1}$min^{-1}), and the lowest for dichlorvos (3.5×10^{4} (mol.L^{-1})$^{-1}$min^{-1})

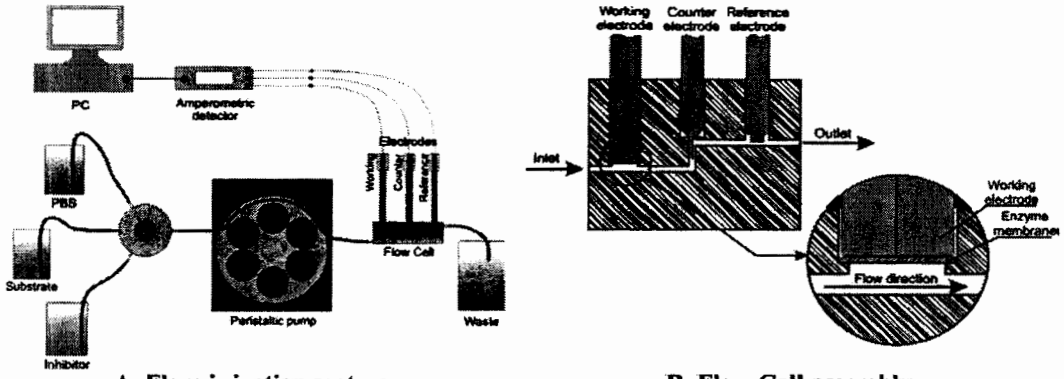

A. Flow-injection system **B. Flow Cell assembly**

Figure 2.28 (A) Flow-injection system; (B) Enzyme membrane-working electrode assembly in the flow-cell. [60]

Moreover, there are various biosensors for indirect determination of pesticides and heavy metals summarized in Table 2.4.

Table 2.4 Summary of Enzymatic biosensor based on FIA for indirect determination

Inhibitors	Enzymes	Immobilization matrix	Techniques	Sample	Linear range /LOD	Nature of inhibition	Reference
Hg^{2+}	Invertase GOx	Cross-linking with GA	Thermometric	-	5 – 80 $\mu g.L^{-1}$	-	Pirvotoiu et al. [22]
Hg^{2+}	Urease	Entrapping in polyacrylamide gel	Potentiometric	Drinking water	2 – 20 $\mu g.L^{-1}$	-	Shi et al. [23]
Hg^{2+} Cu^{2+}, V^{5+} Ni^{2+}	Glycerol 3-P, Alcohol and Sarcosine oxidase		Amperometric	Water sample	LOD = 0.05 $mg.L^{-1}$ Hg^{2+} (glycerol 3-P oxidase), = 2 $mg.L^{-1}$ Cu^{2+} and 0.5 $mg.L^{-1}$ V^{5+} (alcohol oxidase), 1 $mg.L^{-1}$ Ni^{2+} (sarcosine oxidase)	-	Compagmpone et al. [24]
Pesticide; paroxon, cabaryl	AChE	Cross-linking with GA and BSA	Amperometric	Lagoon water, kiwi fruits	1.0 x 10^{-5} $mol.L^{-1}$ 5.0 x 10^{-5} $mol.L^{-1}$	-	La Rosa et al. [62]
Organophosphorus pesticide; dichlorovos	AChE	Entrapping AChE in Al_2O_3 sol-gel matrix	Amperometric	Seawater	0.1 – 80 $\mu mol.L^{-1}$	-	Shi et al. [88]
Hg^{2+}	Glycerol 3-P oxidase	Free enzyme	Amperometric	-	0.05 – 0.5 $mg.L^{-1}$	-	Compagmpone et al. [89]

CHAPTER 3
EXPERIMENTAL

This chapter describes the instruments, equipment, chemicals and reagents used in this research. Chemical preparation, biosensor preparation, the biosensor based flow injection set-up and the measurement procedure were clearly explained a step by step. In addition, sample preparation was described before measuring mercury by the proposed biosensor. Cold vapor atomic absorption spectroscopy was presented in the last section as the reference method.

3.1 Instruments

All instruments shown in Table 3.1 and equipment presented in Table 3.2 were used for this research.

Table 3.1 Instruments for the experiment

Instrument	Model	Company
Atomic absorption spectrophotometer (AAS) Data system	Perkin Elmer® PinAAcle™ 900T WinLab32™ for AA software	Perkin (Shelton, CT, USA)
Microwave digestion	DISCOVER SP-D (CEM)	Thaiunique, THAILAND
Potentiostat/galvanostat	AUTOLAB	Methrohm (PGSTAT12)
Scanning electron microscope	JSM 5410-LV	JEOL

Table 3.2 Equipment

Equipment	Model	Company
Auxiliary electrode	Platinum wire	CH-Instrument, USA
Electrochemical flow cell	-	BASi instrument, USA
Hot plate	-	VELP SCIENTIFICA
Injection port	Injection loop	Rheodyne, USA
Peristaltic pump	Peristaltic pump	Ismatec, Switzerland
pH meter	PCS Testr 35	-
Reference electrode	Ag/AgCl electrode	BASi instrument, USA
Ultrasonic bath	CP360D	Crest ultrasonics
Vortex mixer	Vortex ginie-2 G 560E	Labnet
Working electrode	Screen printed carbon electrode modified with 5 % (m) MnO_2	-

3.2 Chemicals and reagents

Chemicals and reagents were purchased from various companies as shown in Table 3.3.

Table 3.3 List of chemicals and reagents, formula, grade and their suppliers

Chemicals and reagents	Formula	Grade	Company
Ammonium hydroxide	NH_4OH	AR grade	
Cadmium standard solution	Cd (II)	Spectro grade	SCP science
Chromium standard solution	Cr (II)	Spectro grade	SCP science
Copper standard solution	Cu (II)	Spectro grade	SCP science

Table 3.3 List of chemicals and reagents, formula, grade, and their suppliers (Continued)

Chemicals and reagents	Formula	Grade	Company
Disodium hydrogen phosphate heptahydrate	$Na_2HPO_4.7H_2O$	AR grade	Carlo Erba
Enzyme glucose oxidase	-	AR grade	Sigma Aldrich
Ethylenediaminetetraaceticacid disodium salt dihydrate (EDTA)	$C_{10}H_{14}N_2Na_2O_8.2H_2O$	AR grade	Fluka
Glucose	$C_6H_{12}O_6$	-	-
Hydrochloric acid	HCl	37.0	Carlo Erba
Hydrogen peroxide	H_2O_2	30.0	Sigma Aldrich
Iron standard solution	Fe (III)	Spectro grade	SCP science
Lead standard solution	Pb (II)	Spectro grade	SCP science
Manganese standard solution	Mn (II)	Spectro grade	SCP science
Mercury standard solution	Hg (II)	Spectro grade	SCP science
Mineral oil	-	AR grade	Acros
Monosodium dihydrogenphosphatemonohydrate	$NaH_2PO_4.H_2O$	AR grade	Carlo Erba
Nafion		AR grade	Fluka
Nitric acid	HNO_3	AR grade	Carlo Erba
Sodium hydroxide	NaOH	AR grade	SCP science
Potassiumchromate	K_2CrO_4	AR grade	SCP science
Potassium permanganate Stannous chloride dihydrate	$KMnO_4$ $SnCl_2.2H_2O$	AR grade AR grade	Carlo Erba J.T. Baker
Zinc standard solution	Zn (II)	Spectro grade	SCP science

3.3 Chemical preparation

3.3.1 Glucose oxidase solution

100 $mg.mL^{-1}$ glucose oxidase solution was prepared by 0.1xxx g of glucose oxidase powder (250 KUg^{-1}) dissolved in 1 mL of deionized water (DI water). The solution was shaken by a vortex mixer for 5 min and then kept under 4 °C in a refrigerator before use.

3.3.2 0.1mol.L^{-1}ammonium hydroxide solution

310 µL of 25% NH_4OH was diluted and adjusted with DI water into 20 mL volumetric flask.

3.3.3 Neutralized Nafion solution

The Nafion solution was neutralized to pH 7-8 by dropping a small amount of 0.1 $mol.L^{-1}$ NH_4OH (section 3.3.2) into the solution and pH solution was checked by pH paper test.

3.3.4 Glucose oxidase stock solution

Glucose oxidase stock solution was prepared by mixing 40 µL of 0.1 $mg.mL^{-1}$ GOx (section 3.3.1) with 10 µL of neutralized Nafion solution (section 3.3.2) and 50 µL of DI water. The solution was mixed using vortex mixer and then kept at 4 °C in refrigerator before used.

3.3.5 0.1 mol.L^{-1} disodium hydrogen phosphate solution

13.4xxx g of disodium hydrogen phosphate heptahydrate was dissolved and diluted with DI water into 500 mL volumetric flask.

3.3.6 0.1 mol.L^{-1} monosodium hydrogen phosphate solution

6.9xxx g of monosodium dihydrogen phosphate monohydrate was dissolved and diluted with DI water into 500 mL volumetric flask.

3.3.7 1 mol.L^{-1}sodium hydroxide solution

1.xxx g of sodium hydroxide was dissolved and diluted with DI water into 25 mL volumetric flask.

3.3.8 1 mol.L^{-1}hydrochloric acid solution

2.00 mL of 37 % HCl acid was diluted with DI water to 25 mL volumetric flask.

3.3.9 0.1 mol.L^{-1}phosphate buffer solution at pH 7.0

The phosphate buffer pH 7.0 was prepared by mixing 61 mL of 0.1mol.L^{-1} Na_2HPO_4 (section 3.3.5) and 39 mL of 0.1 mol.L^{-1}NaH_2PO_4 (section 3.3.6) and then adjusted to pH 7.0 by addition of a small amount of 1 mol.L^{-1} NaOH or 1 mol.L^{-1} HCl.

3.3.10 1000 mg.L^{-1} hydrogen peroxide solution

83 µL of 30 % (w/v) hydrogen peroxide was diluted with DI water into 25 mL volumetric flask.

3.3.11 Glucose standard solution

100 mL of 1 % (w/v) standard solution of glucose was prepared by dissolving 1.00xx g of glucose powder in phosphate buffer solution at pH 7.0 and left overnight at room temperature, and then always stored at 4 °C in refrigerator before used

3.3.12 10 mg.L^{-1} of mercury (II) ion standard solution

100 µL of 1000 mg.L^{-1} standard mercury solution and diluted with phosphate buffer solution (section 3.3.9) into 10 mL volumetric flask.

3.3.13 0.05 mol.L^{-1}Ethylenediaminetetraacetic acid(EDTA)

0.81xx g of ethylenediaminetetraacetic acid disodium salt dehydrate was dissolved and diluted with 0.1 mol.L^{-1} phosphate buffer solution at pH 7.0 into 50 mL volumetric flask.

3.3.14 Interference solutions

10 mg.L^{-1} cadmium (II), chromium (III), copper (II), iron (III), lead (II), manganese (II) and zinc (II) solutions were prepared in the phosphate buffer pH 7.0

3.3.15 5% (w/v) potassium permanganate solution

1.25xx g of potassium permanganate was dissolved and adjusted with DI water into 25 mL volumetric flask.

3.3.16 20 mg.L^{-1} potassium chromate solution

0.002x g of potassium chromate powder was dissolved and adjusted with the phosphate buffer into 250 mL volumetric flask.

3.3.17 3.0 % (v/v) hydrochloric acid solution

81 mL of 37 % hydrochloric acid was diluted with DI water into 1000 mL volumetric flask.

3.3.18 1.1 % (w/v) stannous chloride solution

1.1 % (w/v) stannous chloride was prepared by dissolving 11.xxxx g of stannous chloride dehydrate powder in 3.0 % (v/v) hydrochloric acid into 1000 mL volumetric flask

3.4 Biosensor preparation

To make enzyme-casting solutions, required volumes of 40 µL of glucose oxidase solution (section 3.3.1) with 10 µL neutralized nafion (section 3.3.3) and 50 µL DI water were mixed, in the order listed, in a plastic vial (1.5 mL microcentifuge tubes).

To make the screen-printed carbon electrode modified with 5 % (m) manganese dioxide (MnO_2/SPCE) immobilized with glucose oxidase, 10 µL of casting solution was drop-coated on a 3.3 (±0.2) mm by 15.0 (±0.2) mm portion of the SPCE's electroactive surface was prepared. The GOx/MnO_2/SPCE was consequently dried at room temperature. The resulting biosensor was either immediately loaded into a flow cell or stored for later use at 4 °C as indicated.

To set-up electrochemical flow cell was assembled, a thin-layer (0.1905 mm) electrochemical flow cell (Part # MF-1087, BASi) and the exploded view of which are shown in Figure 3.1 was used. An Ag/AgCl electrode (3 M KCl, BAsi RE-4, Part # MF-2021) served as the reference electrode (RE). The counter electrode (CE) was the stainless steel back-plate (auxiliary electrode block) of the cell. For screen printed electrode, a 1×4×0.635 cm working electrode (WE) was fixed into a lab made rectangular-slotted PTFE block which makes part of the flow cell by a simple locking mechanism. The WE was separated from the CE by a 0.1905 nm thick polyester gasket with an oval opening to expose about 49.5 (±3.1) mm^2 electroactive surface of the WE.

3.5 Flow injection analysis system

The FIA system cosisted of a peristaltic pump (Ismatec, Switzerland), a six port injection valve with the flow through electrochemical cell as mention above. The apparatus scheme of FIA measurement is shown in Figure 3.2 and appendix A.1.

For all electrochemical measurements a computer-controlled electrochemical workstation (AUTOLAB, PGSTAT12, Metrohm) was used in combination with a corresponding software (GPES).

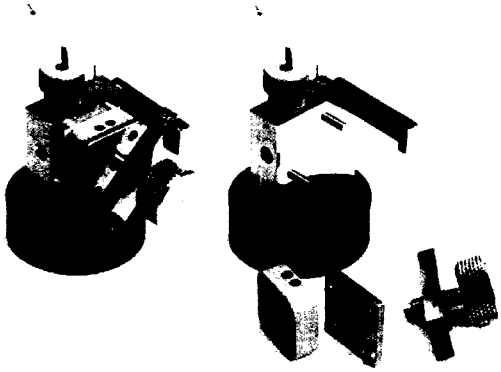

Figure 3.1 Electrochemical flow cells [90]

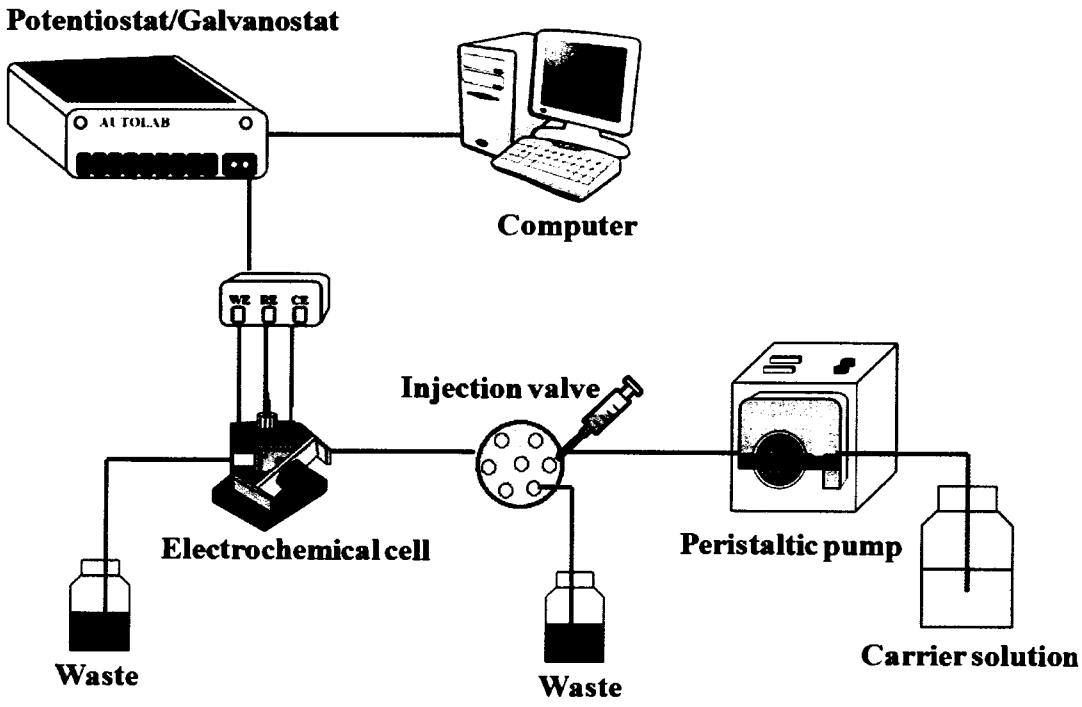

Figure 3.2 Flow injection analysis system

3.6 Measurement procedure

3.6.1 Electrocatalytic reaction of SPCE and MnO_2/SPCE by the cyclic voltammetry

The unique electrochemical behavior of bare SPCE, MnO_2/SPCE and GOx/MnO_2/SPCE was studied measuring by the potentiostat connected with three electrodes (modified electrodes as working electrode, Ag/AgCl as a reference electrode and Pt wire as an auxiliary electrode as mention). Both electrodes were catalytically studied to hydrogen peroxide as electro active substance model and glucose solution. They were working under optimal conditions; 0.1 $mol.L^{-1}$ phosphate buffer solution of pH 7.0 at scan rate of 25 $mV.s^{-1}$. The potential range was -0.90 to +0.90 V versus Ag/AgCl. The cyclic voltammograms are presented and discussed in the section 4.1.

3.6.2 Parameters affecting on the responses of the GOx/MnO_2/SPCE

The parameters at which the measurements based on FIA were carried out are also a critical factor in determining activity of the enzyme electrode such as operating potential, pH solution, immobilized enzyme loading and glucose loading to obtain optimum condition before its inhibition study. The parameters were studied as follows.

3.6.2.1 Operating potential

The operating potentials were varied in the range of 0.4 - 0.5 V versus Ag/AgCl. A 200 $mg.L^{-1}$ glucose standard solution was injected into the phosphate buffer as a carrier solution with conditions fixed at injection volume of 250 µL and flow rate of 1.2 $mL.min^{-1}$. The current peaks were measured by chronoamperometric detector and are shown in section 4.2.1 and appendix B.1.1.

3.6.2.2 pH buffer solution

The effect of the pH solution on the performance of the GOx/MnO_2/SPCE was studied by varying the pH in the range of 5.0 - 8.0. The experimental was done by operating potential of +0.46 V versus Ag/AgCl, injection volume of 250 µL and flow rate of 1.2 $mL.min^{-1}$. 200 $mg.L^{-1}$ glucose standard solutions were injected into the carrier stream in various pH solutions. The results are presented in section 4.2.2 and appendix B.1.2.

3.6.2.3 Enzyme loading

In order to determine the optimum unit of GOx immobilized on the electrode surface for the best response, different units of GOx were studied. Various enzyme amounts of 40, 80, 120 and 160 $U.cm^{-2}$ were drop-coated on MnO_2/SPCEs. The measurement was done by injecting 200 $mg.L^{-1}$ glucose solutions into the carrier stream (phosphate buffer pH 7.0) flowing through various GOx/MnO_2/SPCEs. The experimental conditions were done as follows: operating potential of +0.46 V versus Ag/AgCl, injection volume of 250 µL and flow rate of 1.2 $mL.min^{-1}$. The obtained peak currents versus amount of enzyme units are presented in section 4.2.3 and appendix B.1.3.

3.6.2.4 Glucose loading

The concentration of substrate (glucose) of GOx was studied to obtain adequate enzymatic inhibition. To optimize glucose loading different concentrations of glucose was used; 50, 100, 200, 400, 600, 800 and 1000 $mg.L^{-1}$ dissolved in phosphate buffer solution at pH 7.0. The measurement was done under optimal conditions. The experimental was studied by injecting 500 $mg.L^{-1}$ mercury in various glucose concentrations into the carrier stream (phosphate buffer pH 7.0) flowing through GOx/MnO_2/SPCE. Peak heights versus amount of glucose concentrations are presented in the section 4.2.4 and appendix B.1.4.

3.6.3 Optimization of the flow injection analysis method

In this study, the parameters of flow injection analysis were experimentally investigated in the case of inhibition degree of glucose oxidase such as injection volume and flow rate.

3.6.3.1 Injection volume

The effect of injection volume on the inhibitory of GOx/MnO_2/SPCE was studied with the volume varied at 20, 50, 100, 250 and 500 µL. The relations between inhibition degree and the injection volume were illustrated in FIA system using chronoamperometric detector with operating potential at +0.46 V versus Ag/AgCl, supporting electrolyte 0.1 $mol.L^{-1}$ phosphate buffer solution at pH 7.0, substrate concentration of 200 $mg.L^{-1}$ glucose, GOx loading of 80 $U.cm^{-2}$ and

inhibitor concentration of 500 $\mu g.L^{-1}$mercury. The results are shown in section 4.3.1 and appendix B.1.5.

3.6.3.2 Flow rate

The effect of flow rate on the inhibition of the GOx/MnO_2/SPCE biosensor was investigated in the flow rate at 0.6, 0.8. 1.0, 1.2, 1.4 and 1.6 $mL.min^{-1}$. The relations between inhibition degree and the flow rate were illustrated in FIA system with injection volume of 250 µL using chronoamperometric detector, and done under optimum condition as in section 3.6.3.1. The results are shown in section 4.3.2 and appendix B.1.6.

3.6.4 Inhibition study

Mercury (II) ion is the target ion of the inhibitory of GOx/MnO_2/SPCE and was determined as the inhibitor. The experiments were conducted in two steps. In first, substrate (200 $mg.L^{-1}$ glucose solution) was injected into the carrier stream (phosphate buffer) in FIA system and done under optimum conditions. The current occurred corresponding to H_2O_2 oxidation was measured as I_0. In second step, mercury in glucose solution was injected into the phosphate buffer with the same measurement in which the mercury and enzyme were interacted. The reduction of current (I) was measured. Under inhibition effect of mercuric ion, the current after inhibition is smaller than the current (I_0). Percentage inhibition is calculated and given by the equation 2.14 (section 2.13). In preliminary inhibitory process, three concentrations of mercuric ions (100, 500 and 1000 $\mu g.L^{-1}$ mercury) were studied. The result is shown in section 4.4.

3.6.5 Analytical figures of merit

3.6.5.1 Linear range of mercury

Linear range of mercuric ion was determined for inhibition of GOx/MnO_2/SPCE. The inhibitory effect of various concentrations of mercury on designed biosensor was tested at 100, 200, 300, 400, 500, 600, 700, 800, 900, 1000, 1500 and 2000 $\mu g.L^{-1}$, with the three replicate injections. The FIA system was set as under optimal conditions. For the experimental, 200 $mg.L^{-1}$ glucose was injected into FIA system and current signals were recorded as I_0. Then mercury solutions at

different concentrations were injected into FIA system and the current signal was recorded as I. After that, I_o and I were used for calculation of percentage inhibition (% inhibition) of GOx/MnO_2/SPCE. Finally, % inhibition was plotted versus different mercury concentrations. The results are presented in section 4.5.1 and appendix B.2.2.

3.6.5.2 Limit of detection (LOD)

The LOD was calculated on the basis of 3 SD/b where SD is standard deviation of inhibition degree at lowest concentration of calibration curve (100 $\mu g.L^{-1}$ mercury) and b is the slope of the calibration curve (0.0407 $\%.L.\mu g^{-1}$) illustrated in Figure 4.11(b). The result is shown in the section 4.5.2 and appendix B.2.3.

3.6.5.3 Limit of quantification (LOQ)

The LOQ was calculated on the basis of 10 SD/b where SD is standard deviation of inhibition degree at lowest concentration of calibration curve (100 $\mu g.L^{-1}$) and b is the slope of the calibration curve (0.0407 $\%.L.\mu g^{-1}$) illustrated in Figure 4.11(b). The result is shown in the section 4.5.3 and appendix B.2.4.

3.6.5.4 Repeatability

The repeatability of the GOx/MnO_2/SPCE was evaluated by measuring the inhibition degree of GOx/MnO_2/SPCE to 100 $\mu g.L^{-1}$ mercury (the lowest concentration) with ten replicated injections (n = 10) working under the optimal condition. The results are presented in section 4.5.4 and appendix B.2.5.

3.6.5.5 Reproducibility

The reproducibility of GOx/MnO_2/SPCE was evaluated by measuring the inhibition degree of GOx/MnO_2/SPCE to 100 $\mu g.L^{-1}$ mercury with three independent electrodes (n = 3). Precision of GOx/MnO_2/SPCE (three electrodes) was determined by using % RSD. The results are presented in section 4.5.5.

3.6.5.6 Regeneration

To perform multiple measurements with the same electrode, the regeneration of the GOx/MnO_2/SPCE was studied. The GOx/MnO_2/SPCE can be regenerated after inhibition by EDTA solution. The effect of EDTA at various concentrations of 0.025, 0.050, 0.075 and 0.100 $mol.L^{-1}$ were determined.

The procedure of regeneration was set as under optimal conditions. The first step, three injects of 200 $mg.L^{-1}$ glucose were injected into FIA system and current signals were recorded as I_0. Second, three injects of 1 $mg.L^{-1}$ mercury (diluted with 200 $mg.L^{-1}$ glucose solution) were injected into FIA system and current signals were recorded as I_1 (current after inhibition). Third, EDTA solution was replaced as carrier solution for 1 min. Then, three injects of 200 $mg.L^{-1}$ glucose were injected into FIA system again and current signals were recorded as I_2. Percentage regeneration (% regeneration) was calculated and is presented in section 4.5.6 and appendix B.2.6.

3.6.5.7 Stability

The stability of the GOx/MnO_2/SPCE for storage in three weeks has been investigated after the electrodes were kept in dried conditions at 4 °C in a refrigerator. The currents were measured from the beginning, 1, 2, 3, 4, 5, 6, 7, 8, 9, 10, 11, 12, 13, 14 and 21 days.

The measurement was carried out under optimal conditions. At the beginning, three injects of 200 $mg.L^{-1}$ glucose solution were injected into FIA system and current signals were recorded as C_0 (initial current). The same electrode was kept at 4 °C in a refrigerator. The next day, the electrode was investigated under the same condition and current measurement defined as C_1. C_0 and C_1 were calculated for the relative current. The results are presented in section 4.5.7 and appendix B.3.

3.6.5.8 Interferences

In this study, many heavy metals were estimated on their possible interfering effect on the determination of mercury under the same experimental conditions. The effect of other heavy metals on GOx/MnO_2/SPCE was studied; 100 $mg.L^{-1}$ heavy metals; (Fe (III), Cr (VI), Cr (III), Mn (II), Zn (II), Pb (II), Cd (II) and Cu (II)) mixed with 0.1 $mg.L^{-1}$ mercury were measured in ratio 1:100 (Hg (II) ion : interfering ion.

The measurement was carried out based on the optimum conditions. At first, 200 $mg.L^{-1}$ glucose solution was injected into FIA system and current signals were recorded as I_0 (initial current). Continuously, 100 $\mu g.L^{-1}$ mercury mixed with each metal ion of 10 $mg.L^{-1}$ (diluted and adjusted with 200 $mg.L^{-1}$ glucose solution) was injected into FIA system and the current response was recorded as I (current after

inhibition). I_0 and I were calculated as % inhibition. The results are shown in section 4.5.8 and appendix B.4.

3.6.6 Enzyme kinetics

3.6.6.1 Kinetic catalytic reaction of GOx

The enzyme-substrate kinetics of the biosensor was evaluated by study the catalytic reaction of GOx to glucose substrate. The oxidation current responses in various concentrations of glucose solution catalyzed by GOx were measured under the optimal conditions.

The measurement was done under the carrier flow through and background current was measured. After the background current reached stable, glucose solutions (0.2 - 20.0 $mmol.L^{-1}$) were injected into the carrier phosphate solution and the current was recorded continuously. The results are presented in section 4.6.1 and appendix B.5.

3.6.6.2 Catalytic inhibition of GOx

The inhibitory effect of mercury (II) on the GOx activity conditions to describe catalytic inhibitor type using direct Michealis-Menten and double-reciprocal plot Lineweaver-Burk was studied.

The experimental was done and measured under optimal conditions by injecting 1 $mg.L^{-1}$ mercury into the carrier flow. Afterwards, different glucose concentrations (0.2 - 20.0 $mg.L^{-1}$) were injected systematically. The oxidation current responses catalyzed by GOx were measured and plotted by Michealis-Menten and double-reciprocal plot Lineweaver-Burk. The results are presented in section 4.6.2 and appendix B.5.

3.6.7 Characterization by scanning electron microscope (SEM)

The morphology of MnO_2/SPCE and GOx/MnO_2/SPCE surface was studied by scanning electron microscopy (JSM 5410-LV, JEOL). Samples (MnO_2/SPCE and GOx/MnO_2/SPCE) were slashed from surface of alumina support. Afterward, samples were attached on aluminum stubs that had a small amount of glue on it and then sputter coated with gold and operated in the SEM. The accelerating voltage and magnification for all the images were 20 kV and 5000x, respectively. The results are presented in section 4.7.

3.7 Application of the biosensor to determination of mercury in samples

The different types of sample were studied; shrimps and mackerels obtained from a local market, Warin chamrab district at Ubon Ratchathani province, a dogfish muscle certified reference material for trace metals (DORM-2) from National Research Council of Canada, natural water sampling from a local reservoir at Ubon Ratchatani university campus and spiked samples were carried out.

3.7.1 Sample preparation

Fresh samples (shrimps and mackerels) should be homogeneous and dried in an oven at 100 °C until they reach a constant weight. After drying, portions of approximately 1.xxxx g were weighed for digestion.

Blank and samples were digested by a microwave digester operated with conditions shown in Table 3.4. All samples were put into suitable vessels with continually adding 5 mL conc. HNO_3 and 5 mL of DI water. The vessels were left for at least 10 min without their lids. Afterwards, all vessels were transferred into a microwave digestion system. After digestion and cooling, all digested samples were made up to 10 mL in volumetric flasks; and then, neutralized samples by NaOH to pH 7.0 before measurement by the proposed method and CVAAS were needed.

For the spiked samples, 10 µL of 1000 $mg.L^{-1}$ mercury standard solution were added to the natural water, shrimps and mackerel samples; and made up the final 5 mL volume with DI water. These spikes provided a concentration of 2 $mg.L^{-1}$ mercury.

Table 3.4 Microwave digestion program used

Temp (°C)	Ramp Time (min)	Hold Time (min)	Pressure (PSI)	Power (W)	Stirring
200	04:00	02:00	200	250	Medium

3.7.2 Analysis in real samples

3.7.2.1 Proposed biosensor based on FIA

The determination of mercury in real samples by GOx/MnO_2/SPCE was done by a standard addition method. The 100, 200, 300 and 400 $\mu g.L^{-1}$ mercury concentrations in 200 $mg.L^{-1}$ of glucose solution were prepared as shown in Table 3.5.

Table 3.5 Volumes of stock standard and other reagents needed to prepare a range of standard addition method

	Standard addition solution				
	0	1	2	3	4
Final concentration of mercury ($\mu g.L^{-1}$)	-	100	200	300	400
Volume of sample (mL)	1.00	1.00	1.00	1.00	1.00
Volume of 10000 $mg.L^{-1}$ glucose (mL)	0.10	0.10	0.10	0.10	0.10
Total volume (mL)	5.00	5.00	5.00	5.00	5.00

For the experimental, the FIA system was set as under the optimal conditions. At first, 200 $mg.L^{-1}$ glucose solution was injected into FIA system and obtained current signal was recorded as I_0. The second, solutions of standards explained in Table 3.5 were injected into the flow system, respectively. The current signals were recorded as I (at various concentrations, 100 - 400 $\mu g.L^{-1}$ mercury). Afterwards, % inhibition was calculated and plotted versus mercury concentrations as the standard addition graph. The results are presented in section 4.8.

3.7.2.2 Cold vapor atomic absorption spectroscopy

Standards were prepared in the working range of 0.5 - 10 $\mu g,L^{-1}$ mercury. Mercury was determined using 1.1% (w/v) $SnCl_2$ and its atomization was in a quartz cell heated at 100 °C for mercury vapor analysis. The carrier solution was 3% (v/v) HCl acid.

Using a FIAS-AAS system with working step shown in Table 3.6, the measurement was done by injecting standard (500 µL) into the carrier solution stepwise was transferred into the quartz cell placed in a heating mantle with adaptor in the place of the burner of AAS. The mercury was decomposed and atomized which its

absorbance was systematically recorded. All samples were studied as the same condition as standard solution done. The results are presented in section 4.8 and appendix B-6.

Table 3.6 FIAS pump and valve timing [92]

Step	Time	Pump 1 (rpm)	Pump 2 (rpm)	Valve position		Read trigger
				Fill	Inject	
Prefill	15	100	120	X		
1	10	100	120	X		
2	15	0	120		X	X
3	1	100	120	X		

Where X is not fill

CHAPTER 4
RESULTS AND DISCUSSION

In this research we studied the development and application of a biosensor for the determination of mercury based on enzyme inhibition process which is indirect method. The biosensor was fabricated by glucose oxidase (GOx) in nafion solution immobilized on screen printed carbon electrode (SPCE) modified with 5% (m) manganese dioxide (MnO_2/SPCE) assembled with an electrochemical cell as a detector based on flow injection analysis (FIA).

The chapter reports the work divided into 4 parts, the first part presents about characterization of the GOx/MnO_2/SPCE as the biosensor by electrochemical methods. Continually, the second one focused on how to assemble GOx/MnO_2/SPCE to FIA system. Additionally, parameters affecting the measurement such as operating potential, pH buffer solution, substrate concentration, injection volume and flow rate are presented. The third section explains investigation and validation of GOx/MnO_2/SPCE based on FIA for detecting of mercury explained in terms of linear range, limit of detection, limit of quantification, repeatability, reproducibility, regeneration, interferences, stability and accuracy. Accordingly, enzyme kinetics and catalytic inhibition are essentially presented. Afterwards, surface morphologies of GOx/MnO_2/SPCE are investigated. Continually, applications of GOx/MnO_2/SPCE based on FIA to detect mercury in certified reference material (DORM-2), real samples, and spiked samples are presented. All results are compared with cold vapor atomic absorption spectrophotometry (CVAAS) as a reference method in the last part.

4.1 Characterization of GOx/MnO_2/SPCE by cyclic voltammetry

To confirm manganese dioxide improving electrode sensitivity the electrochemical behavior of bare SPCE and MnO_2/SPCE was investigated and their cyclic voltammograms were recorded in 0.1 mol.L^{-1} phosphate buffer solution of pH

7.0 at a scan rate of 25 $mV.s^{-1}$. The potential range was -0.90 to +0.90 V versus Ag/AgCl [56, 67], also the response of modified SPCE compared to the bare SPCE voltammograms depicted in Figure 4.1.

As the results, there is no Faradaic peak for bare SPCE in the potential range studied. It is observed that a sluggish electron transfer reaction may occur. Compared to modified MnO_2 on SPCE, there are anodic peak current from hydrogen peroxide starting at +0.4 V. Turkusic et al. [56] and Beyene et al. [67] reported that MnO_2 modified carbon electrodes can reduce the H_2O_2 overvoltage and hence diminishing the interference from other species by promotion of electron transfer reactions. Thus, we conclude that MnO_2 acts as electron transfer as explained in section 2.10.

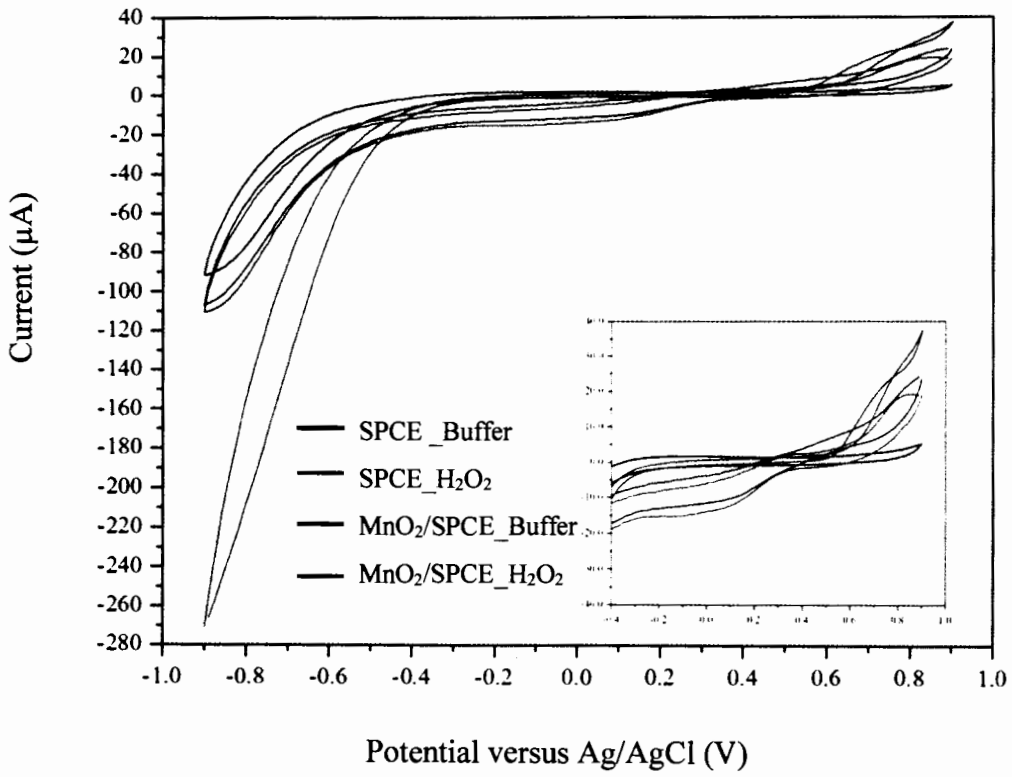

Figure 4.1 Cyclic voltammograms of SPCE and MnO_2/SPCE. Black line is background of SPCE and green line is the presence of 100 $mg.L^{-1}$ H_2O_2. Red line is background of modified MnO_2/SPCE and blue line is the presence of 100 $mg.L^{-1}$ H_2O_2.

Moreover, to investigate the sensitivity of MnO_2/SPCE immobilized with glucose oxidase, cyclic voltammograms of the electrode was shown in Figure 4.2. The results showed that there is anodic peak that occurs in the potential range studied. It proved that glucose is enzymatically oxidized with molecular oxygen forming gluconolactone and H_2O_2. Therefore, there is MnO_2 electron transfer stating at potential of +0.4 V. Moreover, Turkusic et al. [55] reported a biosensor for determination of glucose. MnO_2 and GOx bulk modified screen printed carbon ink was used. The suitable applied potential for determination of glucose was at +0.48 V versus Ag/AgCl.

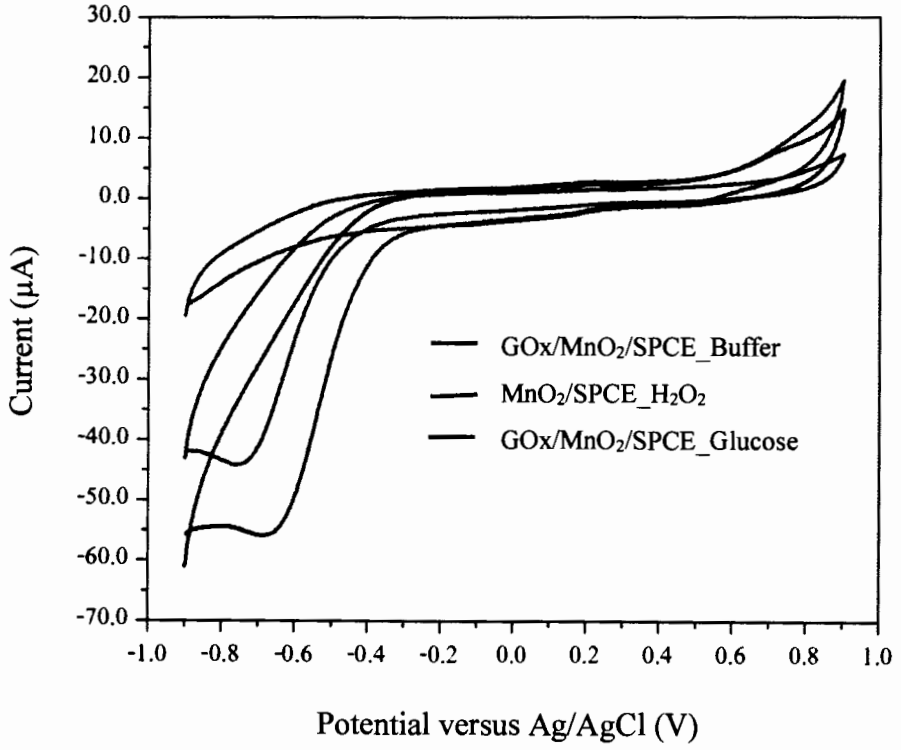

Figure 4.2 Cyclic voltammograms of GOx/MnO_2/SPCE were measured in a 0.1 mol.L^{-1}phosphate buffer solution at pH 7.0 as supporting electrolyte (green line), 100 mg.L^{-1} H_2O_2 (blue line) and 100 mg.L^{-1} glucose (red line) under conditions of potential applied from -0.9 to +0.9 V versus Ag/AgCl with scan rate 25 mV.s^{-1}.

As the results, the oxidation of glucose was measured using GOx/MnO_2/SPCE at applied potential about +0.4 V versus Ag/AgCl. Before applying GOx/MnO_2/SPCE to

detect mercury by inhibition process, parameters affecting on the responses of the GOx/MnO_2/SPCE were essentially studied in the next section.

4.2 Parameters effecting on the responses of the GOx/MnO_2/SPCE

The parameters at which the measurements are carried out are also a critical factor to determine the activity of the enzyme electrode. These parameters effecting on the response of the enzyme electrode are operating potential, pH of solution, enzyme loading and glucose loading.

4.2.1 Operating potential

The effect of potential applied at the electrode was investigated. All studied potentials from +0.40 to +0.50 V versus Ag/AgCl [85, 93-94] were optimized by inject of 200 $mg.L^{-1}$ glucose solution into the carrier solution and the current signals were obtained at various potential studied (the experimental in section 3.6.2.1). The results showed the dependence of current (μA) versus the potential applied displayed in Figure 4.3 and appendix B.1.1. The electrode showed high current responses with potential higher than +0.40 up to +0.46 V, then the signal was off. Similar result to Schachl et al. [93] that they fabricated a carbon paste electrode bulk modified with MnO_2 as an amperometric detector for determination of H_2O_2 in FIA that operating potential of +0.46 V versus Ag/AgCl was obviously obtained. Moreover, they developed a carbon thick film electrode modified with an MnO_2 film for determination of H_2O_2 in FIA that applied potential was used at +0.48 V versus Ag/AgCl[94]. In 2011, Samphao et al. [85] developed an amperometric biosensor for indirect determination of mercury by inhibition of GOx immobilized on a carbon paste electrode bulk modified with MnO_2 that operating potential was chosen at +0.46 V versus Ag/AgCl. Therefore, operating potential of +0.46 V was taken for further studies.

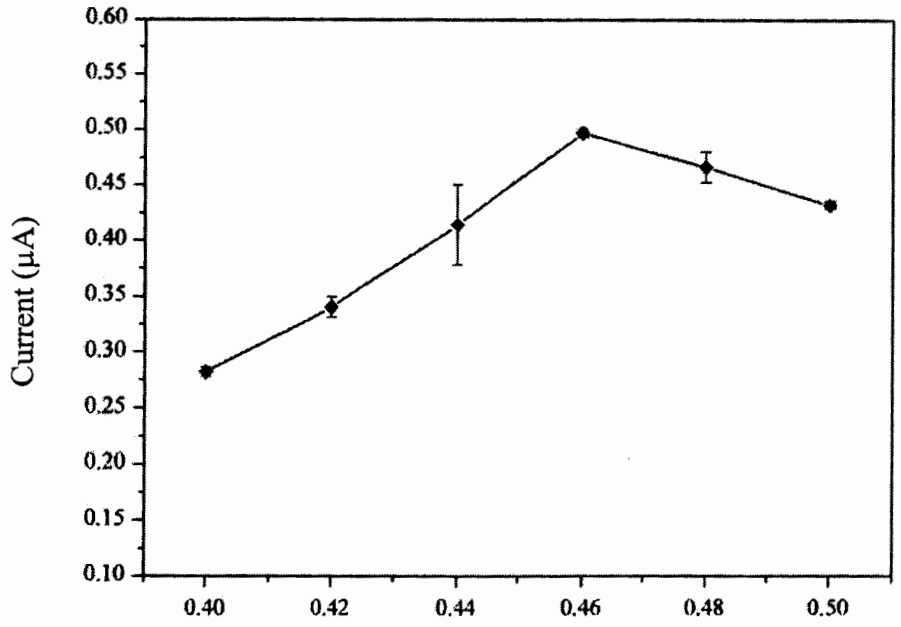

Figure 4.3 Effect of operating potential on the amperometric response of GOx/MnO_2/SPCE

4.2.2 pH buffer solution

An optimum pH range is vital to the sensitivity of enzyme biosensor as it influences both the bioactivity of the enzyme and electrochemical behavior of MnO_2. It has been reported that extreme pH may possibly modify the kinetics of measurements as a result of disturbing the redox state of the enzyme reaction. The effect of pH on the biosensor response was investigated in the range of 5.0 - 8.0 (section 3.6.2.2) and the results are shown in Figure 4.4 and appendix B.1.2.

As the results show, it can be deduced that the electrode exhibited an optimum response at pH 7.0 over the experiment pH range of 5.0 - 8.0 in 0.1 $mol.L^{-1}$ phosphate buffer solutions. It can also be noted that electrochemical response of the electrode was very poor when exposed to strong acidic or alkaline environment. This is because high acidity and strong alkalinity causes a decrease in GOx activity. Moreover, the pH solution depended on the chemical reaction to MnO_2. The electrochemical reconversion of modifier was dependent on the hydronium ion which shows the effect of hydronium ion in equation 4.1 and 4.2.

$$MnOOH \longrightarrow MnO_2 + H^+ + e^- \quad (4.1)$$

$$MnO + H_2O \longrightarrow MnO_2 + 2H^+ + 2e^- \quad (4.2)$$

The pH optimum found in this work is in accordance with previous investigations where a glucose electrode was used. Bankar et al. [43] reviewed most of the strains used commercially for the productions of GOx at an optimum pH 6.0 - 7.0 for growth and enzyme production. Chey et al. [95] developed potentiometric glucose biosensor based on immobilization of GOx on ZnOnanorods for indirect determination of mercuric ion that they have reported the highest activity of the enzyme at pH 7.0. Kong et al. [46] fabricated an amperometric glucose biosensor with immobilization of GOx onto ZnO nanotube that they presented the biosensor showing an optimal response at pH 7.0.

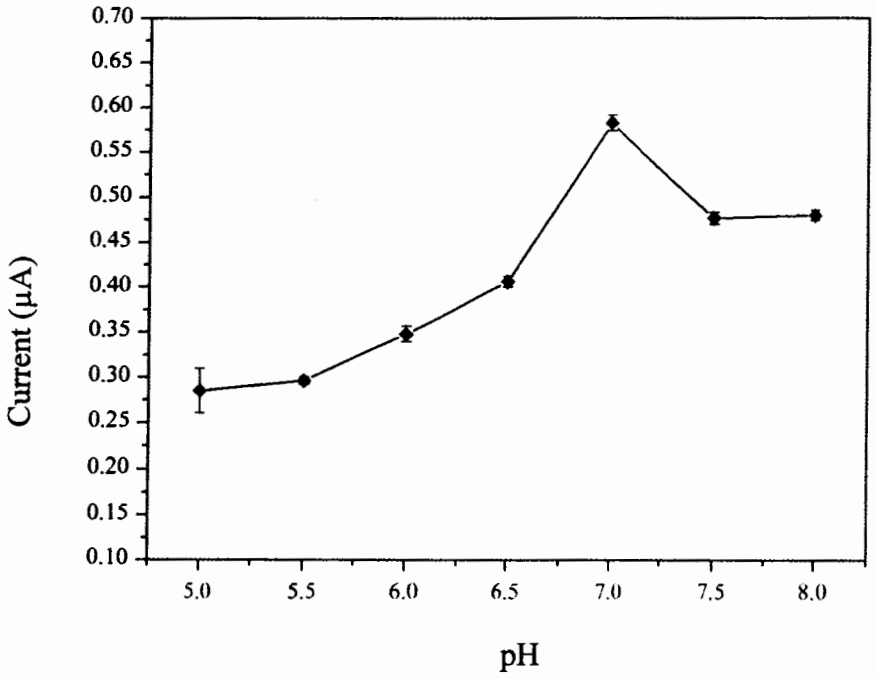

Figure 4.4 Effect of pH solution on the amperometric response of GOx/MnO_2/ SPCE

On the basis of the results above and according with previous works, the phosphate buffer solution at pH 7.0 was selected for the subsequent experiments.

4.2.3 Enzyme loading

Typically enzyme loading affects to an amperometric response of the electrode. To improve the biosensor performance, the amount of GOx should be sufficient to achieve a broad linear response range. The trend is such that with increasing GOx loading, more H_2O_2 is formed and hence leading to an increase in current. Different concentrations of GOx (40, 80, 120 and 160 $U.cm^{-2}$) immobilized onto electrode surface were used to determine the optimum response for enzyme inhibition of the further experiment (section 3.6.2.3). The effect of the enzyme loading on the sensitivity of the chronoamperometric signal is shown in Figure 4.5 and appendix B.1.3. High sensitivity was found when 80 $U.cm^{-2}$ was used. When the amount of enzyme on the surface becomes higher, the sensitivity decreases due to the increased thickness of the membrane which deteriorates the diffusion of glucose. The highest sensitivity to inhibitor was found for a membrane containing low enzyme loading by Sotiropoulou and Chaniotakis. [96], Shan et al. [97] and Mohammadi et al. [52]. Ciucu et al [98] studied a set of five membranes with different amounts of AChE; the response of the biosensors decrease with decrease of the enzyme concentration and the response was off beyond. Therefore, GOx loading of 80 $U.cm^{-2}$ on the electrode surface was chosen for further studies.

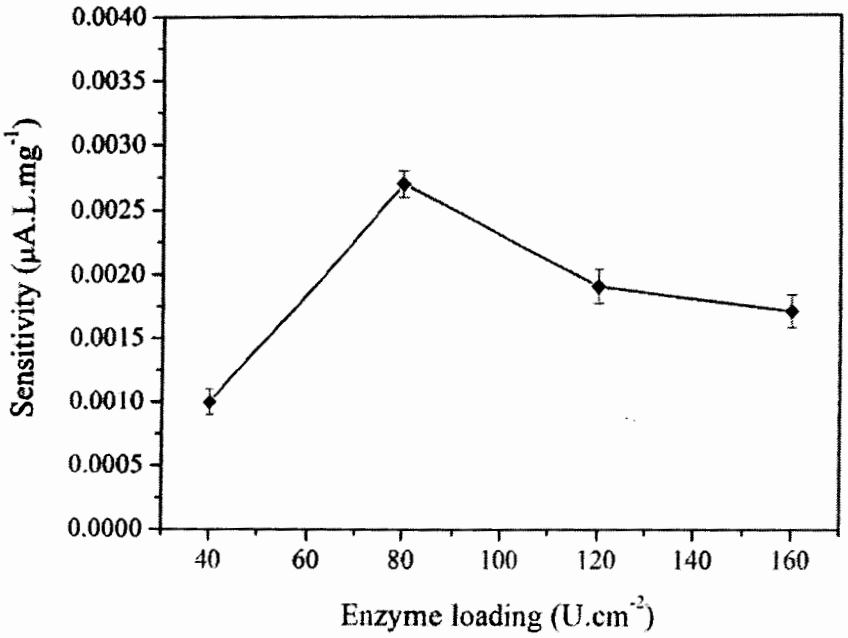

Figure 4.5 Effect of GOx loading on the sensitivity the GOx/MnO_2/SPCE

4.2.4 Glucose loading

The substrate concentration can affect the degree of inhibition that was reported by Kok et al. [99]. They concluded that the inhibition level (%) increases with increasing of the substrate concentration, and have worked with a saturating substrate concentration in the case of pesticide inhibition and in the studies for the detection of mercury by inhibition of glucose oxidase. The sensitivity of glucose loading was basic approach investigated. The percentage of inhibition was evaluated from the response of the active and inhibited forms of the enzyme. Therefore, all the enzyme molecules in the medium have to take part in the reaction and this could only be possible in substrate concentrations corresponding to the saturation portion of the activity versus glucose curves. In this research the substrate concentration was studied in the range 50 - 1000 $mg.L^{-1}$ glucose (the experimental in section 3.6.2.4). As the results shown in Figure 4.6 and appendix B.1.4, 200 $mg.L^{-1}$ glucose used as the substrate for glucose oxidase was the optimum value for inhibition study.

It was noted that the usage of the high glucose concentration would not yield good results when the detection is carried out by simultaneous addition of analyte (mercury). Under such condition, the inhibition mechanism is competitive inhibition process, so that the glucose would compete with mercury for the enzyme active site and inhibition, especially at low analyte concentration, could not be detected.

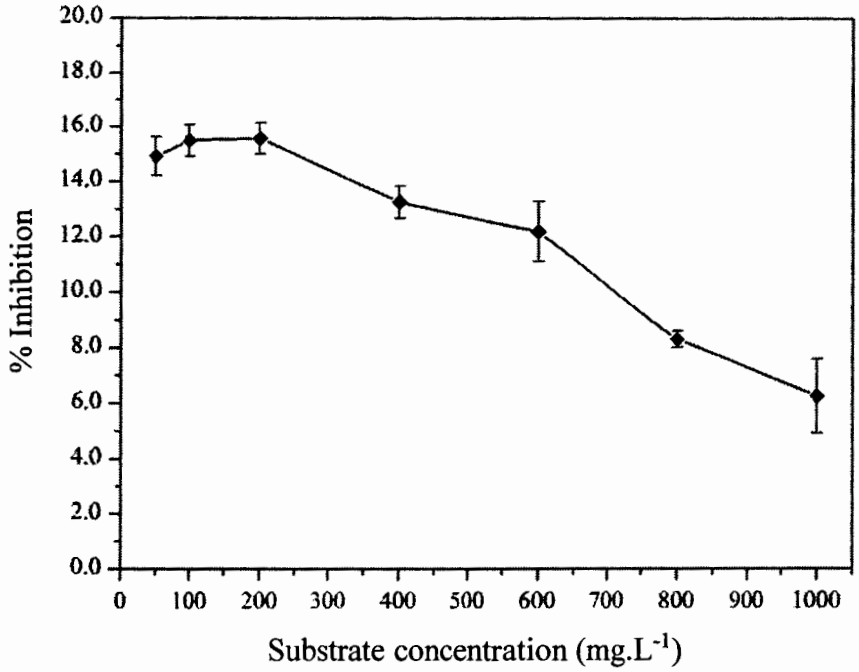

Figure 4.6 Effect of glucose loading on the inhibition of the GOx/MnO_2/SPCE with 500 µg.L^{-1} mercury

Similar working with other enzymatic inhibition, Dzyadevych et al. [100] showed that sensitivity of a butyrylcholinesterase (BuChE) biosensor toward tomatine decreases with an increase in the substrate concentration. Liu et al. [21] developed biosensor for determination of trace mercury in compost extract by inhibition based glucose oxidase that they reported the substrate competes with inhibitor when the substrate concentration is high, so the increase of substrate concentration lead to the decrease of inhibition of inhibitor on the enzyme.

In summary, the parameters effecting on the response of the GOx/MnO_2/SPCE were obtained; operating potential of +0.46 V versus Ag/AgCl, pH buffer solution of 0.1 mol.L^{-1} phosphate buffer solution at pH 7.0, enzyme loading of 80 U.cm^{-2} GOx and substrate concentration of 200 mg.L^{-1} glucose were experimentally optimum conditions for further inhibition studies. This research has used the GOx/MnO_2/SPCE as the biosensor assembled with the electrochemical cell coupled with FIA; thus, some parameters effecting on the response of FIA system are crucial and studied in the next topic.

4.3 Optimization of the flow injection analysis method

The parameters influence to dispersion of an injected fluid zone: sample volume, flow rate of carrier and merging fluid streams, geometrical dimensions and configuration of transport conduits and online reactor, and pattern of flow segmentation. In this study, the parameters were experimentally investigated in the case of inhibition degree of glucose oxides.

4.3.1 Effect of FIA injection volume

An optimum injection volume is necessary to deliver the sample into the carrier stream for the maximum current response into the biosensor cell. The variation of current response with the injected sample volume in the 20 - 500 μL range was studied (experimental in section 3.6.3.1). The relationship between inhibition degree and the injection volume is illustrated in Figure 4.7 and appendix B.1.5.

The result of inhibition degree increases when the injection volumes are up to 250 μL. Those results can be inferred that smaller volume was inadequate for the inhibition process while the larger injection volume was for enzyme-substrate saturation. Moreover, the board peak current occurred when the loop volume exceeded at 500 μL (Figure 4.8). Thus, in the present FIA system for the indirect mercury determination, a 250 μL sample loop was selected for further studies. The injection volume found in this work is in accordance with previous investigations where an enzyme inhibition electrode was used; La Rosa et al. [62] developed an amperometric flow-through biosensor for the determination of pesticide by inhibition of AChE that they described the inhibition degree increase with increasing injection volume.

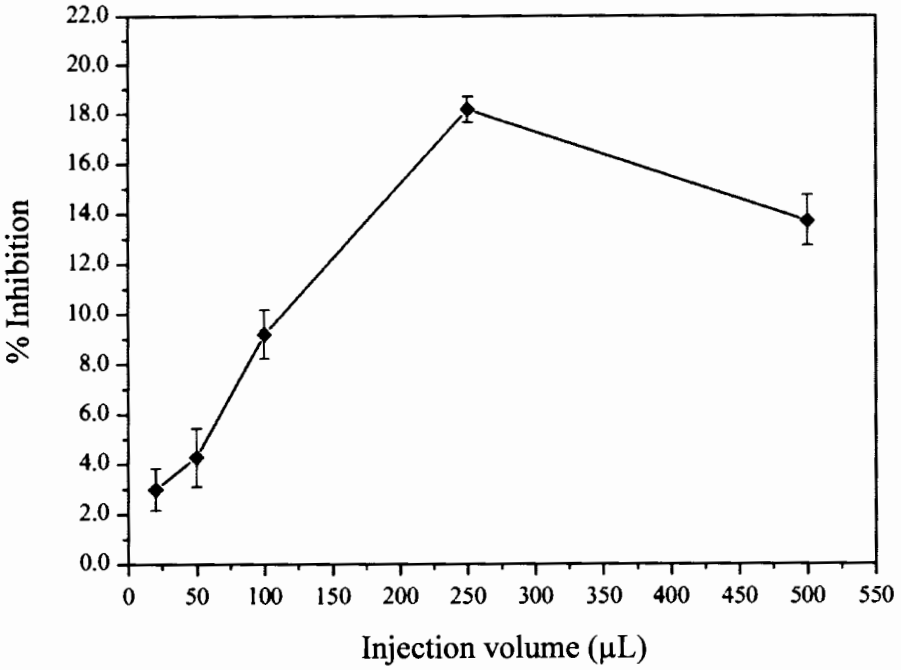

Figure 4.7 Effect of injection volume on the inhibition of the GOx/MnO_2/SPCE with 500 μg.L^{-1}mercury

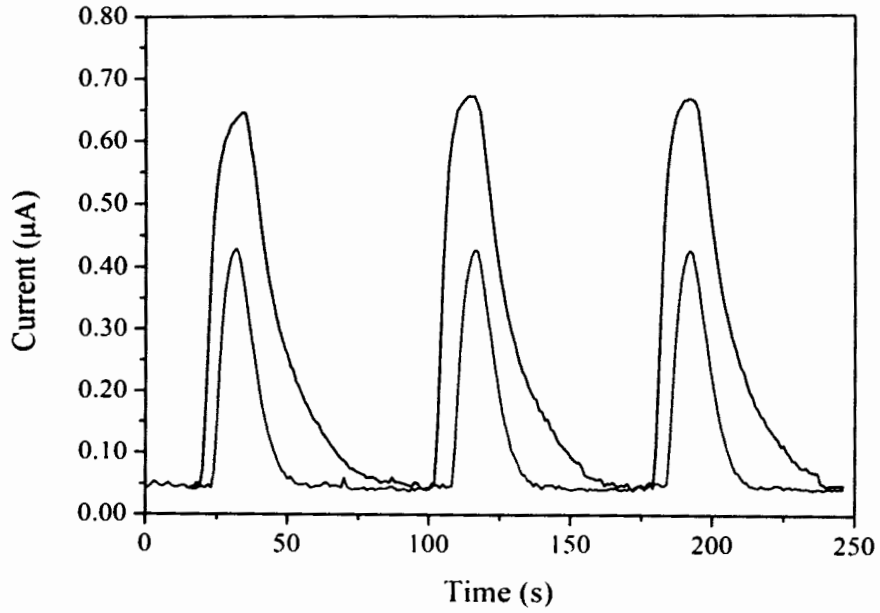

Figure 4.8 The current responses on the injection volume of 250 μL (blue line) and 500 μL (black line)

4.3.2 Effect of FIA flow rate

Ruzicka and Hansen [57] mentioned that dispersion diminishes with a decrease in flow rate because the slow flow rate increases the retention time of the sample into the detector.

In this work, an optimum flow rate is necessary to deliver all reactants through the detector cell. The effects of the flow rate on the intensity of current were studied over the range 0.6 - 1.6 $mL.min^{-1}$ in each stream (the experimental in section 3.6.3.2). The result for enzyme inhibition is shown in Figure 4.9 and appendix B.1.6. The inhibition degree for mercury detection was increased with an increase in flow rate up to 1.2 $mL.min^{-1}$. Inhibition degree was down when the flow rate was greater than 1.6 $mL.min^{-1}$. Moreover, the broad peak current occurred when the flow rate less than 0.6 $mL.min^{-1}$ (Figure 4.10). Thus, the optimal flow rate of 1.2 $mL.min^{-1}$ was chosen to maintain the maximum sensitivity for our subsequent experiments.

The flow rate optimum found in this work is in accordance with previous investigations where an enzyme inhibition electrode was used. La Rosa et al. [62] developed an amperometric flow-through biosensor for the determination of pesticide by inhibition of AChE. They explained a fast flow rate results in low inhibition degree as would be expected, since the inhibitor is in contact with the enzyme for shorter time periods. Therefore, slow flow rates would be desirable in order to maximize the inhibition response. Shi et al. [23] developed biosensor for determination of mercury(II) traces in drinking water by inhibition of an urease reactor in FIA system that they reported the optimum flow rate of 1.2 $mL.min^{-1}$ that shown the highest inhibition response.

According to previous studies, $GOx/MnO_2/SPCE$ based on FIA was further studied under optimum condition; operating potential of +0.46 V versus Ag/AgCl, 0.1 $mol.L^{-1}$ phosphate buffer solution at pH 7.0, 80 $U.cm^{-2}$ GOx as a enzyme concentration, 200 $mg.L^{-1}$ glucose loading as a substrate concentration, 250 µL injection loop and 1.2 $mL.min^{-1}$ of flow rate. The next topic, inhibition study of GOx was investigated.

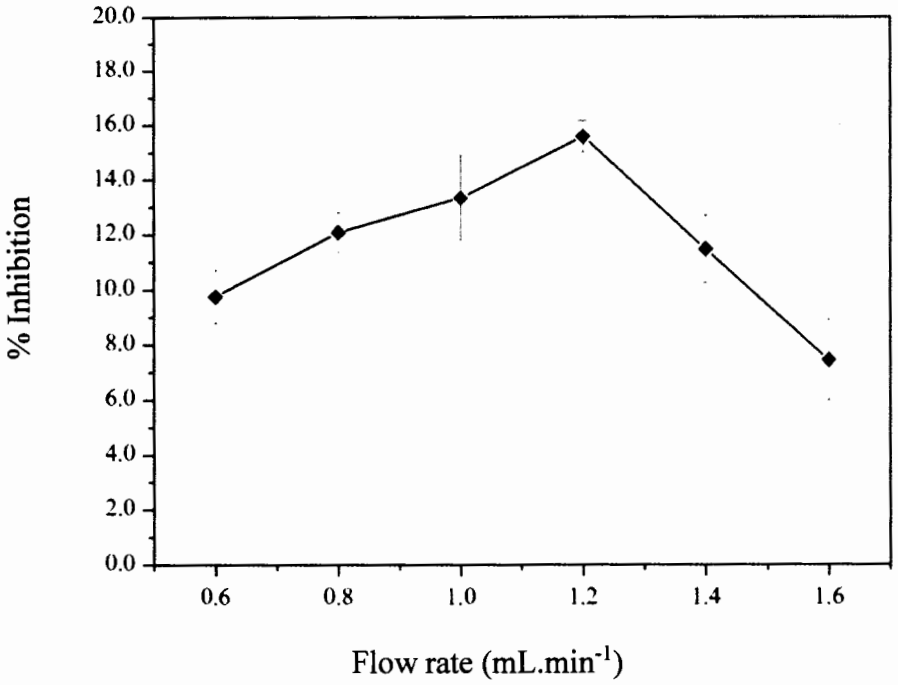

Figure 4.9 Effect of flow rate on the inhibition of GOx/MnO_2/SPCE with 500 $\mu g.L^{-1}$ mercury

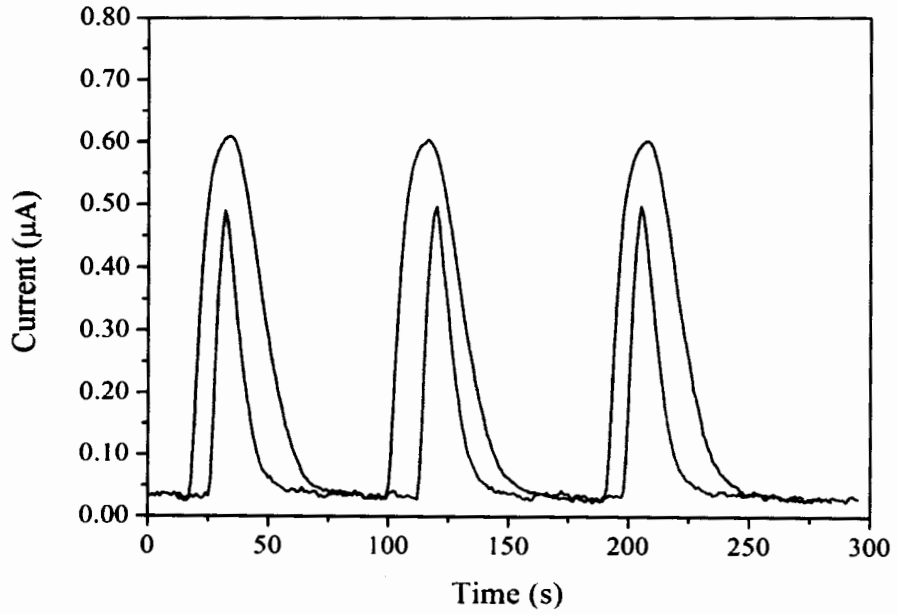

Figure 4.10 The current responses on the flow rate of 0.6 $mL.min^{-1}$ (black line) and 1.2 $mL.min^{-1}$ (blue line)

4.4 Inhibition study

For the determination of mercury by inhibition of GOx, the glucose concentration was held constant at 200 $mg.L^{-1}$, and the decrease of the response signal was monitored after the presence of mercury. The response current drops when mercury presented in the test solution in which degree of inhibition was proportional to the concentration of mercuric (II) ion that the method allows calculation of the percentage inhibition, defined using a formula in equation 2.9 (section 2.13). The mechanism of the enzymatic inhibition was described by Gibbs et al. [50] that mercury probably was bound sulfhydyl or hydroxyl groups of the glucose oxidase close to or at its active center.

As the flow injection performs, measurements were done on the wide range (100 - 1000 $\mu g.L^{-1}$) of mercury in the solution injected (the experimental in section 3.6.4). Example of signal recording from the detector is shown in Figure 4.11. As the results, the current decreased when adding mercury into the solution due to enzyme inhibition therefore H_2O_2 was not produced following enzyme catalytic reaction.

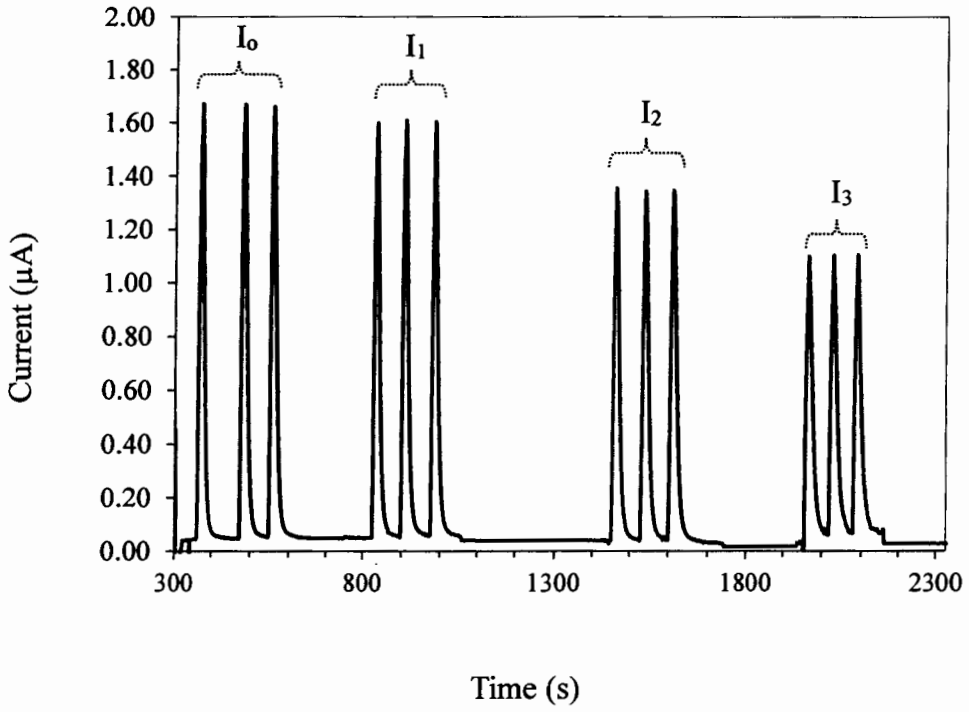

Figure 4.11 FIA grams recorded for determination of mercury based on inhibition of GOx. I_o is injection of 200 mg.L^{-1} glucose as a substrate (initial enzyme activity). I_1, I_2 and I_3 are injection of 100, 500 and 1000 μg.L^{-1} mercury that mixed with 200 mg.L^{-1} glucose, respectively (enzyme activity after inhibition).

As the results above, the parameters effecting GOx/MnO_2/SPCE and the inhibition of GOx based on FIA were completely investigated. Validated methods of GOx/MnO_2/SPCE based on FIA for the indirect determination of mercury in terms of linear range, limit of detection, limit of quantification, repeatability, reproducibility, regeneration, interferences, stability and accuracy were essentially studied and they are presented in the next section.

4.5 Analytical figures of merit

The following figures of merit sever as indicators for the characteristics of an analytical technique with regards to a specific analyte.

4.5.1 Linear range

Linear range of mercury ion was determined for inhibition of GOx/MnO_2/SPCE. The GOx activities was measured using FIA under experimental conditions; 0.1 mol.L^{-1} phosphate buffer solution at pH 7.0 as supporting electrolyte, enzyme loading of 80 U.cm^{-2}, operating potential at +0.46 V versus Ag/AgCl, substrate concentration of 200 mg.L^{-1} glucose, injection volume of 250 µL and flow rate of carrier solution of 1.2 mL.min^{-1}. The inhibitory effect of mercury on designed biosensor was tested at different concentrations (100 - 2000 µg.L^{-1} mercury) diluted in 200 mg.L^{-1} glucose solution using FIA systems, with the three replicated injections as explained in experimental section 3.6.5.1. The mercury concentrations were injected into the carrier steam. These FIA grams are illustrated by decreasing of current when inhibition of GOx activity increasing. Afterwards, the relationships between percentage inhibition and different concentrations would be calculated and plotted in which it is shown in Figure 4.13 (a) and appendix B.2.2. The maximum inhibition percentage (% Inhibition) of GOx observed was 40.13 % at concentration of 1000 µg.L^{-1} mercury. At higher concentrations of mercury (>1000 µg.L^{-1}) the inhibition degree response was found to level off.

The response of the GOx/MnO_2/SPCE to mercury exhibited good linearity in the concentration range (100 - 1000 µg.L^{-1}) and the inhibition degree varies according to the following linear equation $y = 0.0407x - 0.5760$ with the correlation coefficient of $r^2 = 0.9975$ and the sensitivity of 0.0407 %.L.μg^{-1} (Figure 4.13 (b)).

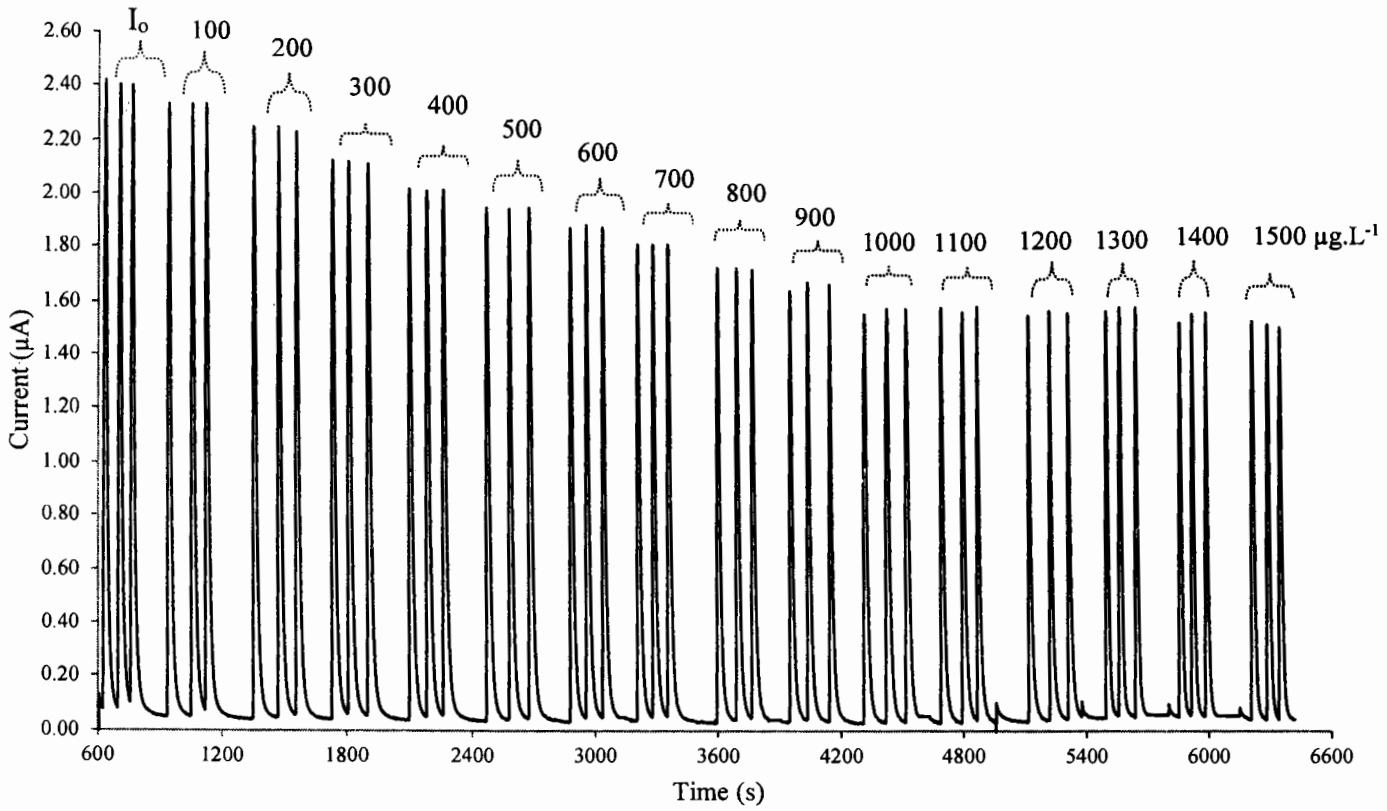

Figure 4.12 FIA gram of the biosensor on the current responses of the GOx/MnO_2/SPCE to mercury based on inhibition of GOx activity. I_o (initial current of enzyme activity) and 100 - 1500 µg.L^{-1} mercury (residual current of enzyme activity)

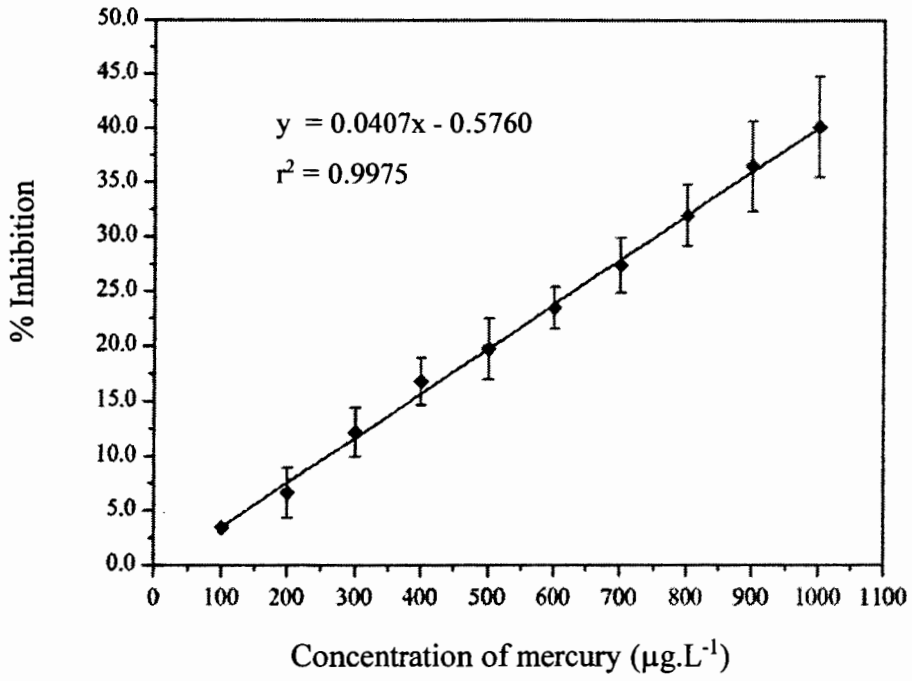

Figure 4.13 Linear dynamic range for detection of mercury based on inhibition of the GOx/MnO_2/SPCE

4.5.2 Limit of detection

The limit of detection (LOD) was calculated on the basis of 3 SD/b where SD is standard deviation of inhibition degree at the lowest concentration of calibration curve (100 $\mu g.L^{-1}$ mercury) (0.39, n = 3) and b is the slope of the calibration curve (0.0407 $\%.L.\mu g^{-1}$) illustrated in Figure 4.13 (b). The LOD of GOx/MnO_2/SPCE for determination of mercury was 29 $\mu g.L^{-1}$.

This work obtained the result of LOD in which it is low limit of detection compared to previous works; Samphao et al. [85], Malitesta and Guascito [77] developed amperometric biosensor for determination of Hg^{2+} by inhibition of GOx. They reported that LOD for the determination mercury is 500 $\mu g.L^{-1}$. Volotovsky et al. [82] developed amperometric biosensor for determination of Ag^{+}, $Hg^{2+}$and $Cu^{2+}$by inhibition of urease. Their result of LOD to detect Hg^{2+} was 200 $\mu g.L^{-1}$.

4.5.3 Limit of quantification

The limit of quantification (LOQ) was calculated on the basis of 10 SD/b where SD is standard deviation of inhibition degree at the lowest concentration of calibration curve (100 $\mu g.L^{-1}$) (0.39, n = 3) and b is the slope of the calibration curve (0.0407 $\%.L.\mu g^{-1}$) illustrated in Figure 4.13 (b). The LOQ of GOx/MnO_2/SPCE for quantification of mercury based on FIA system was 96 $\mu g.L^{-1}$.

Our work obtained the result of LOQ in which it is low limit of quantification compared to previous works; Guascito et al. [20] developed amperometric biosensor for determination of metal ions by inhibition of GOx. They reported the LOQ for determination of mercury of 1000 $\mu g.L^{-1}$. Compagnone et al. [24] studied amperometric biosensor for determination of heavy metals by enzyme inhibition based on FIA. They have reported that mercury inhibited glycerol 3-P oxidase at LOQ of 500 $\mu g.L^{-1}$.

4.5.4 Repeatability

To evaluate the repeatability of a GOx/MnO_2/SPCE, the inhibition degrees were measured at lowest concentration of calibration curve (100 $\mu g.L^{-1}$ mercury) with ten replicated injections (the experimental in section 3.6.5.4). As the results, the FIA gram was shown in Figure 4.14. The GOx/MnO_2/SPCE has been presented high precision with relative standard deviation (RSD) of 3.68% (The inhibition degrees were shown in appendix B.2.5).

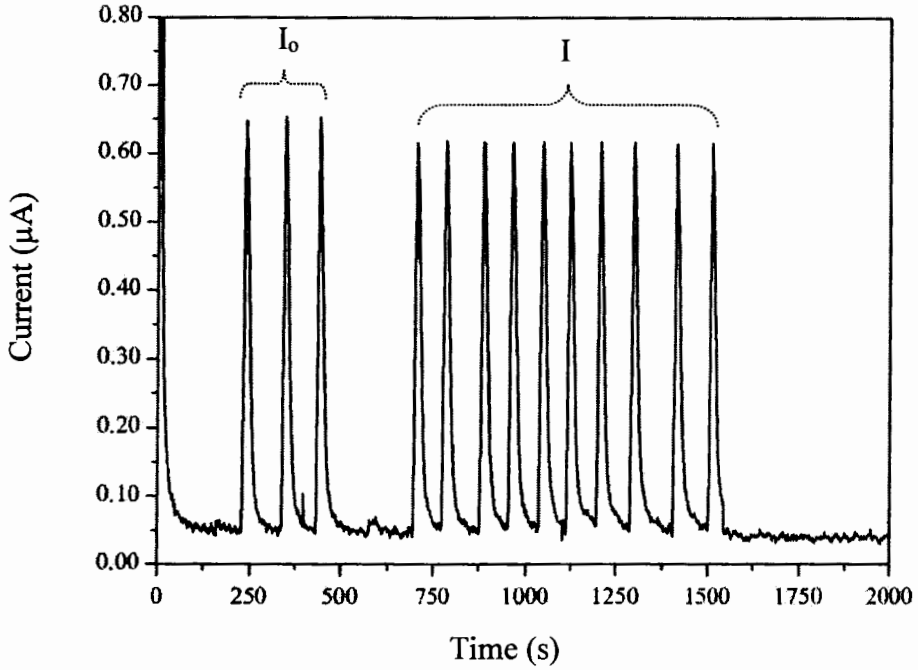

Figure 4.14 FIA amperometric response of the GOx/MnO_2/SPCE to the repeatability of inhibition by100 μg.L^{-1} mercury

4.5.5 Reproducibility

To estimate the precision of the GOx/MnO_2/SPCE, the electrode to electrode reproducibility was evaluated by using three independent electrodes fabricated under the same conditions. The inhibition responses were measured at the lowest concentration (100 μg.L^{-1} mercury). As the results, the FIA gram is shown in Figure 4.15. The inhibition degrees for three electrode assays were 3.50, 3.46 and 3.75 % inhibition, respectively; thus, %RSD was obtained at 4.40%. The reproducibility of the GOx/MnO_2/SPCE for determination of mercury has a high precision when compare to the bi-enzymatic whole cell conductometric biosensor for heavy metal ions and pesticides detection in water samples was developed by Chouteau et al. [101] that they reported reproducibility measurements with %RSD was less than 8%.

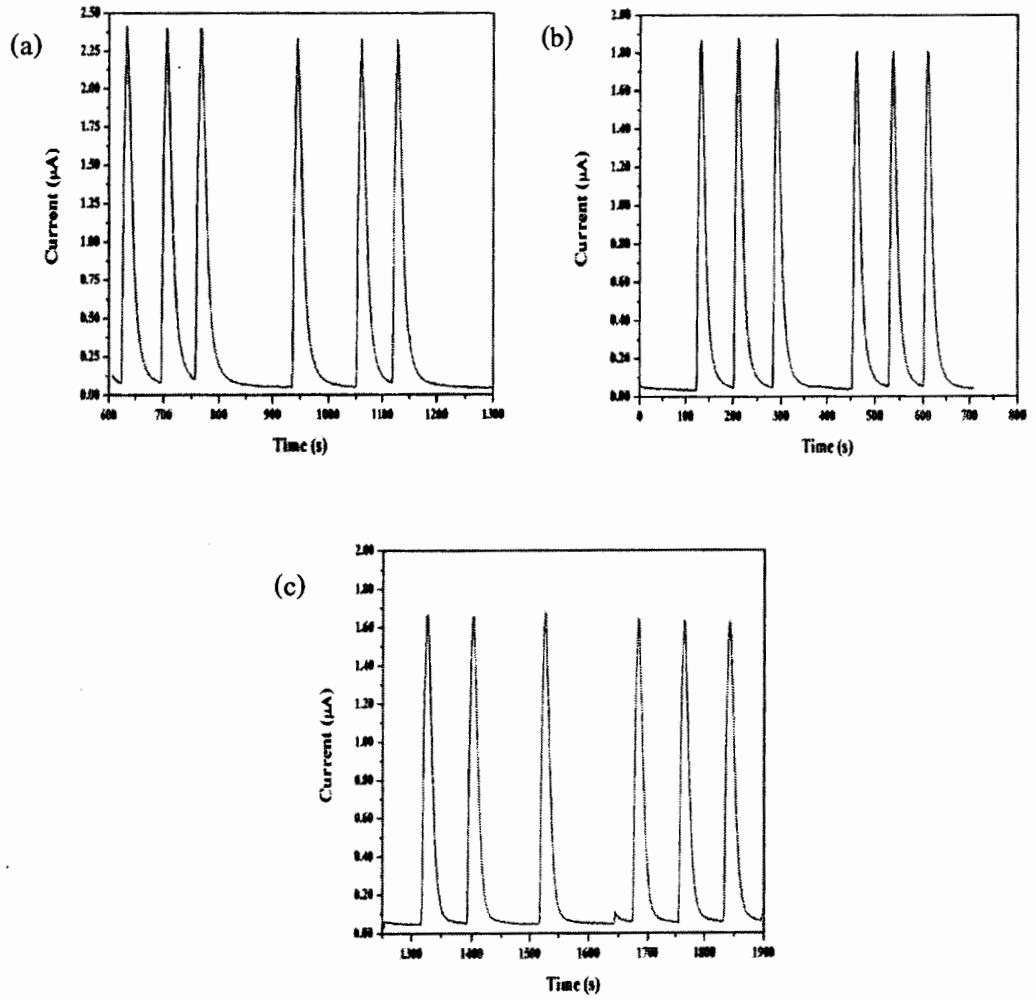

Figure 4.15 FIA amperometric response of the GOx/MnO_2/SPCE to reproducibility of inhibition by 100 μg.L^{-1} mercury (three electrodes; (a), (b) and (c))

The investigation and validation of GOx/MnO_2/SPCE based on FIA to detect mercury were sum up; linear range of 100 - 1000 μg.L^{-1}, limit of detection of 29 μg.L^{-1}, limit of quantification of 96 μg.L^{-1}, repeatability of 3.68 %RSD and reproducibility of 4.40 %RSD were experimentally obtained. Continually, to perform multiple measurements with the same electrode, the regeneration of GOx/MnO_2/SPCE was investigated in the next section.

4.5.6 Regeneration

After the exposure of the GOx/MnO_2/SPCE to mercury, the activity of the enzyme at the electrode surface had to be restored in order to perform multiple measurements with the same electrode. The GOx/MnO_2/SPCE could be regenerated after inhibition by using of metal chelating agent. Ethylenediaminetetraacetic acid (EDTA) could be an effective regenerating agent for the GOx based biosensor after contact with the heavy metal. The regeneration efficiency was dependent on the history of the electrode with respect to mercury exposure.

The effect of EDTA concentrations based on FIA was performed by different EDTA concentrations flow through GOx/MnO_2/SPCE surface (the experimental in section 3.6.5.6). Example of signal recording for study of regeneration presented in Figure 4.16, which shows the typical current versus time plot during the inhibition and regeneration process of the biosensor.

A series of solutions with different EDTA concentrations are then used to obtain the corresponding percentage regeneration (% regeneration). Percentage regeneration is given by the following expression $\frac{I_2}{I_0} \times 100$ where, I_0 is the reference peak height given by biosensor before inhibition, and I_2 is the peak height after regeneration.

The percentages of regeneration (% regeneration) were measured at different EDTA concentrations (0.025, 0.05, 0.075 and 0.1 $mol.L^{-1}$). The results showed % regeneration versus EDTA concentration displayed in Figure 4.17 and appendix B.2.6. The GOx/MnO_2/SPCE showed high regeneration responses with EDTA concentration higher than 0.025 $mol.L^{-1}$ up to 0.05 $mol.L^{-1}$, then the regeneration degree was off. Moreover, at 0.05 $mol.L^{-1}$ EDTA presents the lowest standard deviation, so that 0.05 $mol.L^{-1}$ EDTA was chosen for regenerating the activity of GOx.

Similarly, Malitesta and Guascito [77] has been recently obtained a full and rapid restoration of response by treatment of Hg^{2+}-inhibited GOx biosensor with EDTA solution.

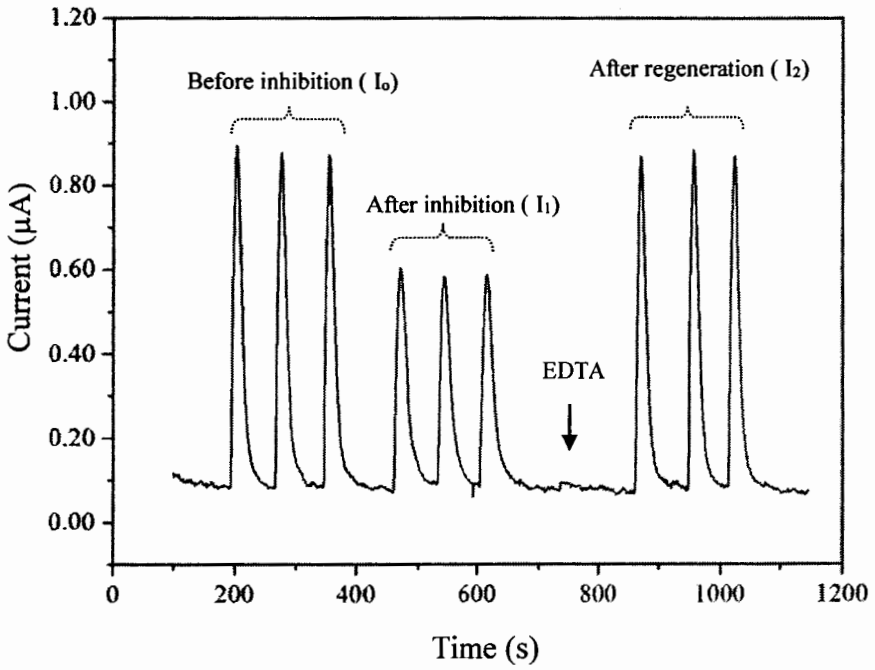

Figure 4.16 FIA amperometric response of the GOx/MnO_2/SPCE to the regeneration using EDTA ; I_o is initial current, I_1 is current after inhibit with 1 mg.L^{-1} mercury, I_2 is current after regenerated with 0.05 mol.L^{-1} EDTA and flow through the biosensor for 2 min.

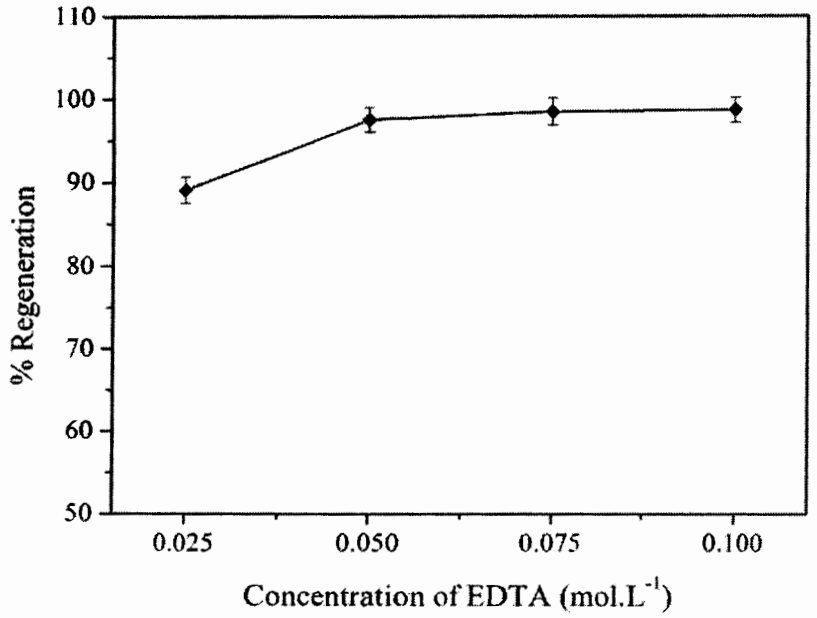

Figure 4.17 The effect of EDTA concentration to the regeneration of the GOx/MnO_2/SPCE

4.5.7 The storage stability

The storage stability of the GOx/MnO_2/SPCE has been investigated after the electrodes were stored in dry conditions at 4 °C in a refrigerator [102]. The current were measured when stored for 3 weeks (the experiments in the section 3.6.5.7).

The result of storage stability of GOx/MnO_2/SPCE was presented in Figure 4.18, and appendix B-3 which shows the relative current (%) versus storage time (days). The relative current (%) given by the following expression $\frac{C_1}{C_0}$x100 where, C_0 is the initial current given by GOx/MnO_2/SPCE before stored at 4 °C (the initial current), and C_1 is the current after stored at 4 °C (1 - 21 days). As the results, the relative current response of 89.3% and 76.0% were obtained after stored for 7 and 14 days, respectively.

In conclusion, the proposed biosensor could be stored more than three weeks with high activity. The biosensor is comparable for stability with a work reported by Liu et al. [102]. They developed an amperometric glucose biosensor based on entrapped GOx in the composite of carbon nanotubes/chitosan and its stability yields for 15 days at 4 °C.

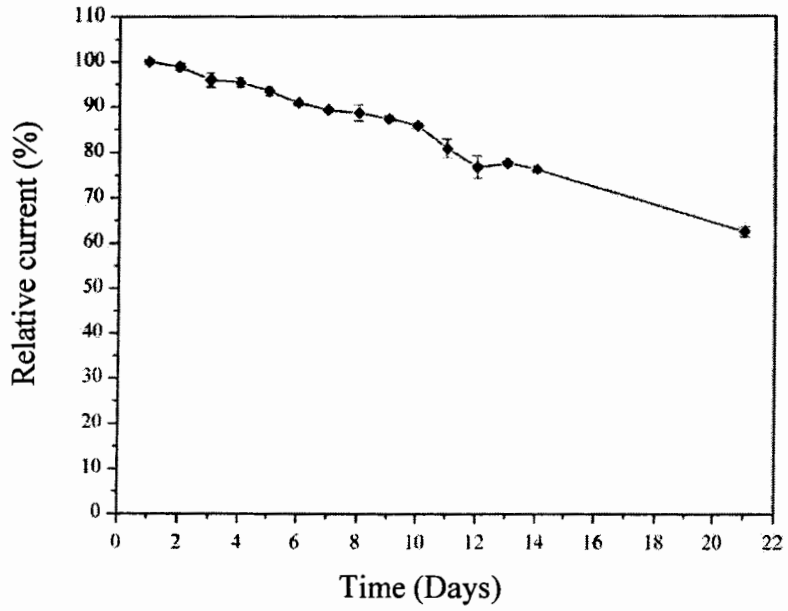

Figure 4.18 Effect of the storage stability on the current response of the GOx/MnO_2/SPCE

4.5.8 Interferences

Selectivity is an important factor for the performance of an inhibition-based enzyme catalytic process. In this study, many heavy metals were investigated on their possible interfering effect on the determination of mercury under the same experimental conditions.

To examine the interference effect of heavy metals on GOx/MnO_2/SPCE, the inhibition degree of 10 $mg.L^{-1}$ heavy metals (Fe (III), Cr (VI), Cr (III), Mn (II), Zn (II), Pb (II), Cd (II) and Cu (II)) mixed with 0.1 $mg.L^{-1}$ mercury were measured (1: 100 ; Hg (II) ion : interfering ions). The inhibition degrees were compared with inhibition degree of 100 $\mu g.L^{-1}$mercury (the experimental in the section 3.6.5.8). As the results, inhibition degree plotted versus types of metal ions is presented in Figure 4.17 (a); one notices that heavy metals including Pb (II), Cd (II) and Cu (II) interfere the determination as they also inhibit the activity of GOx. However, the three other heavy metals at concentration of 10 $mg.L^{-1}$ is very high concentration which environment is not contaminant in this level that reported by Athar and Vohara [103] and Callendar [104].

Moreover, the result in Figure 4.19 (a); Pb (II) Cd (II) and Cu (II) have a significant effect at 10 $mg.L^{-1}$. Therefore, interference at lower concentration (1 $mg.L^{-1}$) of three metal ions was studied under same method (the experimental in section 3.6.5.8). Inhibition degree was plotted versus types of metal ions (1 : 10 ; Hg : interfering ion) as shown in Figure 4.19 (b). As the results the inhibition degree of all metal ions is not significantly different that mercury is not inferred by others at concentration level of 1 $mg.L^{-1}$.

In this research, there are no inferences effecting to mercuric detection for this biosensor based on FIA.

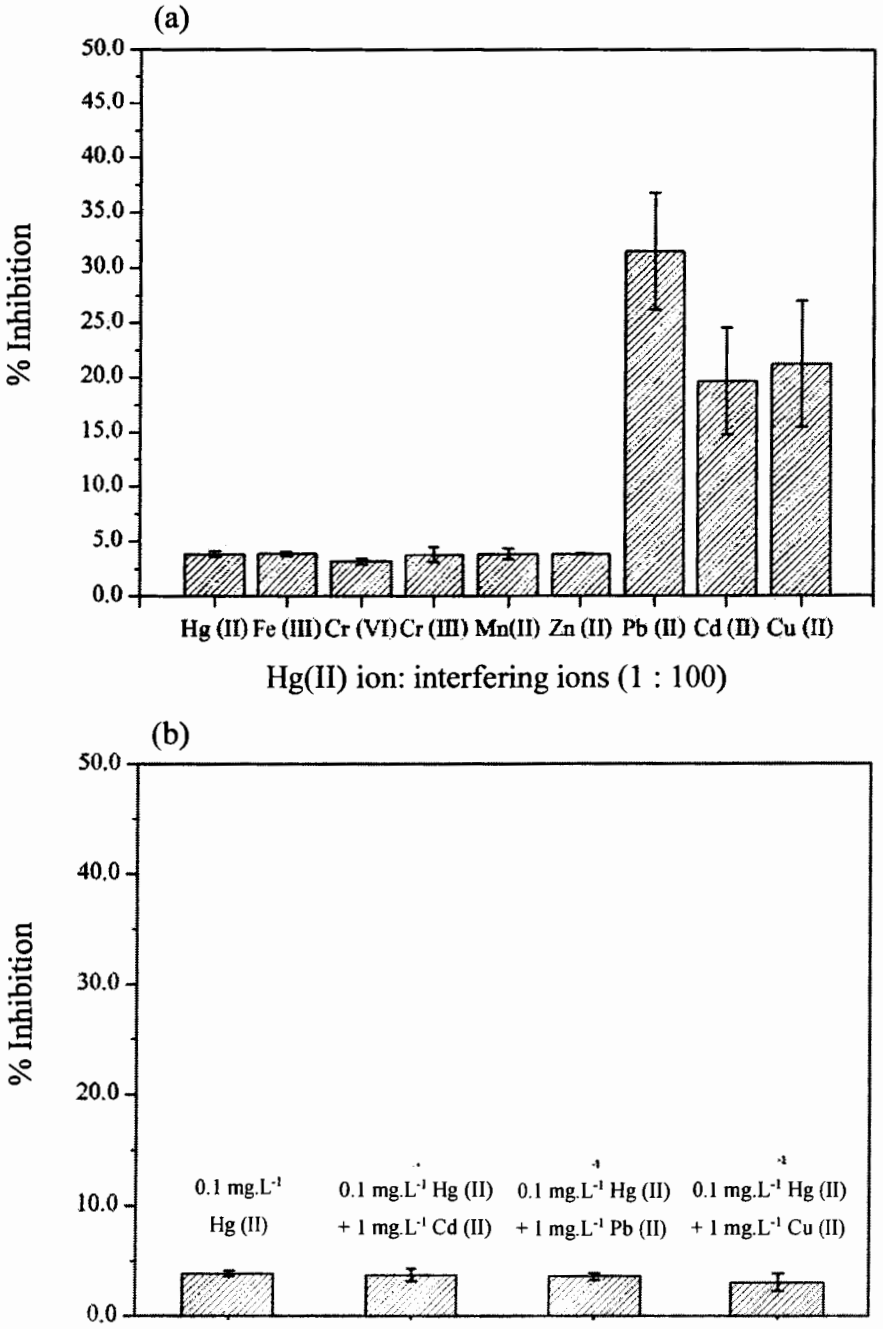

Figure 4.19 Effect of interferences on the inhibition degree of the GOx/MnO_2/SPCE biosensor; (a)Hg (II) ion: interfering ion (1 : 100) and (b) Hg (II) ion : interfering ion (1 : 10)

To understand kinetic reaction and catalytic inhibition of GOx was studied and is presented in the next section.

4.6 Enzyme kinetics

Enzyme kinetic reactions can be studied in a variety of ways to explore different aspects of catalysis. Enzyme-substrate and enzyme-inhibitor complexes should be studied due to understanding its activity. In this research GOx was immobilized with MnO_2/SPCE which was used to detect mercury based on its inhibitory process. Therefore, kinetic catalytic reaction and inhibition of GOx were studied in this part.

4.6.1 Kinetic catalytic reaction of GOx

To investigate the enzyme-substrate kinetics, the performance of GOx/MnO_2/SPCE response to different glucose concentrations (0.2 - 20 mmol.L^{-1}) based on FIA system was studied.

The oxidation current responses catalyzed by GOx was measured under the optimal conditions. After the background current in phosphate buffer pH 7.0 was reached stable, glucose solutions (0.2 - 20.0 mmol.L^{-1}) were injected into the carrier solution and the current was recorded continuously (the experimental in section 3.6.6.1).

As the results, the FIA gram (Figure 4.20) of the GOx/MnO_2/SPCE to the successive step injections of glucose into the carrier solution. A subsequent injection of glucose at different concentration of 0.2 - 20 mmol.L^{-1} provoked a remarkable increase in the oxidation current. Continually, the currents were plotted versus different glucose concentrations which it can be seen the plot in Figure 4.21 and appendix B-5.

In explanation, the enzyme-substrate kinetics could be described by the apparent Michaelis-Menten constant (K_m) and Lineweaver-Burk equation (double reciprocal plot) which depicts the enzyme-substrate kinetics of biosensor.

From Figure 4.20, one can further observe that the biosensor response gradually deviates from the linear feature as the glucose concentration up to 20 mmol.L^{-1} representing a typical characteristic of Michaelis-Menten kinetics.

The K_m is investigated; Michelis-Menten method were evaluated with 5.88 $mmol.L^{-1}$ and highest current (I_{max}) of 4.45 μA as shown in Figure 4.21 (a). The second method, Line weaver-Burk equation (double-reciprocal plot) was plotted between 1/I and 1/S (Figure 4.21 (b). The intercepts on the 1/I and 1/[S] axes give the values of $1/I_{max}$ and $1/K_m$. Then, the K_m and I_{max} for the immobilized enzyme in double-reciprocal method can be calculated to be 5.80 $mmol.L^{-1}$ and 4.41 μA, respectively. The obtained K_m was very good agreement with the value for the free enzyme (K_m = 6.2 $mmol.L^{-1}$ reported by Rosi et al. [44]). Similar result of apparent K_m for the immobilized and free enzymes suggested that the accessibility of glucose molecules to the enzyme active sites was not different by immobilization. Two methods of enzyme substrate kinetics presented no significant different values of K_m and I_{max}.

There are some previous works reporting calculated K_m of GOx immobilized in difference matrixes such as glucose biosensors based on ZnO:Conanoclusters (K_m = 21 $mmol.L^{-1}$) reported by Zhao et al. [45], polypyrrole films (K_m = 37.6 $mmol.L^{-1}$) reported by Uang et al. [105], and nano-$CaCO_3$ (K_m = 21.4 $mmol.L^{-1}$) reported by Shan et al. [106].

In summary, the obtained K_m from this proposed research is rather low (5.80 $mmol.L^{-1}$). The lower K_m means the higher enzymatic activity; thus, the GOx/MnO_2/SPCE modified biosensor possesses a high affinity to glucose.

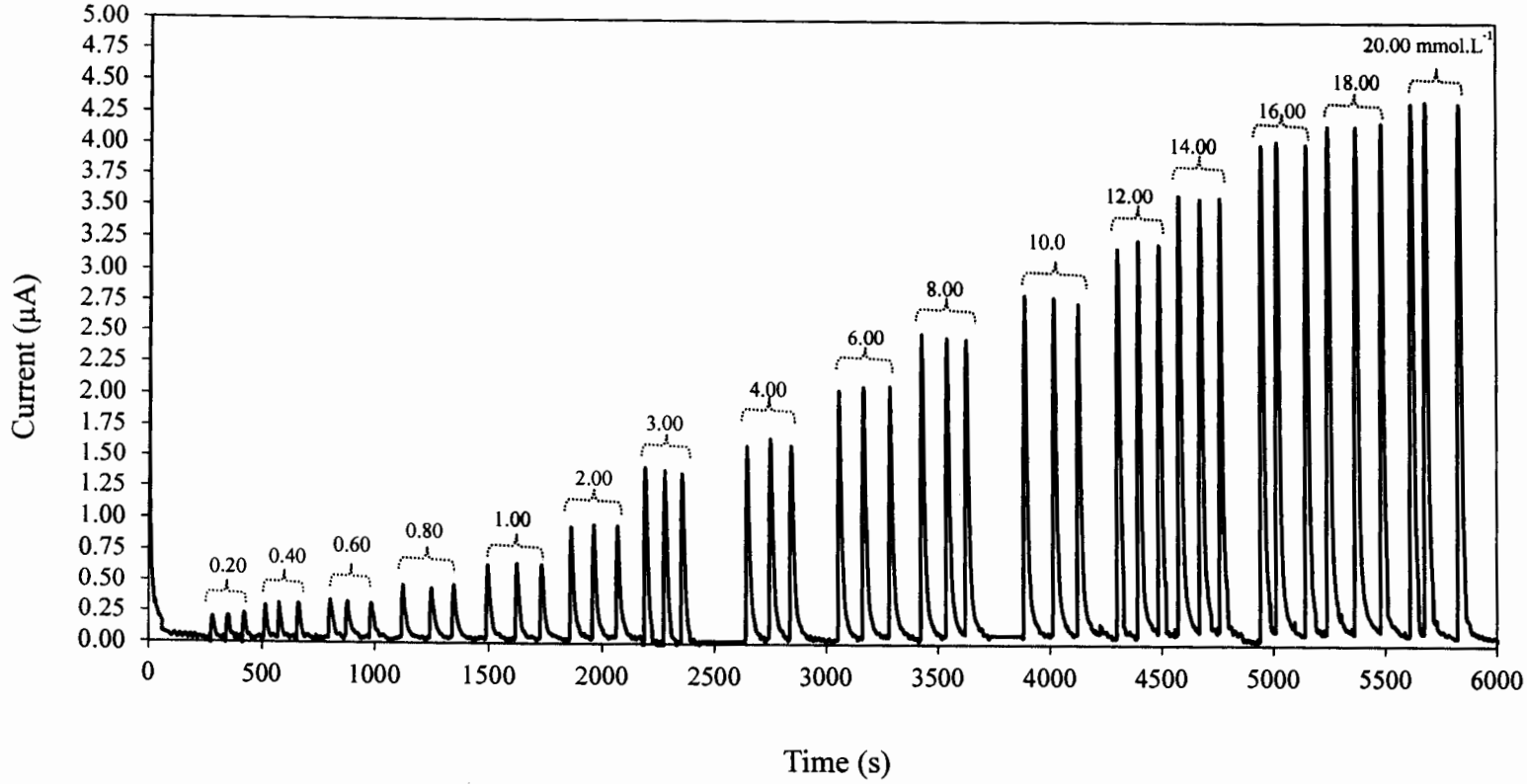

Figure 4.20 The FIA gram of the GOx/MnO_2/SPCE to the injection of glucose at 0.2 - 20.0 mmol.L^{-1}

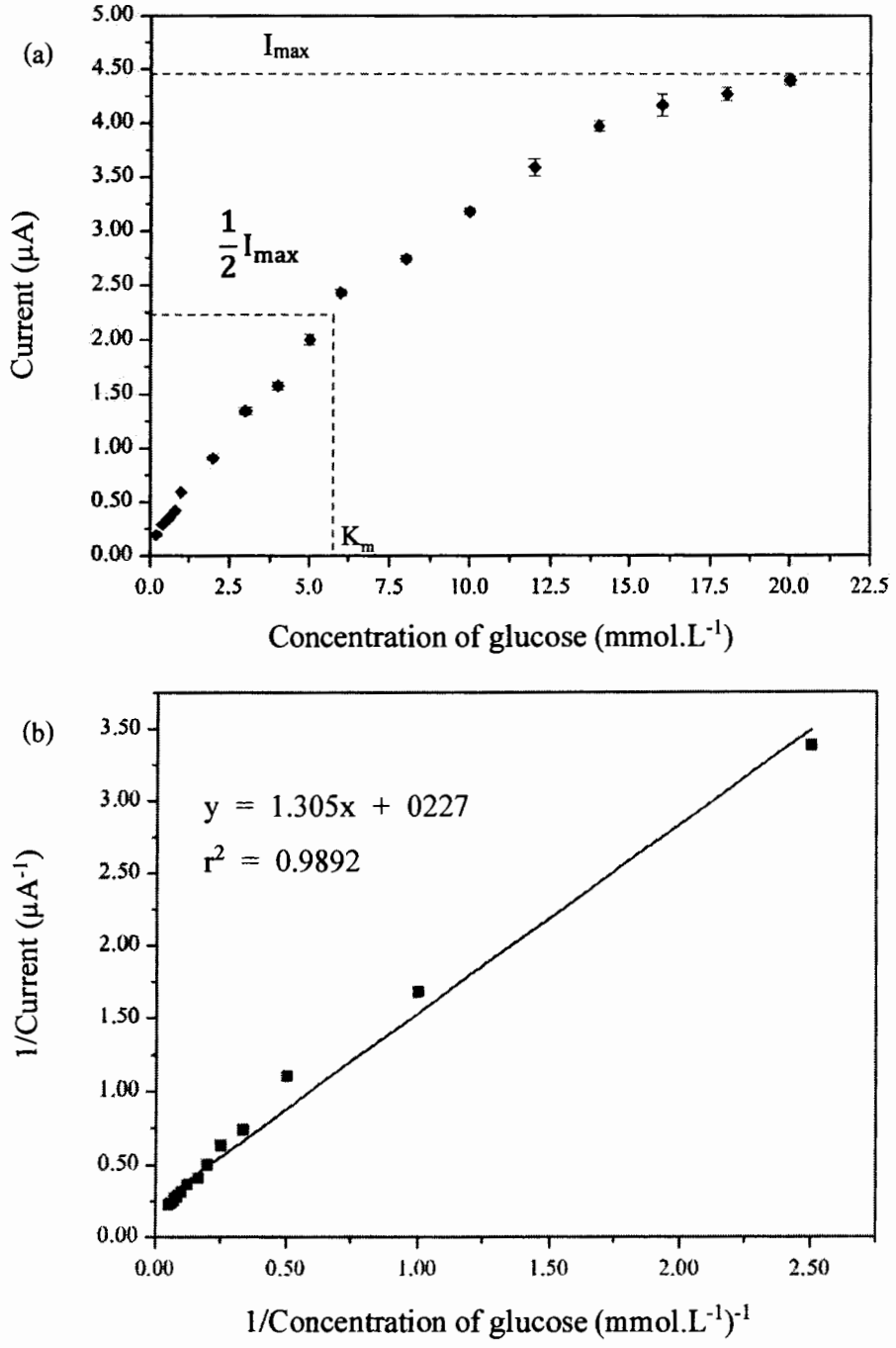

Figure 4.21 (a) Dependence of enzymatic activity on glucose concentration during glucose oxidation by the GOx/MnO_2/SPCE (direct Michaelis-Menten) (b) double reciprocal plots for the GOx/MnO_2/SPCE

4.6.2 Catalytic inhibition of GOx

To confirm the mode of inhibition of GOx by mercury, the catalytic inhibition of GOx was studied. The oxidation current after inhibition by mercury solution (fixed at 1 $mg.L^{-1}$) was measured under the optimal conditions (the experimental in section 3.6.6.2)

The result was plotted between current and different glucose concentration after inhibited mercury (appendix B.5), and fit these data to the direct Michaelis-Menten as shown in Figure 4.22. Determination of the values of K_m and I_{max} directly from the nonlinear least-squares best fits of the data. Then, comparing with plug these values of K_m and I_{max} into the double-reciprocal (Lineweaver-Burk equation) to obtain a linear function, and plot this linear function after inhibited by mercury with the same double-reciprocal plot (Figure 4.23).

In this way the Michealis-Menten method and double-reciprocal plots can be used to determine inhibitor modality from the pattern. Based on the mechanism to inhibit the enzyme activity, the inhibitor (Hg^{2+}) may further be classified into competitive, noncompetitive, and uncompetitive inhibitors (described in section 2.6). For an enzyme-catalyzed reaction, the effect of the inhibitor on the current versus substrate concentration curve is shown in Figure 4.22 and Figure 4.23.

In Figure 4.23 was presented for direct Michaelis-Menten; presence (red line) and absence inhibitor (black line) can be observed when present inhibitor with no change K_m but I_{max} decreased (red line) that it is the unique of noncompetitive inhibition reported by Guascito et al. [20], Bachan Upadhyay [47] and Krawczynski et al. [15]. And the result of these measurements presents in Figure 4.23 explained in the pattern of Lineweaver-Burk plot suggested that it is noncompetitive inhibition of GOx (no change K_m but I_{max} increased).

As results reported of value of K_m and I_{max} in Table 4.1 that it is concluded that inhibition pattern of GOx is noncompetitive inhibition. Guascito et al. [20] and Ghica et al. [83] reported the same type of inhibition mechanism by mercury (II) ions.

Table 4.1 Comparison of K_m and I_{max} before and after inhibit GOx with mercury

Method	Before inhibition		After inhibition	
	K_m (mmol.L^{-1})	I_{max} (μA)	K_m (mmol.L^{-1})	I_{max} (μA)
Lineweaver-Burk	5.80	4.41	5.80	2.70
Michaelis-Menten	5.88	4.45	5.88	2.70

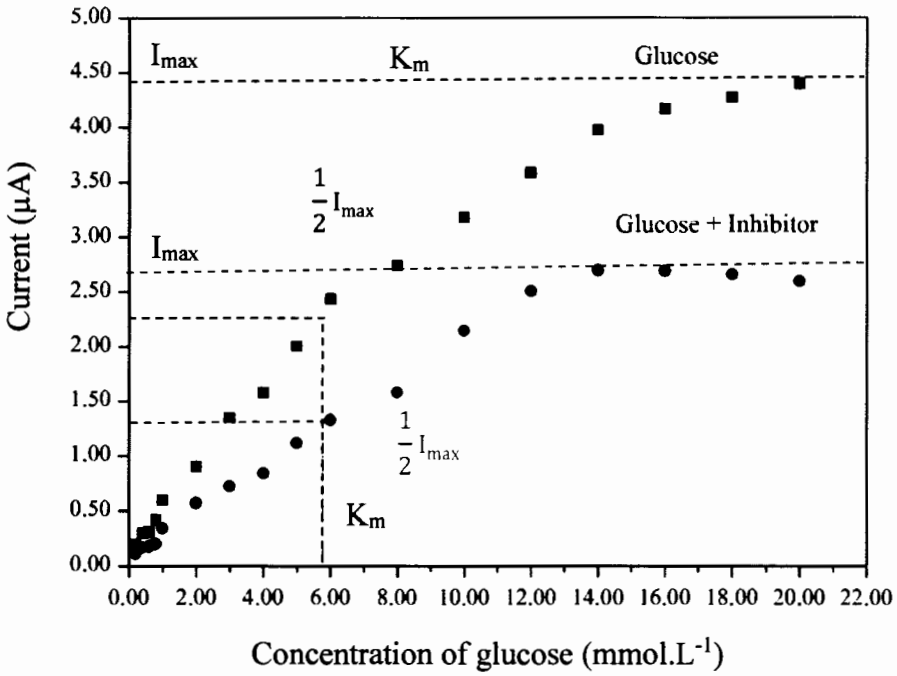

Figure 4.22 Dependence of enzymatic activity on glucose concentration during glucose oxidation by the GOx/MnO_2/SPCE (direct Michaelis-Menten) that comparing before (black line) and after (red line) inhibition with 1 mg.L^{-1} mercury

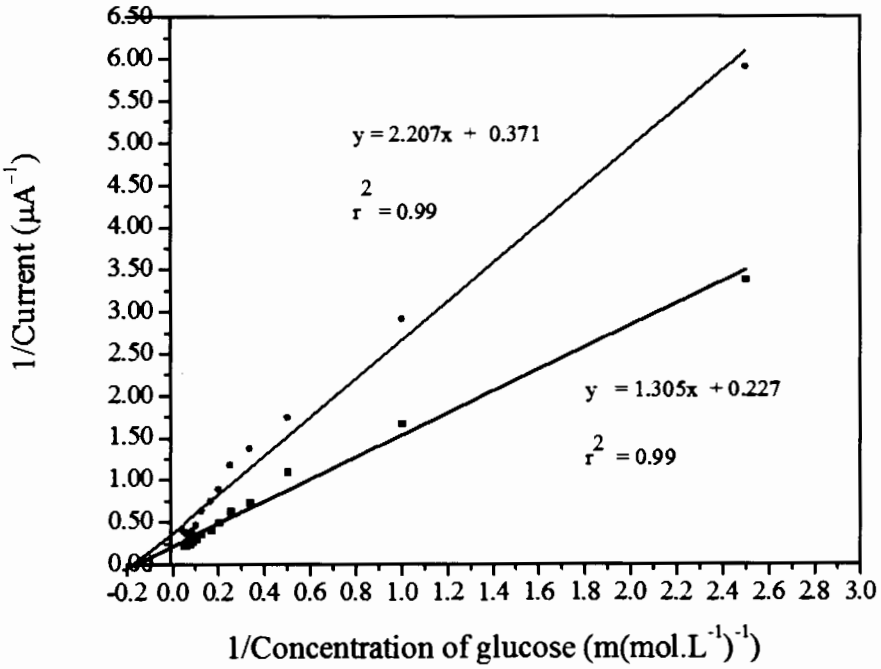

Figure 4.23 Double reciprocal plots for GOx/MnO_2/SPCE that comparing before (black line) and after (red line) inhibition with 1 mg.L^{-1} mercury

Continually, morphology of bare MnO_2/SPCE and GOx/MnO_2/SPCE was studied to see how the enzyme and matrixes distribution, the electrode surfaces were characterized by scanning electron microscope (SEM) and results are shown in the next section.

4.7 Characterization by scanning electron microscope (SEM)

The morphology of the MnO_2/SPCE electrode was investigated by SEM. Figure 4.24 (a) shows the surface of a typical MnO_2/SPCE. The surface morphology showed good definition of carbon particles, resulted in a sponge-like, branched, porous-structured, high-surface area on a SPE, ideal for inclusion of enzyme. On the other hand, the morphology of the GOx/MnO_2/SPCE electrode is shown in Figure 4.24 (b), the enzyme immobilization can be observed by a change in morphology to clusters of protein on the surface of the MnO_2/SPCE. Moreover, it can be seen that the GOx was coated by Nafion film these particles should be embedded in the Nafion matrix and due to the cage effects of the clusters of Nafion. Fortier et al. [107] reported the resulting polymer-enzyme film was covered by a thin layer of Nafion to avoid its subsequent dissolution in water to dissolve the enzyme without any significant loss of enzymatic activity. Some cavities are obviously present on the surface of the electrode, possibly resulting from the volatilization of solvents during the formation of film. This film not only prevents the loss of immobilized enzyme but also can improve the anti-interfere ability of the GOx/MnO_2/SPCE electrode because protons on the SO_3H (sulfonic acid) groups of Nafion [107]. In addition pores allow movement of cations but the membranes do not conduct anions or electrons.

(a) (b)

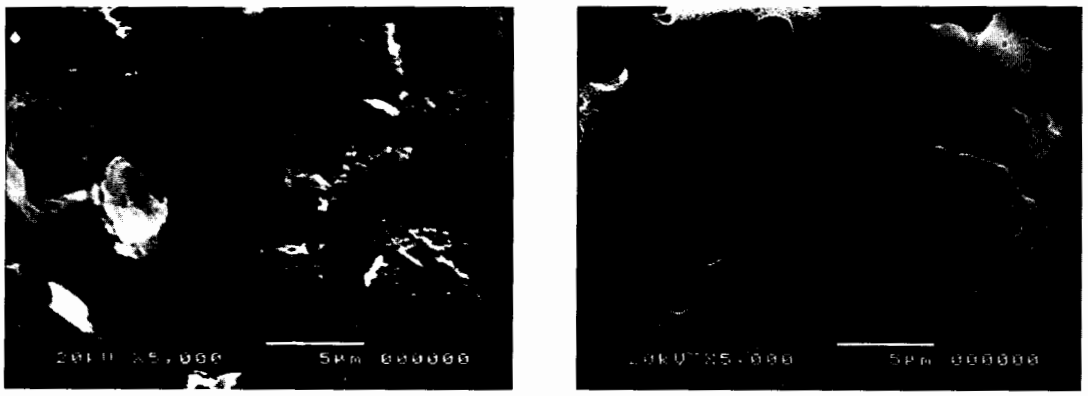

Figure 4.24 SEM image of (a) MnO_2/SPCE and (b) Nafion/GOx/MnO_2/SPCE

Furthermore, to ensure the accuracy of GOx/MnO_2/SPCE, application of GOx/MnO_2/SPCE for determination of mercury in certified reference material

(DORM-2) and real samples were investigated and the results are presented in the next section.

4.8 Mercury analysis in real samples

Mercury becomes increasingly concentrated in the marine food chain, in a process referred to as biomagnifications, and can reach extremely high levels in fish and other marine. The consumption of these fish and other marine organisms is the main route of human exposure to mercury. Thus the contaminant of mercury in mackerel (*rastrelligerbrachysoma*) and shrimp (*macrobrachiumlanchesteri*) were studied because the most popular consumption. In addition the concentration of mercury in natural water was measured. Further, to ensure the accuracy of the sample preparation, digestion and analysis, dogfish muscle certified reference material for trace metals (DORM-2) were also analyzed. Natural water, shrimps and mackerel samples were spiked with 2 $mg.L^{-1}$ mercury (the sample preparation, digestion and analysis presented in section 3.7).

To ensure the accuracy of the sample preparation, digestion and analysis, the DORM-2 was also examined which certified values of DORM-2 has been established at 4.64 ± 0.26 $mg.Kg^{-1}$ mercury. As the result the proposed method can be detected of 4.55 ± 0.07 $mg.Kg^{-1}$ mercury. The recoveries from these samples were also excellent, with an accuracy of 98%.

The mercury concentrations in seven samples were compared between the proposed method ($GOx/MnO_2/SPCE$) and the standard method (CVAAS). The result is presented in Table 4.2 and appendix B.7.

Table 4.2 The mercury concentration in different sample that measured with GOx/MO_2/SPCE and CVAAS

Samples	Expected result	Mercury concentration ($mg.Kg^{-1}$)		Recovery (%)	Relative difference (%)
	($mg.Kg^{-1}$)	Proposed method	CVAAS		
1) DORM-2	4.64 ± 0.26*	4.55 ± 0.07	4.71 ± 0.35	98	-3.4
2) local natural water	-	ND.	ND.	-	
3) shrimps	-	ND.	ND.	-	-
4) mackerel	-	ND.	ND.	-	-
5) spiked water	2.00	2.02 ± 0.18	2.01 ± 0.02	101	+0.5
6) spiked shrimps	2.00	1.90 ± 0.11	1.88 ± 0.05	95	+1.1
7) spiked mackerel	2.00	1.92 ± 0.03	2.03 ± 0.07	96	+5.4

ND. = none detection

DORM-2 = certified reference material 4.64 ± 0.26 $mg.Kg^{-1}$ mercury

LOD of CVAAS = 1 $\mu g.L^{-1}$ mercury

The validity of the method was checked by recovery determinations. The recoveries were found to be between 95% - 101%. The relative differences between both methods ranged from 0.5 - 5.4 % with respect to the reference determination and are in good agreement.

In order to evaluate the developed method, the results from both methods were compared shown in Figure 4.25. Applying the paired t-test, the t-value is significantly smaller than the tabulated critical value at a degree of freedom of 2, indicating that there is no significant statistical difference between these results at a confidence interval for 95% probability (appendix B.7). The results indicated that the mercury concentration as determined from the two methods agrees significantly well with each other.

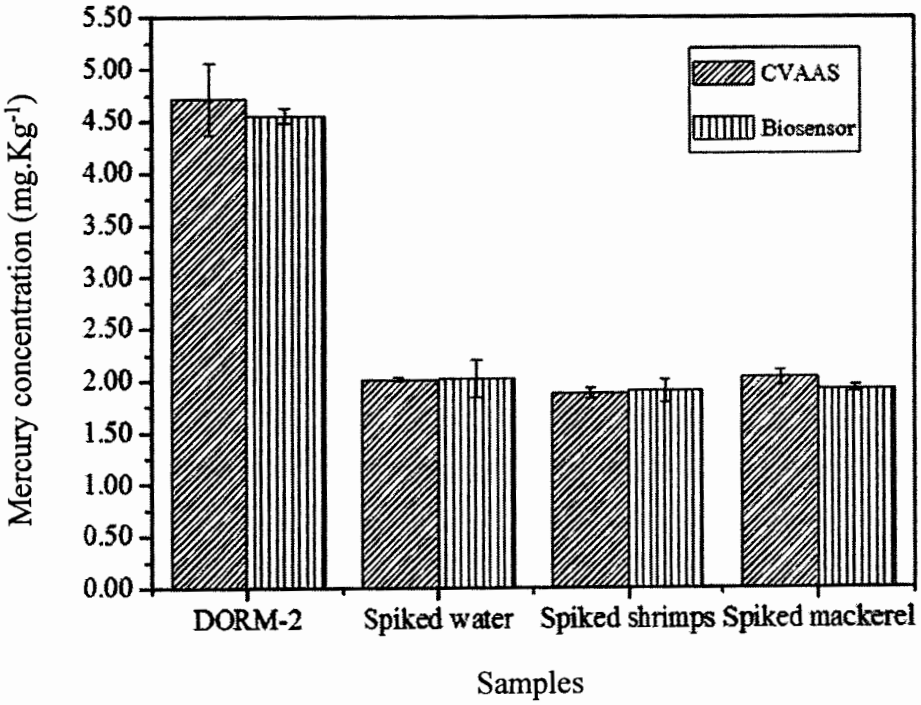

Figure 4.25 Comparison of mercury determination from CVAAS and biosensor

CHAPTER 5
CONCLUSION

The aim of this research has been focused on the development and application of a biosensor for the determination of mercury based on enzyme inhibition process which is indirect method. The biosensor was fabricated by GOx in Nafion solution immobilized on MnO_2/SPCE assembled with an electrochemical cell as a detector based on flow injection analysis (FIA).

As the results of optimization studies; an operating potential of +0.46 V versus Ag/AgCl, supporting electrolyte of 0.1 $mol.L^{-1}$ phosphate buffer solution at pH 7.0, GOx loading of 80 $U.cm^{-2}$, substrate concentration of 200 $mg.L^{-1}$ glucose solution, injection volume of 250 µL and flow rate of 1.2 $mL.min^{-1}$ were obtained.

The determination of mercury was obtained of the linear range of 100 - 1000 $\mu g.L^{-1}$, and the inhibition degree varies according to the following linear equation $y = 0.0407x - 0.5760$ with the correlation coefficient of $r^2 = 0.9975$ and the sensitivity of 0.0407 $\%.L.\mu g^{-1}$. The limit of detection was 29 $\mu g.L^{-1}$ mercury (3 SD/slope) and limit of quantification was 96 $\mu g.L^{-1}$(10 SD/slope). The repeatability and reproducibility were 3.68% (10 measurements, 100 $\mu g.L^{-1}$ mercury) and 4.40% (3sensor), respectively.

After inhibition, the GOx/MnO_2/SPCE surface regenerated by 0.05 $mol.L^{-1}$ EDTA for 2 min was obtained. The storage stability of the GOx/MnO_2/SPCE has been investigated after the electrodes were stored in dry conditions at 4 °C in a refrigerator and its stability yielded for 21 days with relative current of 62%. Furthermore, the study of interferences of an inhibition-based enzyme catalytic process with heavy metals were investigated on their possible interfering effect on the determination of mercury under the same experimental conditions; the results are only Pb (II), Cd (II) and Cu (II) having a significant effect at high concentration of 10 $mg.L^{-1}$ but no effect at the 1 $mg.L^{-1}$.

The kinetic catalytic reaction of GOx was studied. The apparent Michaelis-Menten (K_m) constant and I_{max} could be calculated to be 5.80 mmol.L^{-1} and 4.41 μA, respectively. The obtained K_m was in very good agreement with the value of the free enzyme GOx (K_m = 6.2 mmol.L^{-1}). Besides, the kinetic inhibition of GOx was determined. The K_m and I_{max} were obtained with 5.80 mmol.L^{-1} and 2.70 μA, respectively and compared with free enzyme. The results was found that no change K_m but I_{max} decreased is the unique of noncompetitive inhibition.

Furthermore, the accuracy of GOx/MnO_2/SPCE to detect mercury was studied; GOx/MnO_2/SPCE was applied to certified reference material (DORM-2) and real samples. As the results, the agreement with expected results is excellent, with the recovered values all falling 5 % of the expected values. In order to test the developed method, mercury concentration in samples analyzed by the developed method was compared with CVAAS. The analyzed mercury concentrations were compared with the values measured by the CVAAS method, using paired *t*-test. The results indicated that the mercury concentration as determined from the two methods is significantly agreement.

REFERENCES

REFERENCES

[1] Counter, S. A. and Buchanan, L. H. "Mercury exposure in children: a review", **Toxicology and Applied Pharmacology**. 198(2): 209-230; July, 2004.

[2] Manzoori, H. and et al. "Determination of mercury by cold vapour atomic absorption spectrometry after preconcentration with dithizone immobilized on surfactant-coated alumina", **Journal of Analytical Atomic Spectrometry**. 13(4): 305-308; April, 1998.

[3] Hight, S. C. and Cheng, J. "Determination of total mercury in seafood by cold vapor-atomic absorption spectroscopy (CVAAS) after microwave decomposition", **Food Chemistry**. 91(3): 557-570; July, 2005.

[4] Puk, R. and Weber, J. H. "Determination of mercury(II), monomethylmercury cation, dimethylmercury and diethylmercury by hydride generation, cryogenic trapping and atomic absorption spectrometric detection", **Analytica Chimica Acta**. 292(1–2): 175-183; June, 1994.

[5] Mao Tseng, C. and et al. "Rapid determination of inorganic mercury and methylmercury in biological reference materials by gydride generation, cryofocusing, atomic absorption spectrometry after open focused microwave-assisted alkaline digestion", **Journal of Analytical Atomic Spectrometry**. 12(7): 743-750; July, 1997.

[6] Han, F. and et al. "Rapid determination of mercury in plant and soil samples using inductively coupled plasma atomic emission spectroscopy, a comparative study", **Water, Air, and Soil Pollution**. 170(1-4): 161-171; February, 2006.

[7] Campbell, M. J. and et al. "Influence of chemical species on the determination of mercury in a biological matrix (cod muscle) using inductively coupled plasma mass spectrometry", **Journal of Analytical Atomic Spectrometry**. 7(4): 617-621; April, 1992.

REFERENCES (CONTINUED)

[8] Nixon, D. E., Burritt, M. F. and Moyer, T. P. "The determination of mercury in whole blood and urine by inductively coupled plasma mass spectrometry", **Spectrochimica Acta Part B: Atomic Spectroscopy**. 54(8): 1141-1153; August, 1999.

[9] Tyson, J. F. "Flow injection analysis techniques for atomic-absorption spectrometry; a review", **Analyst**. 110(5): 419-429; May, 1985.

[10] Cowell, D. C. and et al. "The detection and identification of metal and organic pollutants in potable water using enzyme assays suitable for sensor development", **Biosensors and Bioelectronics**. 10(6–7): 509-516; September, 1995.

[11] Gogol, E. and et al. "Amperometric biosensors based on nafion coated screen-printed electrodes for the determination of cholinesterase inhibitors", **Talanta**. 53(2): 379-389; November, 2000.

[12] Andreescu, S., Fournier, D. and Marty, J. L. "Development of highly sensitive sensor based on bioengineered acetylcholinesterase immobilized by affinity method", **Analytical Letters**. 36(9): 1865-1885; February, 2003.

[13] Han, S. and et al. "A methylene blue-mediated enzyme electrode for the determination of trace mercury (II), mercury (I), methylmercury, and mercury–glutathione complex", **Biosensors and Bioelectronics**. 16(1): 9-16; January, 2001.

[14] Alexander, P. W. and Rechnitz, G. A. "Enzyme inhibition assays with an amperometric glucose biosensor based on a thiolate self-assembled monolayer", **Electroanalysis**. 12(5): 343-350; March, 2000.

[15] Krawczynski vel Krawczyk, T., Moszczynska, M. s. and Trojanowicz, M. "Inhibitive determination of mercury and other metal ions by potentiometric urea biosensor", **Biosensors and Bioelectronics**. 15(11): 681-691; December, 2000.

REFERENCES (CONTINUED)

[16] Korpan, Y. and et al. "A novel enzyme biosensor for steroidal glycoalkaloids detection based on pH-sensitive field effect transistors", **Bioelectrochemistry**. 55(1): 9-11; January, 2002.

[17] Arkhypova, V. N. and et al. "Development and optimisation of biosensors based on pH-sensitive field effect transistors and cholinesterases for sensitive detection of solanaceous glycoalkaloids", **Biosensors and Bioelectronics**. 18(8): 1047-1053; August, 2003.

[18] Guerrieri, A. and et al. "A disposable amperometric biosensor for rapid screening of anticholinesterase activity in soil extracts", **Analyst**. 127(1): 5-7; January, 2002.

[19] Ivanov, A. and et al. "Cholinesterase sensors based on screen-printed electrodes for detection of organophosphorus and carbamic pesticides", **Analytical and Bioanalytical Chemistry**. 377(4): 624-631; October, 2003.

[20] Guascito, M. R. and et al. "Inhibitive determination of metal ions by an amperometric glucose oxidase biosensor: Study of the effect of hydrogen peroxide decomposition", **Sensors and Actuators B: Chemical**. 131(2): 394-402; May, 2008.

[21] Liu, J. X. and et al. "Determination of trace mercury in compost extract by inhibition based glucose oxidase biosensor", **Transactions of Nonferrous Metals Society of China**. 19(1): 235-240; February, 2009.

[22] Pirvutoiu, S. and et al. "Flow injection analysis of mercury (II) based on enzyme inhibition and thermometric detection", **Analyst**. 126(9): 1612-1616; November, 2001.

[23] Shi, R., Stein, K. and Schwedt, G. "Determination of mercury(II) traces in drinking water by inhibition of an urease reactor in a flow injection analysis (FIA) system", **Fresenius' Journal of Analytical Chemistry**. 357(6): 752-755; March, 1997.

REFERENCES (CONTINUED)

[24] Compagnone, D. and et al. "Fast amperometric FIA procedure for heavy metal detection using enzyme inhibition", **Analytical Letters**. 34(1): 17-27; February, 2001.

[25] Eggins, B. **Biosensors: an introduction**. New York: Wiley, Teubner, 1996.

[26] Canh, T. M. **Biosensors**. Paris: Chapman, Hall, 1993.

[27] Mohanty, S. P. and Kougianos, E. "Biosensors: a tutorial review", **Potentials, IEEE**. 25(2): 35-40; January, 2006.

[28] McNaught, A. and Wilinson, A. **Compendium of chemical terminology**. Oxford: Blackwell Scientific, 1997.

[29] Monošík, R., Streďanský, M. and Šturdík, E., "Biosensors - classification, characterization and new trends", **In Acta Chimica Slovaca**. 5(1): 109-120; January, 2012.

[30] Turner, A. P. "Biosensors-sense and sensitivity", **Science**. 290(5495): 1315-1317; November, 2000.

[31] Guilbault, G. G. and et al. "Biosensors - 42 years and counting", **Analytical Letters**. 37(8): 1481-1496; December, 2004.

[32] Webb, E. C. **Enzyme nomenclature 1992, Recommendations of the Nomenclature Committee of the International Union of Biochemistry and Molecular Biology on the Nomenclature and Classification of Enzymes**. n.p. : Academic Press, 1992.

[33] Bairoch, A. "The enzyme data bank", **Nucleic acids research**. 21(13): 3155-3156; March, 1993.

[34] Marks, R. **Handbook of biosensors and biochips**. Portland: Wiley, 2007.

[35] Copeland, R. A. **Enzymes: a practical introduction to structure, mechanism, and data analysis**. New York: Wiley-VCH, 2000.

[36] Leavingbio, "Enzyme Action", **Enzyme**. http://leavingbio.net/enzymes.htm. April 8, 2014.

REFERENCES (CONTINUED)

[37] Datta, S., Christena, L. R. and Rajaram, Y. R. S. "Enzyme immobilization: an overview on techniques and support materials", **3 Biotech**. 3(1): 1-9; February, 2013.

[38] Pimpen, P. "Enzyme immobilization", **Enzyme**. http://www.foodnetwork solution.com/wiki/word/4162/immobilized-enzyme. May 25, 2014.

[39] Docstoc. "Enzyme immobilization", **Immobilized Enzyme Systems**. http://www.docstoc.com/docs/110852920/lecture-notes-enzyme-immobilization-of-enzyme. May 25, 2014.

[40] Rensselaer. "Crosslinking", **Cross-Linking**. http://www.rpi.edu/dept/chem-eng/Biotech-Environ/IMMOB/crosslink.htm. May 25, 2014.

[41] Kobos, R. "Enzyme-based electrochemical biosensors", **TrAC Trends in Analytical Chemistry**. 6(1): 6-9; January, 1987.

[42] Wang, Y. and Caruso, F. "Mesoporous Silica Spheres as Supports for Enzyme Immobilization and Encapsulation", **Chemistry of Materials**. 17(5): 953-961; February, 2005.

[43] Bankar, S. B. and et al. "Glucose oxidase - an overview", **Biotechnology Advances**. 27(4): 489-501; July, 2009.

[44] Rossi, L., Quach, A. and Rosenzweig, Z. "Glucose oxidase–magnetite nanoparticle bioconjugate for glucose sensing", **Analytical and Bioanalytical Chemistry**. 380(4): 606-613; October, 2004.

[45] Zhao, Z. W. and et al. "A novel amperometric biosensor based on ZnO:Co nanoclusters for biosensing glucose", **Biosensors and Bioelectronics**. 23(1): 135-139; August, 2007.

[46] Kong, T. and et al. "An amperometric glucose biosensor based on the immobilization of glucose oxidase on the ZnO nanotubes", **Sensors and Actuators B: Chemical**. 138(1): 344-350; April, 2009.

[47] Bachan Upadhyay, L. S. and Verma, N. "Enzyme inhibition based biosensors: a review", **Analytical Letters**. 46(2): 225-241; January, 2013.

REFERENCES (CONTINUED)

[48] Amine, A. and et al. "Enzyme inhibition-based biosensors for food safety and environmental monitoring", **Biosensors & bioelectronics**. 21(8): 1405-1423; February, 2006.

[49] Aiken, A. M. and et al. "Heavy metal-induced inhibition of Aspergillus niger nitrate reductase: applications for rapid contaminant detection in aqueous samples", **Analytica Chimica Acta**. 480(1): 131-142; March, 2003.

[50] Gibbs, P. N., Gore, M. G. and Jordan, P. M. "Investigation of the effect of metal ions on the reactivity of thiol groups in human 5-aminolaevulinate dehydratase", **The Biochemical journal**. 225(3): 573-580; March, 1985.

[51] Evtugyn, G. A., Budnikov, H. C. and Nikolskaya, E. B. "Sensitivity and selectivity of electrochemical enzyme sensors for inhibitor determination", **Talanta**. 46(4): 465-484; August, 1998.

[52] Mohammadi, H. and et al. "Mercury-enzyme inhibition assays with an amperometric sucrose biosensor based on a trienzymatic-clay matrix", **Analytica Chimica Acta**. 543(1–2): 143-149; July, 2005.

[53] Gayet, J. C. and et al. "Detection of heavy metal salts with biosensors built with an oxygen electrode coupled to various immobilized oxidases and dehydrogenases", **Biosensors and Bioelectronics**. 8(3-4): 177-183; April, 1993.

[54] Ebright, Y. W. and et al. "Incorporation of an EDTA-metal complex at a rationally selected site within a protein: application to EDTA-iron DNA affinity cleaving with catabolite gene activator protein (CAP) and Cro", **Biochemistry**. 31(44): 10664-10670; November, 1992.

[55] Turkusic, E. and et al. "Amperomtric determination of glucose with an MnO_2 and glucose oxidase bulk-modified screen-printed carbon ink biosensor", **Analytical Letters**. 34(15): 2633-2647; November, 2001.

[56] Turkusic, E. and et al. "Amperometric determination of bonded glucose with an MnO_2 and glucose oxidase bulk-modified screen-printed electrode using flow-injection analysis", **Talanta**. 65(2): 559-564; January, 2005.

REFERENCES (CONTINUED)

[57] Ruzicka, J. and Hansen, E. H. **Flow Injection Analysis**. The United State of America: A wiley interscience, 1975.

[58] Kissinger, P. T. and Heineman, W. R. "Cyclic voltammetry", **Journal of Chemical Education**. 60(9): 702; March, 1983.

[59] Bard, A. J. and Faulkner, L. R. **Electrochemical methods: fundamentals and applications**. New York: John wiley, SONS. INC., 1980.

[60] Marinov, I. and et al. "Amperometric inhibition-based detection of organophosphorus pesticides in unary and binary mixtures employing flow-injection analysis", **Sensors and Actuators B: Chemical**. 160(1): 1098-1105; December, 2011.

[61] Mulchandani, A. and et al. "Biosensors for direct determination of organophosphate pesticides", **Biosensors and Bioelectronics**. 16(4-5): 225-230; June, 2001.

[62] La Rosa, C. and et al. "Amperometric flow-through biosensor for the determination of pesticides", **Analytica Chimica Acta**. 308(1-3): 129-136; June, 1995.

[63] Liu, G. and Lin, Y. "Biosensor based on self-assembling acetylcholinesterase on carbon nanotubes for flow injection/amperometric detection of organophosphate pesticides and nerve agents", **Analytical Chemistry**. 78(3): 835-843; February, 2006.

[64] Li, X. H. and et al. "Amperometric biosensor based on immobilization acetylcholinesterase on manganese porphyrin nanoparticles for detection of trichlorfon with flow injection analysis system", **Electroanalysis**. 19(24): 2551-2557; December, 2007.

[65] Zheng, Y. H. and et al. "Detection of dichlorvos residue by flow injection calorimetric biosensor based on immobilized chicken liver esterase", **Journal of Food Engineering**. 74(1): 24-29; May, 2006.

REFERENCES (CONTINUED)

[66] Mohammadi, H. and et al. "Determination of mercury (II) by invertase enzyme inhibition coupled with batch injection analysis", **Analyst**. 127(8): 1088-1093; April, 2002.

[67] Beyene, N. W. and et al. "(Bio) sensors based on manganese dioxide-modified carbon substrates: retrospections, further improvements and applications", **Talanta**. 64(5): 1151-1159; December, 2004.

[68] Melo, J. V. and et al. "Urea Biosensors Based on Immobilization of Urease into Two Oppositely Charged Clays (Laponite and Zn−Al Layered Double Hydroxides)", **Analytical Chemistry**. 74(16): 4037-4043; September, 2002.

[69] Kuswandi, B. "Simple optical fibre biosensor based on immobilised enzyme for monitoring of trace heavy metal ions", **Analytical and Bioanalytical Chemistry**. 376(7): 1104-1110; August, 2003.

[70] Rodriguez, B. B., Bolbot, J. A. and Tothill, I. E. "Development of urease and glutamic dehydrogenase amperometric assay for heavy metals screening in polluted samples", **Biosensors and Bioelectronics**. 19(10): 1157-1167; May, 2004.

[71] Bello Rodringuez, B., Bolbot, J. A. and Tothill, I. E. "Urease-glutamic dehydrogenase biosensor for screening heavy metals in water and soil samples", **Analytical & bioanalytical chemistry**. 380(2): 284-292; September, 2004.

[72] Alexander, P. W. and Rechnitz, G. A. "Enzyme Inhibition Assays with an Amperometric Glucose Biosensor Based on a Thiolate Self-Assembled Monolayer", **Electroanalysis**. 12(5): 343-350; March, 2000.

[73] Pirvutoiu, S. and et al. "Application of the enzyme thermistor for determination of mercury and other heavy metals using free and immobilised alcohol oxidase", **Romania Biotechnological Letters**. 7975-986; November, 2002.

REFERENCES (CONTINUED)

[74] Ciucu, A. and et al. "Biosensors for heavy metals determination based on enzyme inhibition", **UPB Buletin Stiintific, Series B: Chemistry and Materials Science (Romania)**. 63(4): 33-44; April, 2001.

[75] Doong, R. A. and Tsai, H. C. "Immobilization and characterization of sol-gel-encapsulated acetylcholinesterase fiber-optic biosensor", **Analytica Chimica Acta**. 434(2): 239-246; May, 2001.

[76] Tsai, H. C. and Doong, R. A. "Simultaneous determination of pH, urea, acetylcholine and heavy metals using array-based enzymatic optical biosensor", **Biosensors and Bioelectronics**. 20(9): 1796-1804; March, 2005.

[77] Malitesta, C. and Guascito, M. R. "Heavy metal determination by biosensors based on enzyme immobilised by electropolymerisation", **Biosensors and Bioelectronics**. 20(8): 1643-1647; February, 2005.

[78] May May, L. and Russell, D. A. "Novel determination of cadmium ions using an enzyme self-assembled monolayer with surface plasmon resonance", **Analytica Chimica Acta**. 500(1): 119-125; December, 2003.

[79] Soldatkin, A. and et al. "Improvement of urease based biosensor characteristics using additional layers of charged polymers", **Analytica Chimica Acta**. 403(1): 25-29; January, 2000.

[80] Evtyugin, G. and et al. "A cholinesterase sensor based on a graphite electrode modified with 1, 3-disubstituted calixarenes", **Journal of Analytical Chemistry**. 58(12): 1151-1156; December, 2003.

[81] Zeng, G. M. and et al. "Determination of trace chromium (VI) by an inhibition-based enzyme biosensor incorporating an electropolymerized aniline membrane and ferrocene as electron transfer mediator", **International Journal of Environmental Analytical Chemistry**. 84(10): 761-774; September, 2004.

REFERENCES (CONTINUED)

[82] Volotovsky, V., Young Jung, N. and Kim, N. "Urease-based biosensor for mercuric ions determination", **Sensors and Actuators B: Chemical**. 42(3): 233-237; August, 1997.

[83] Ghica, M. and Brett, C. A. "Glucose oxidase inhibition in poly(neutral red) mediated enzyme biosensors for heavy metal determination", **Microchimica Acta**. 163(3-4): 185-193; October, 2008.

[84] Cosnier, S. and et al. "A fast and direct amperometric determination of Hg^{2+} by a bienzyme electrode based on the competitive activities of glucose oxidase and laccase", **Electroanalysis**. 23(8): 1776-1779; August, 2011.

85] Samphao, A. and et al. "Indirect determination of mercury by inhibition of glucose oxidase immobilized on a carbon paste electrode", **International Journal of Electrochemical Science**. 7(1): 1001-1010; February, 2012.

[86] Bertocchi, P. and et al. "Flow injection analysis of mercury (II) in pharmaceuticals based on enzyme inhibition and biosensor detection", **Journal of Pharmaceutical and Biomedical Analysis**. 20(1-2): 263-269; June, 1999.

[87] Jeanty, G. and et al. "Flow-injection amperometric determination of pesticides on the basis of their inhibition of immobilized acetylcholinesterases of different origin", **Analytical and Bioanalytical Chemistry**. 373(8): 691-695; June, 2002.

[88] Shi, M. and et al. "A mediator-free screen-printed amperometric biosensor for screening of organophosphorus pesticides with flow-injection analysis (FIA) system", **Talanta**. 68(4): 1089-1095; February, 2006.

[89] Compagnone, D. and et al. "Amperometric biosensors for the determination of heavy metals", European Symposium on Optics for Environmental and Public Safety, **International Society for Optics and Photonics.** 141-152; 1995.

REFERENCES (CONTINUED)

[90] BASi your scientific connection. "BASi Reference Electrode", **HPLC Electrochemical detector**. http:// www.basinc.com/products/ec/flowcells. php. May 10, 2015.

[91] Alonso, G. A. and et al. "An approach to an inhibition electronic tongue to detect on-line organophosphorus insecticides using a computer controlled multi-commuted flow system", **Sensors**. 11(4): 3791-3802; March, 2011.

[92] Hineman, A. **"Determination of As, Se and Hg in Waters by Hydride Generation/Cold Vapor Atomic Absorption Spectroscopy"**. Ontario, Canada: Perkin Elmer, Inc., 2014.

[93] Schachl, K. and et al. "Amperometric determination of hydrogen peroxide with a manganese dioxide-modified carbon paste electrode using flow injection analysis", **Analyst**. 122(9): 985-989; April, 1997.

[94] Schachl, K. and et al. "Amperometric determination of hydrogen peroxide with a manganese dioxide film-modified screen printed carbon electrode", **Fresenius' Journal of Analytical Chemistry**. 362(2): 194-200; September, 1998.

[95] Chey, C. O. and et al. "Indirect determination of mercury ion by inhibition of a glucose biosensor based on ZnO nanorodos", **Sensors**. 1215063-15077; November, 2012.

[96] Sotiropoulou, S. and Chaniotakis, N. A. "Lowering the detection limit of the acetylcholinesterase biosensor using a nanoporous carbon matrix", **Analytica Chimica Acta**. 530(2): 199-204; February, 2005.

[97] Shan, D., Mousty, C. and Cosnier, S. "Subnanomolar cyanide detection at polyphenol oxidase/clay biosensors", **Analytical Chemistry**. 76(1): 178-183; January, 2004.

[98] Ciucu, A. A., Negulescu, C. and Baldwin, R. P. "Detection of pesticides using an amperometric biosensor based on ferophthalocyanine chemically modified carbon paste electrode and immobilized bienzymatic system", **Biosensors and Bioelectronics**. 18(2): 303-310; March, 2003.

REFERENCES (CONTINUED)

[99] Kok, F. N., Bozoglu, F. and Hasirci, V. "Construction of an acetylcholinesterase-choline oxidase biosensor for aldicarb determination", **Biosensors and Bioelectronics**. 17(6): 531-539; June, 2002.

[100] Dzyadevych, S. V. and et al. "Early-warning electrochemical biosensor system for environmental monitoring based on enzyme inhibition", **Sensors and Actuators B: Chemical**. 105(1): 81-87; February, 2005.

[101] Chouteau, C. and et al. "A bi-enzymatic whole cell conductometric biosensor for heavy metal ions and pesticides detection in water samples", **Biosensors and Bioelectronics**. 21(2): 273-281; August, 2005.

[102] Liu, Y. and et al. "The direct electron transfer of glucose oxidase and glucose biosensor based on carbon nanotubes/chitosan matrix", **Biosensors and Bioelectronics**. 21(6): 984-988; December, 2005.

[103] Athar, M. and Vohora, S. B. **Heavy Metals and Environment**. New York: New Age International (P) Limited, 1995.

[104] Callender, E. "Heavy metals in the environment-historical trends", **Treatise on geochemistry**. 15(3): 967-105; June, 2003.

[105] Uang, Y. M. and Chou, T. C. "Fabrication of glucose oxidase/polypyrrole biosensor by galvanostatic method in various pH aqueous solutions", **Biosensors and Bioelectronics**. 19(3): 141-147; November, 2003.

[106] Shan, D. and et al. "Development of amperometric biosensor for glucose based on a novel attractive enzyme immobilization matrix: Calcium carbonate nanoparticles", **Biosensors and Bioelectronics**. 22(8): 1612-1617; March, 2007.

[107] Fortier, G. and et al. "Development of Biosensors Based on Immobilization of Enzymes in Eastman AQ Polymer Coated with a Layer of Nafion", **Analytical Letters**. 23(9): 1607-1619; October, 1990.

APPENDICES

APPENDIX A
EXPERIMENTAL DETAILS

A.1 Enzymes immobilization and FIA set up

(a)

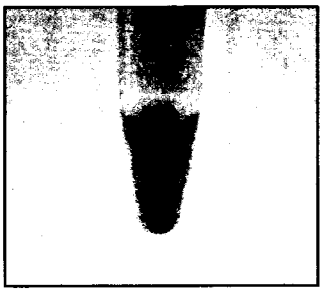

Enzyme casting solution

(b)

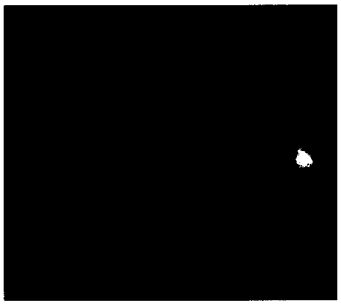

Biosensor preparation

(c)

A side view of the electrochemical cell

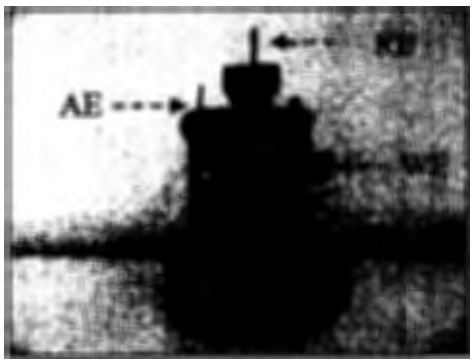

A back view of the electrochemical cell

Figure A.1 (a) GOx casting solution, (b) immobilization of GOx on to MnO_2/SPCE, (c) the electrochemical cell; where AE is auxiliary electrode (platinum electrode), RE is reference electrode (Ag/AgCl electrode) and WE is working electrode (GOx/MnO_2/SPCE)

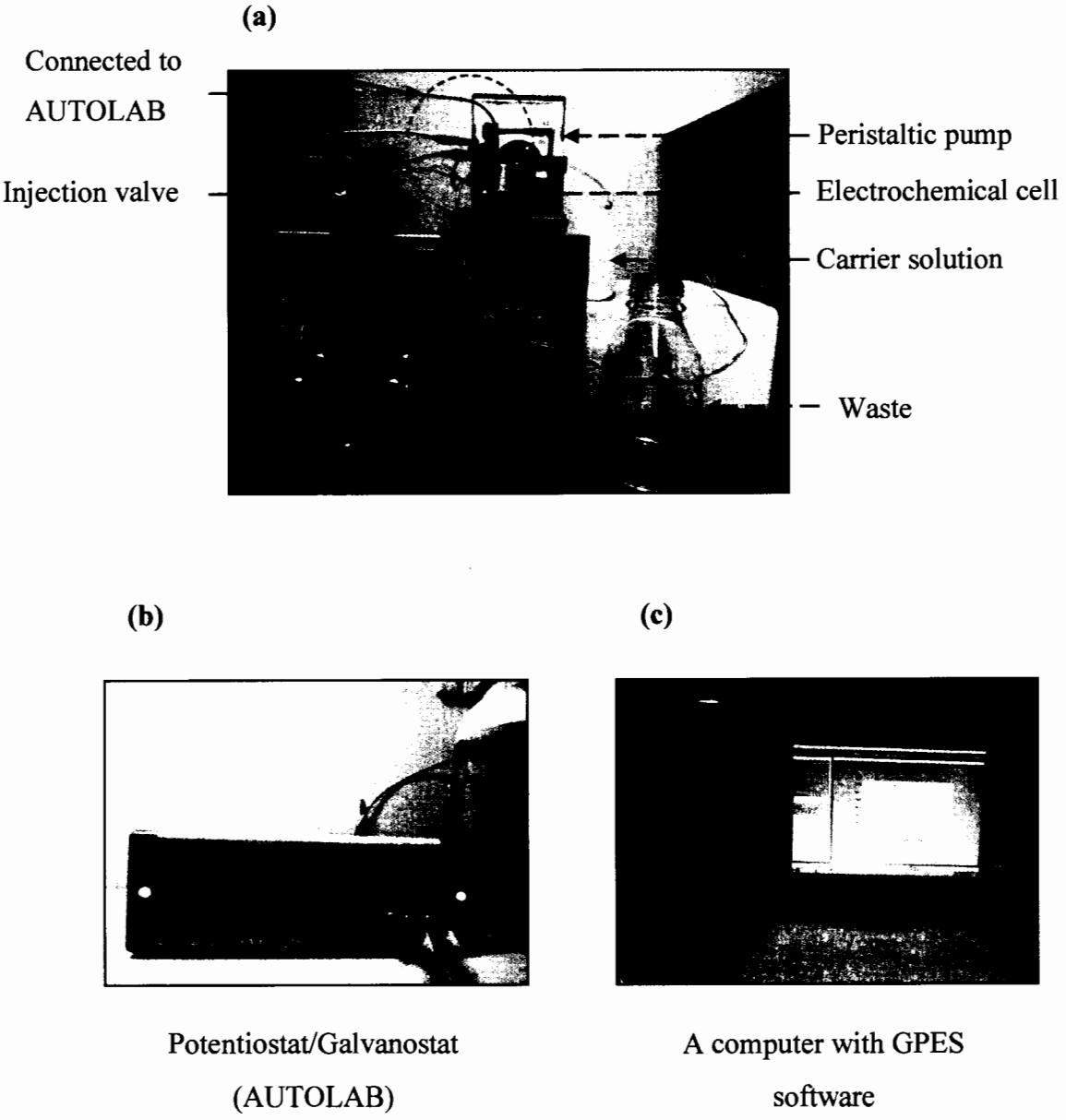

Figure A.2 (a) FIA set up, (b) potentiostat/galvanostat and (c) computer

APPENDIX B

THE RESULTS OF ANALYSIS

B.1 Parameters affecting on the responses of the GOx/MnO_2/SPCE

B.1.1 Operating potential

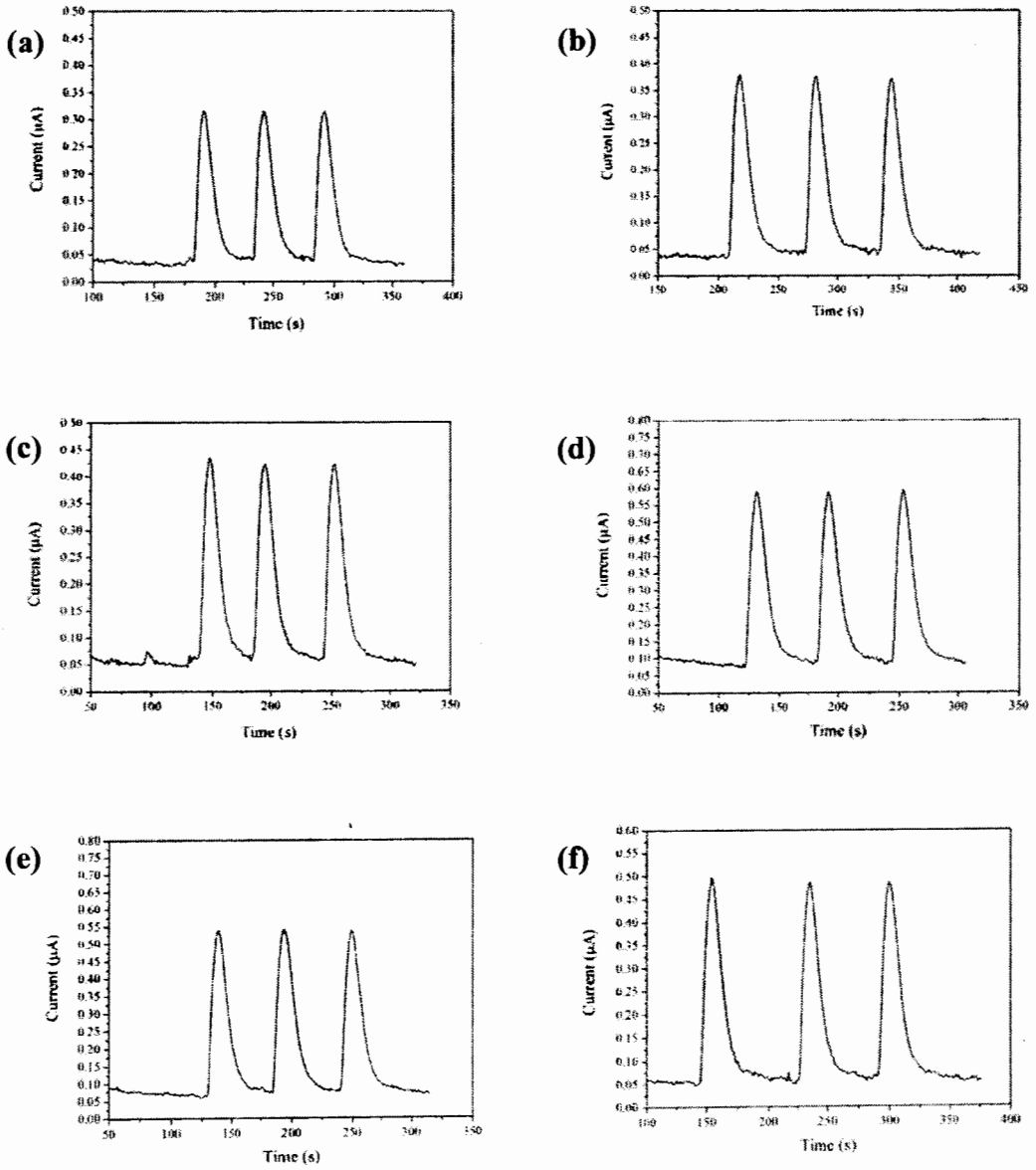

Figure B.1 Current responses on the operating potential; (a) +0.40 V, (b) +0.42 V, (c) +0.44 V, (d) +0.46 V, (e) +0.48 V and (e) +0.50 V versus Ag/AgCl

As the results shown in Figure 4.3 (chapter 4) current responses of GOx/MnO_2/SPCE on the operating potential (Figure B.1) are presented in the Table B.1.

Table B.1 The current of GOx/MnO_2/SPCE on the operating potential

Operating potential (V versus Ag/AgCl)	Average current (μA)*			
	1	2	3	(Mean ± SD); (n=3)
+ 0.40	0.282	0.287	0.278	0.282 ± 0.004
+ 0.42	0.340	0.331	0.349	0.340 ± 0.009
+ 0.44	0.380	0.410	0.452	0.414 ± 0.036
+ 0.46	0.493	0.497	0.500	0.497 ± 0.004
+ 0.48	0.475	0.473	0.451	0.466 ± 0.014
+ 0.50	0.435	0.428	0.433	0.432 ± 0.003

*Current (μA) is current of catalytic reaction (μA) – current of background (μA)

B.1.2 pH buffer solutions

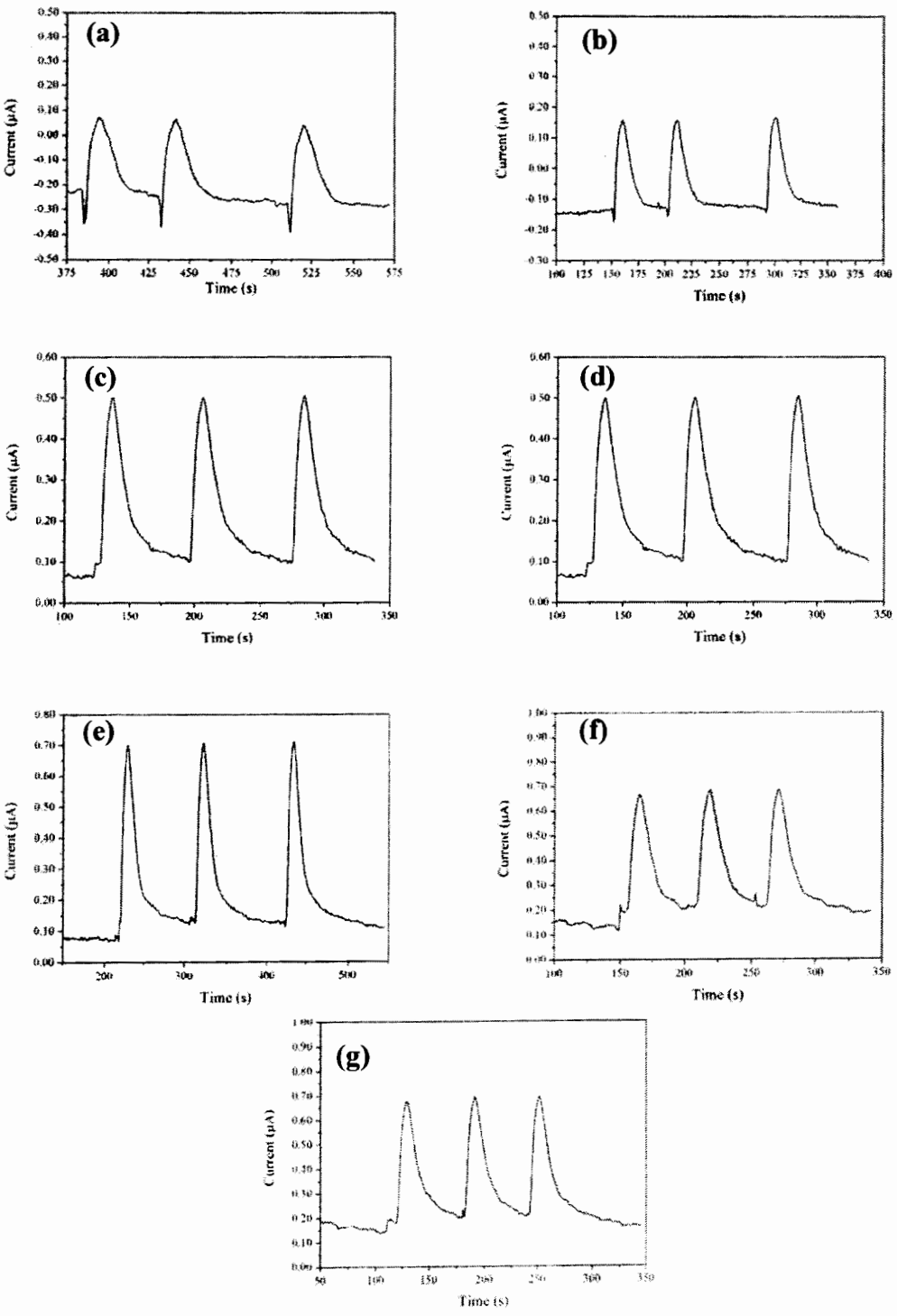

Figure B.2 Current responses on the pH of phosphate buffer; (a) pH 5.0, (b) pH 5.5, (c) pH 6.0, (d) pH 6.5, (e) pH 7.0, (f) pH 7.5 and (g) pH 8.0

As the results shown in Figure 4.4 (chapter 4) current responses of GOx/MnO_2/SPCE pH of phosphate buffer (Figure B.2) are presented in the Table B.2.

Table B.2 The current of GOx/MnO_2/SPCE on the pH phosphate buffer solution

pH buffer	Average current (μA)*			
	1	2	3	(Mean ± SD); (n=3)
5.0	0.297	0.257	0.301	0.285 ± 0.025
5.5	0.297	0.299	0.291	0.296 ± 0.004
6.0	0.348	0.339	0.356	0.348 ± 0.009
6.5	0.399	0.409	0.409	0.405 ± 0.006
7.0	0.575	0.580	0.592	0.582 ± 0.009
7.5	0.470	0.483	0.475	0.476 ± 0.007
8.0	0.477	0.486	0.475	0.479 ± 0.006

*Current (μA) is current of catalytic reaction (μA) – current of background (μA)

B.1.3 Enzyme loading

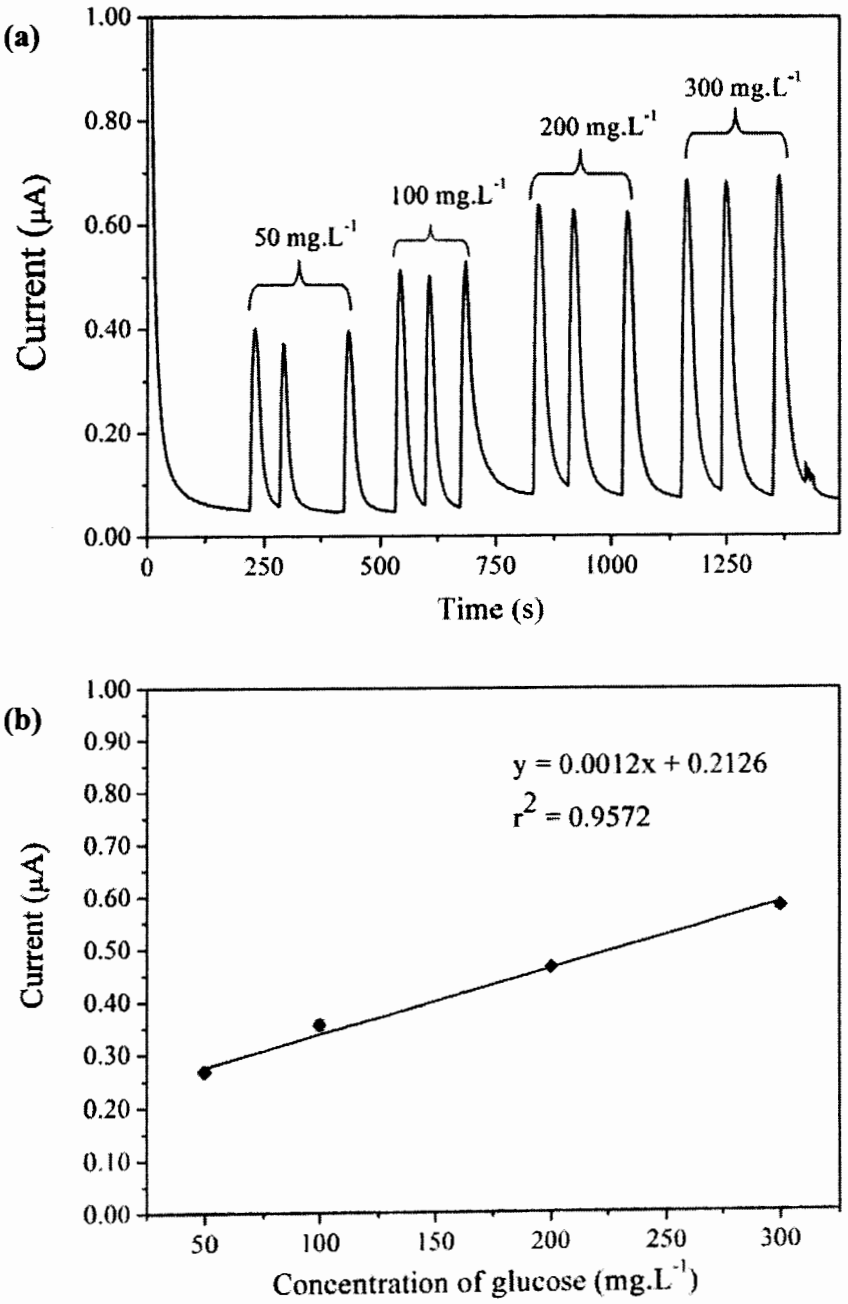

Figure B.3 (a) FIA grams of GOx/MnO_2/SPCE on 40 U.cm^{-2} GOx loading and (b) current responses of GOx/MnO_2/SPCE to glucose concentration 50 - 300 mg.L^{-1}

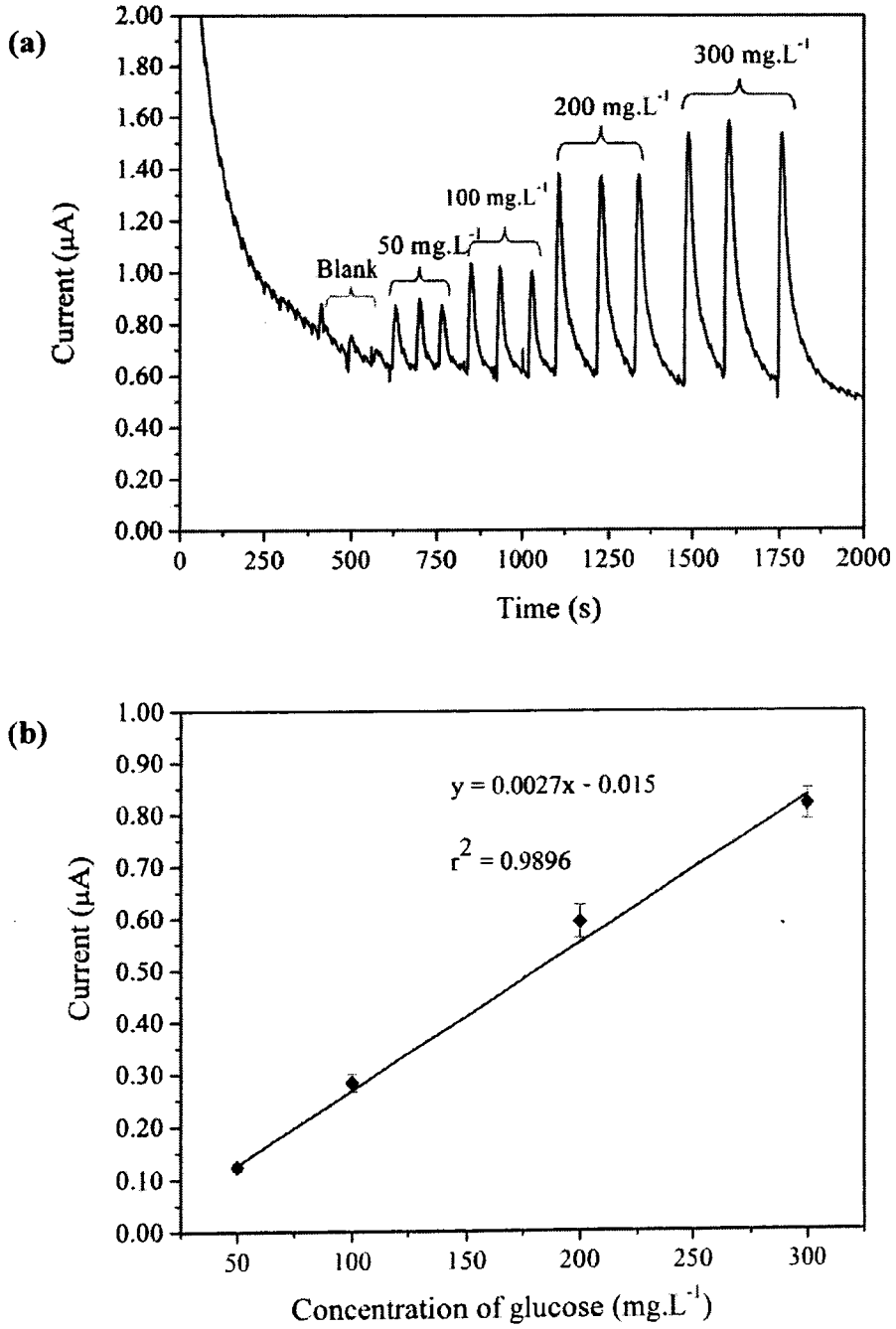

Figure B.4 (a) FIA grams of GOx/MnO_2/SPCE on 80 U.cm^{-2} GOx loading and (b) current responses of GOx/MnO_2/SPCE to glucose concentration 50 - 300 mg.L^{-1}

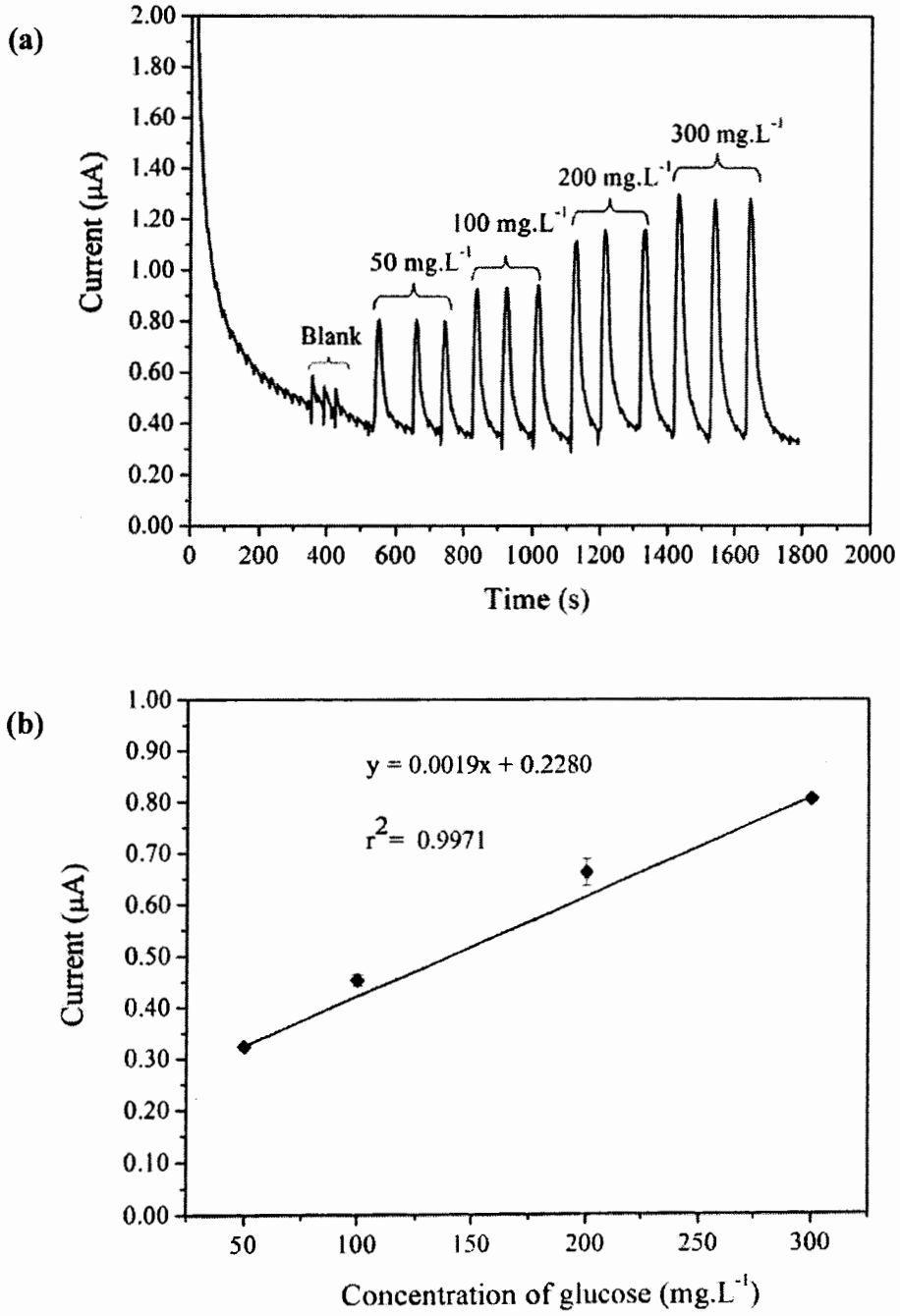

Figure B.5 (a) FIA grams of GOx/MnO_2/SPCE on 120 U.cm^{-2} GOx loading and (b) current responses of GOx/MnO_2/SPCE to glucose concentration 50 - 300 mg.L^{-1}

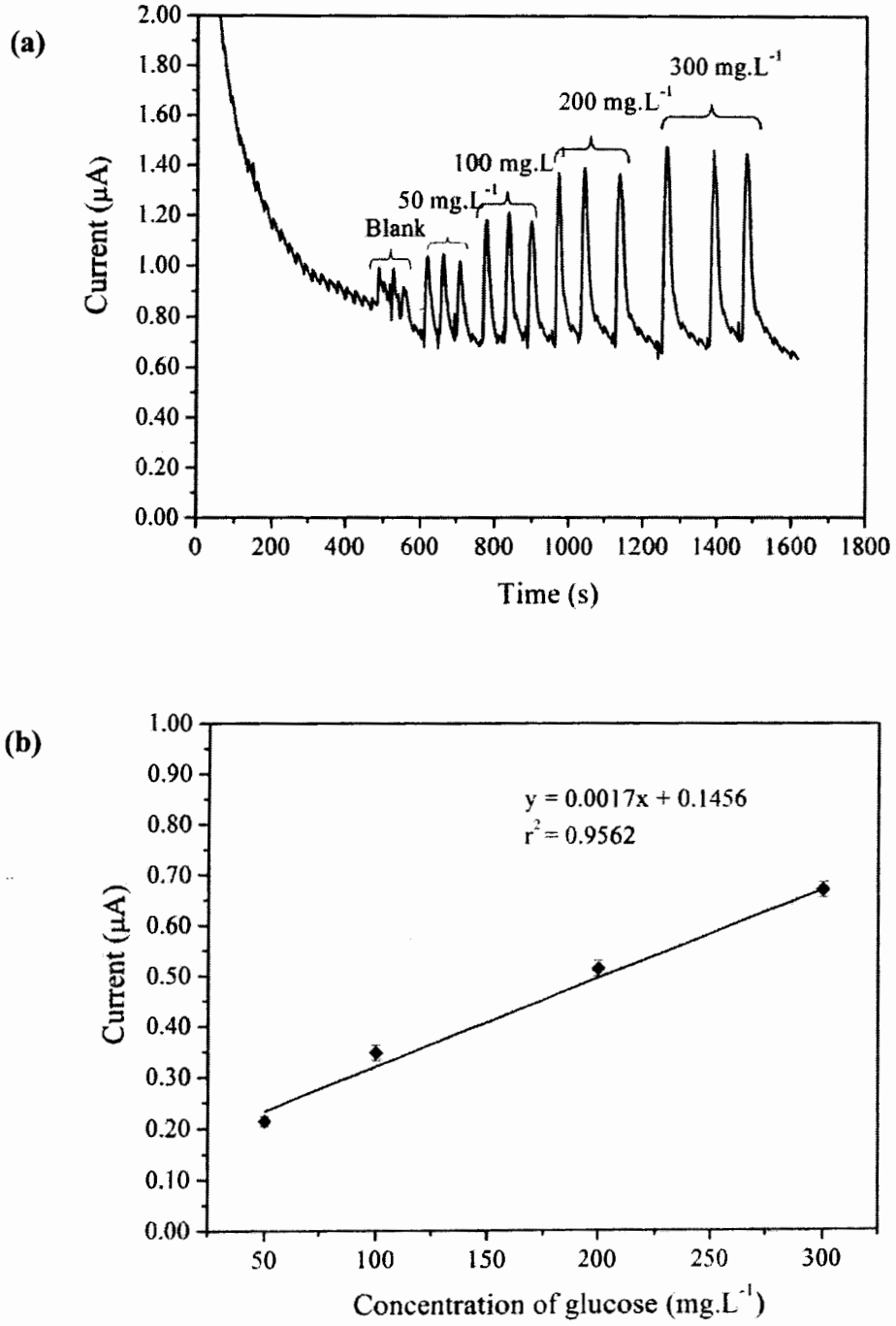

Figure B.6 (a) FIA grams of GOx/MnO_2/SPCE on 160 U.cm^{-2} GOx loading and (b) current responses of GOx/MnO_2/SPCE to glucose concentration 50 - 300mg.L^{-1}

B.1.4 Glucose loading

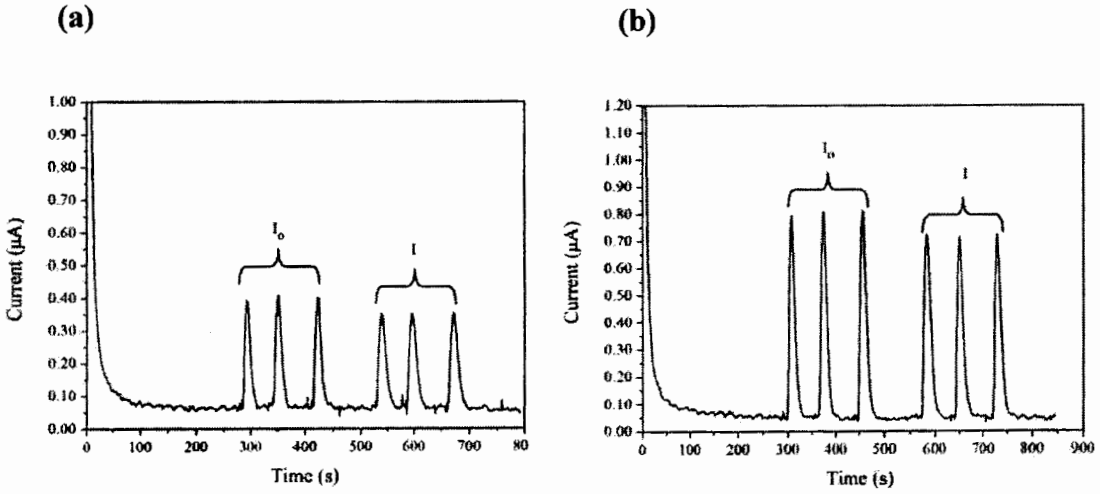

Figure B.7 Current responses of GOx/MnO_2/SPCE to glucose concentration; (a) 50 mg.L^{-1} and (b) 100 mg.L^{-1}

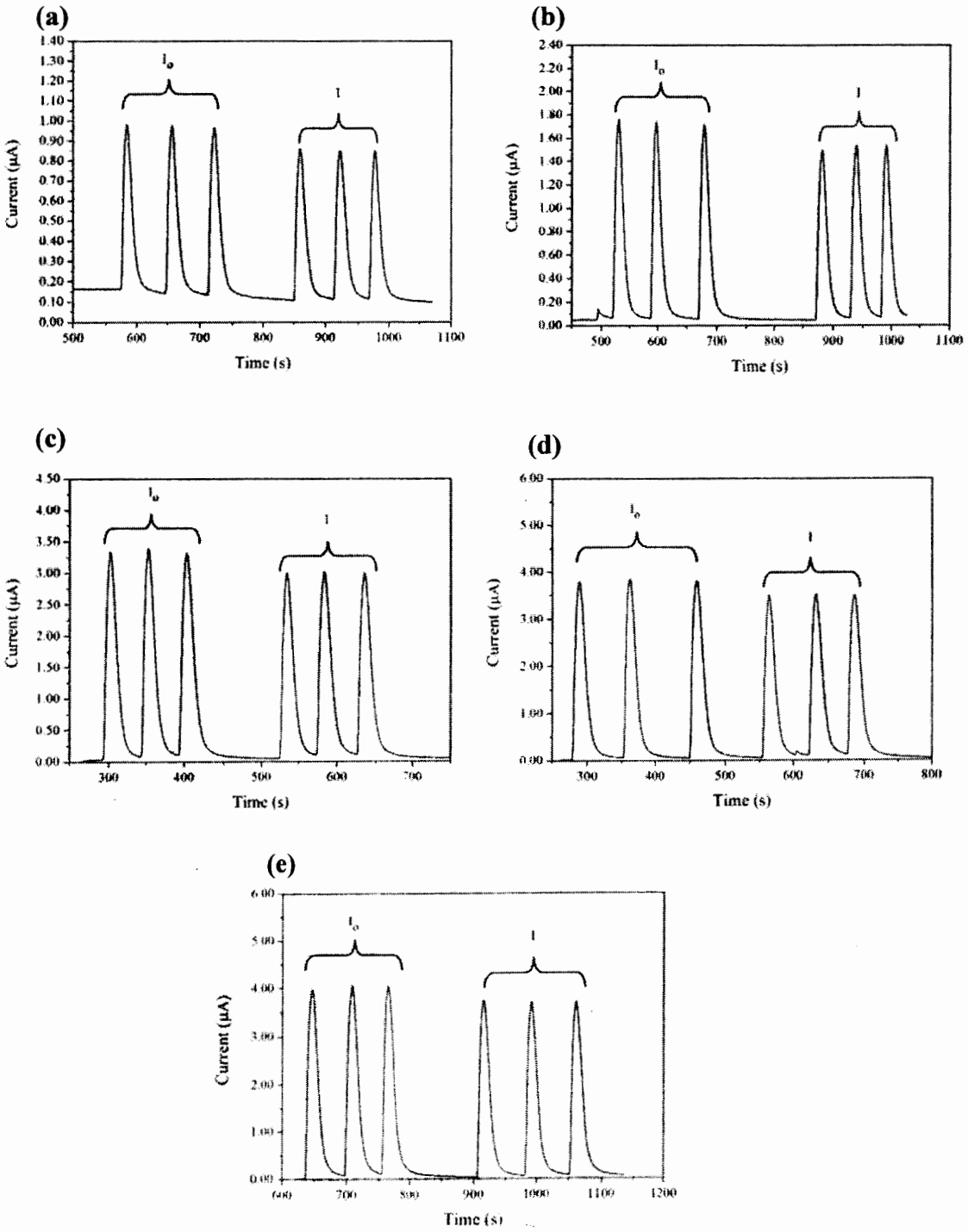

Figure B.8 Current responses of GOx/MnO_2/SPCE to glucose concentration; (a) 200 mg.L^{-1}, (b) 400 mg.L^{-1}, (c) 600 mg.L^{-1}, (d) 800 mg.L^{-1} and (e) 1000 mg.L^{-1}

As the results shown in Figure 4.6 (chapter 4) % inhibition of $GOx/MnO_2/SPCE$ to 0.5 $mg.L^{-1}$ mercury on the various glucose concentrations (Figure B.7 and B.8) are presented in the Table B.3.

Table B.3 The inhibition degree of $GOx/MnO_2/SPCE$ to glucose loading

Glucose concentration ($mg.L^{-1}$)	**% Inhibition**			
	1	**2**	**3**	**(Mean ± SD); (n=3)**
50	14.75	15.71	14.32	14.92 ± 0.71
100	15.46	16.10	14.93	15.49 ± 0.59
200	15.01	15.40	16.30	15.57 ± 0.66
400	12.87	13.93	12.85	13.22 ± 0.62
600	11.20	13.34	12.01	12.18 ± 1.08
800	8.17	8.65	8.09	8.30 ± 0.30
1000	7.13	6.91	4.71	6.25 ± 1.34

B.1.5 Injection volume

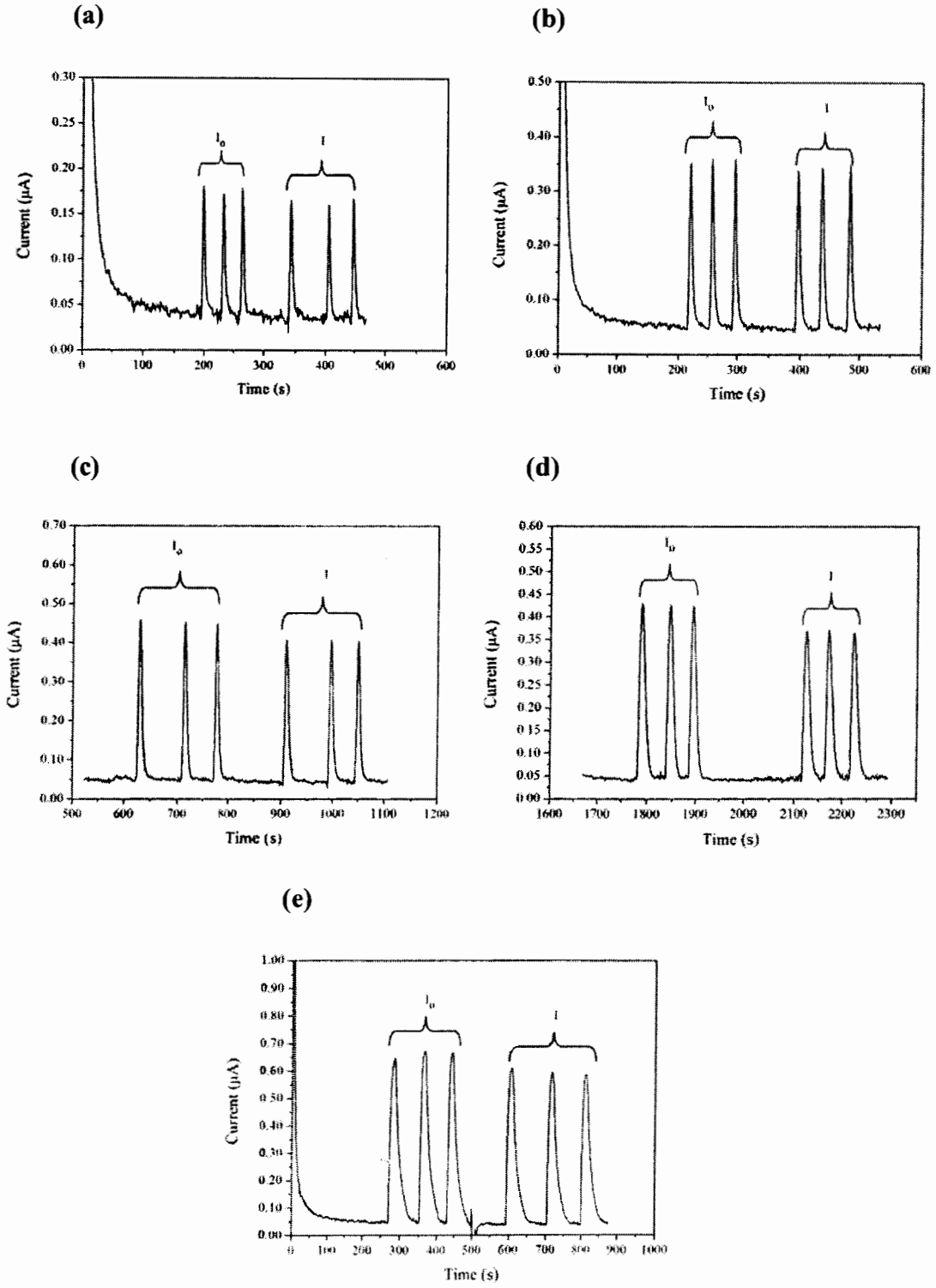

Figure B.9 Current response of GOx/MnO_2/SPCE to the injection volume: (a) 20 μL, (b) 50 μL, (c) 100 μL, (d) 250 μL and (e) 500 μL

As the results shown in Figure 4.7 (chapter 4) % inhibition of GOx/MnO_2/SPCE to 0.5 $mg.L^{-1}$ mercury on the various injection volumes (Figure B.9) are presented in the Table B.4.

Table B.4 The inhibition degree of GOx/MnO_2/SPCE on injection volume

Injection volume (µL)	% Inhibition			
	1	2	3	(Mean ± SD); (n=3)
20	3.94	2.37	2.67	2.99 ± 0.84
50	3.63	3.56	5.63	4.27 ± 1.88
100	8.76	10.32	8.51	9.19 ± 0.98
250	18.67	18.26	17.64	18.19 ± 0.52
500	13.33	14.87	12.95	13.72 ± 1.02

B.1.6 Flow rate

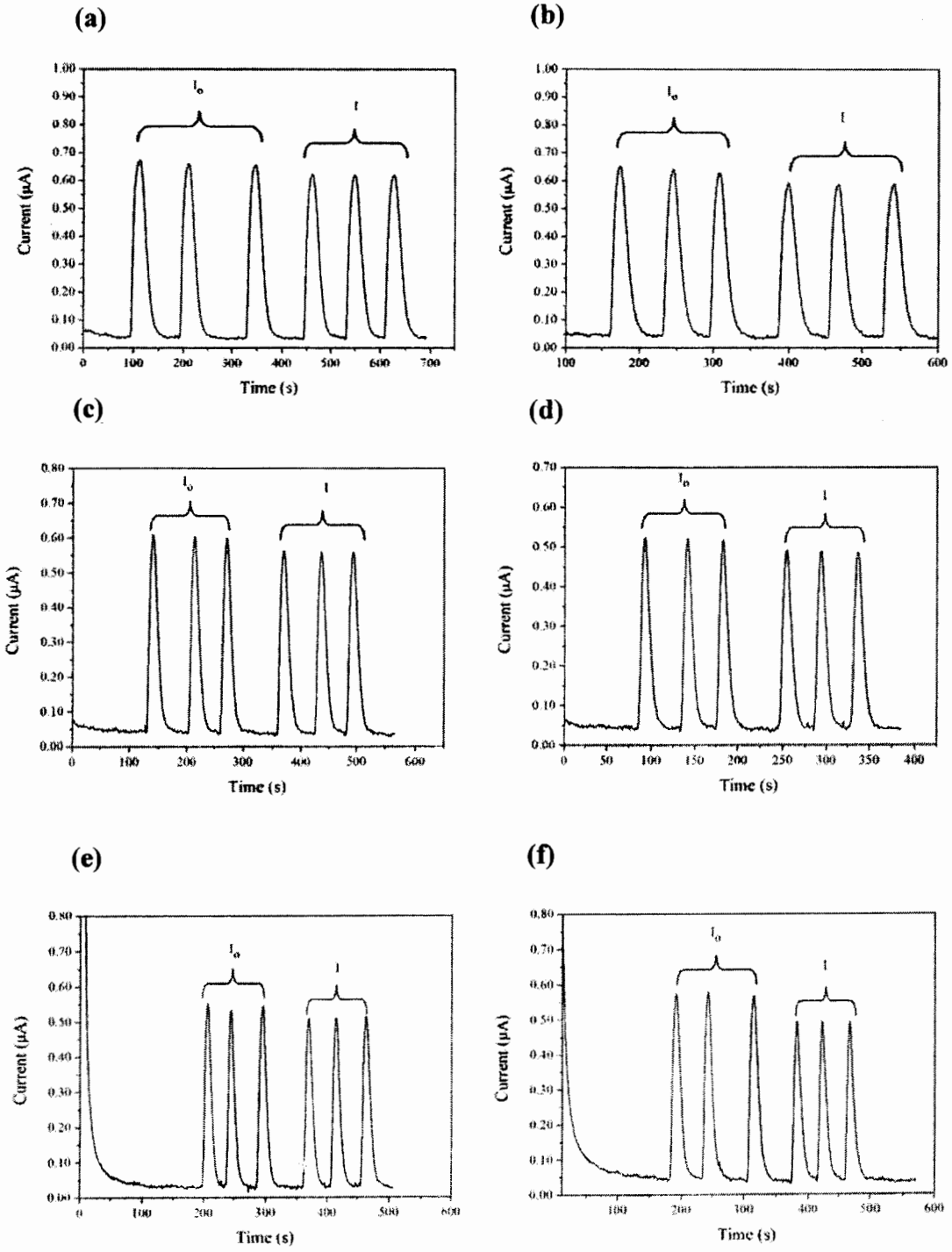

Figure B.10 Current responses of $GOx/MnO_2/SPCE$ on flow rate; (a) 0.6 $mL.min^{-1}$, (b) 0.8 $mL.min^{-1}$, (c) 1.0 $mL.min^{-1}$, (d) 1.2 $mL.min^{-1}$, (d) 1.4 $mL.min^{-1}$, and (e) 1.6 $mL.min^{-1}$

As the results shown in Figure 4.9 (chapter 4) % inhibition of GOx/MnO_2/SPCE with 0.5 mg.L^{-1} mercury on the various flow rates (Figure B.10) are presented in the Table B.5.

Table B.5 The inhibition degree of GOx/MnO_2/SPCE on flow rate of carrier solution

Flow rate (mL.min^{-1})	% Inhibition			
	1	2	3	(Mean ± SD); (n=3)
0.6	10.88	9.17	9.19	9.75 ± 0.98
0.8	11.29	12.76	12.20	12.08 ± 0.74
1.0	13.90	14.53	11.58	13.33 ± 1.56
1.2	16.06	15.74	14.93	15.57 ± 0.58
1.4	10.47	12.83	11.12	11.47 ± 1.22
1.6	9.14	6.56	6.60	7.43 ± 1.48

B.2 Analytical figures of merit

B.2.1 Dynamic range

As the results % inhibition of GOx/MnO_2/SPCE with mercury (100 - 4500 $\mu g.L^{-1}$) are presented in the Table B.2.1.

Table B.6 The inhibition degree of GOx/MnO_2/SPCE on various mercury concentrations

Mercury concentration ($\mu g.L^{-1}$)	% Inhibition			
	1	2	3	(Mean ± SD); (n=3)
100	4.32	3.70	3.12	3.71 ± 0.60
500	19.11	19.73	15.46	18.10 ± 2.31
1000	30.93	31.37	32.46	31.59 ± 0.79
1500	45.07	45.13	42.20	44.20 ± 1.56
2000	49.57	49.20	49.13	49.30 ± 0.24
2500	52.13	51.47	50.84	51.48 ± 0.64
3000	57.77	57.95	57.37	57.70 ± 0.30
3500	57.21	56.40	57.05	56.89 ± 0.43
4000	57.00	56.26	55.09	56.11 ± 0.96
4500	57.37	57.86	56.09	57.10 ± 0.92

B.2.2 Linear range

As the results shown in Figure 4.13 (chapter 4) % inhibition of GOx/MnO_2/SPCE with mercury (100 - 1500 $\mu g.L^{-1}$) is presented in the Figure B-2.1 and % inhibition of GOx/MnO_2/SPCE with mercury (100 - 1000 $\mu g.L^{-1}$) is presented in the Table B.7.

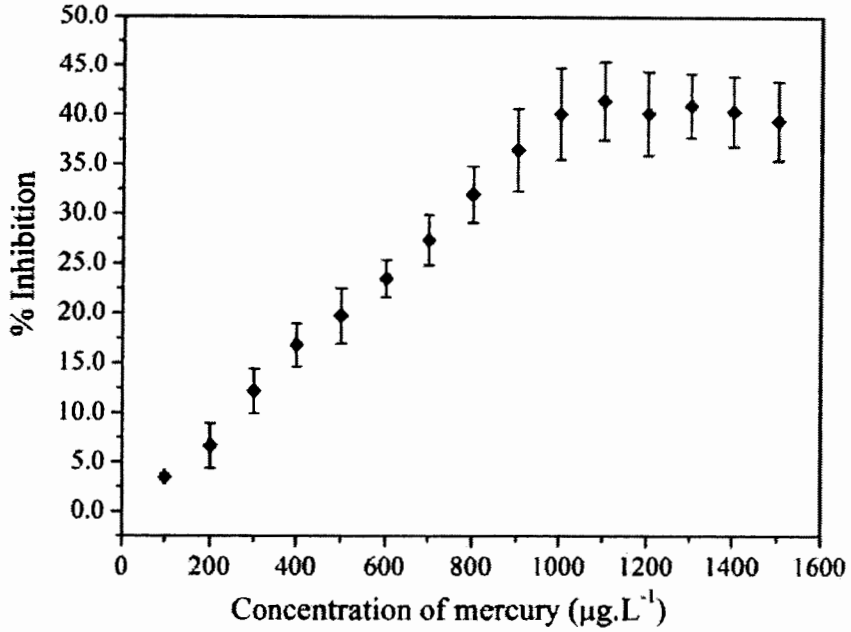

Figure B.11 Linear dynamic range for detection of mercury based on inhibition of the GOx/MnO_2/SPCE

Table B.7 The inhibition degree of GOx/MnO_2/SPCE on the linear range

Mercury concentration ($\mu g.L^{-1}$)	% Inhibition			
	1	2	3	(Mean ± SD); (n=3)
100	3.83	3.54	3.07	3.48 ± 0.39
200	4.25	6.79	8.82	6.62 ± 2.29
300	10.07	11.87	14.54	12.16 ± 2.25
400	14.77	16.55	19.06	16.79 ± 2.16
500	17.11	19.52	22.64	19.76 ± 2.77
600	22.60	22.21	25.64	23.48 ± 1.88
700	27.24	24.90	29.96	27.37 ± 2.53
800	34.06	28.73	33.09	31.96 ± 2.84
900	38.65	31.70	39.07	36.47 ± 4.14
1000	41.50	34.96	43.92	40.13 ± 4.64

B.2.3 Limit of detection

As the results shown in section 4.5.2 (chapter 4)the limit of detection (LOD) is calculated by equation B.1

$$\text{LOD} = \frac{3\text{SD}}{\text{Slope}} \tag{B.1}$$

Where standard deviation is at 0.39 of the inhibition degree at 100 $\mu g.L^{-1}$ mercury and slope is at 0.0407 from the linear range, y= 0.0407x - 0.5760, r^2 = 0.9975 (in Figure 4.11 chapter 4), are calculated below.

$$\text{LOD} = \frac{3(0.39\ \%\text{Inhibition})}{0.0407\ \frac{\%\text{Inhibition}}{\mu g.L^{-1}}}$$

$$\text{LOD} = 29\ \mu g.\ L^{-1}\ \text{mercury}$$

Limit of detection of the proposed biosensor is 29 $\mu g.L^{-1}$ mercury.

B.2.4 Limit of quantification

As the results shown in section 4.5.3 (chapter 4) the limit of quantification (LOQ)is calculated by equation B.2.

$$\text{LOQ} = \frac{10\text{SD}}{\text{Slope}} \tag{B.2}$$

Where standard deviation is at 0.39 of the inhibition degree at 100 $\mu g.L^{-1}$ mercury and slope is at0.0407 from the linear range, y= 0.0407x - 0.5760, r^2 = 0.9975 (in Figure 4.11 chapter 4), are calculated below.

$$\text{LOQ} = \frac{10(0.39\ \%\text{Inhibition})}{0.0407\ \frac{\%\text{Inhibition}}{\mu g.L^{-1}}}$$

$$\text{LOQ} = 96\ \mu g.\ L^{-1}\ \text{mercury}$$

Limit of quantification of the biosensor is 96 $\mu g.L^{-1}$ mercury.

B.2.5 Repeatability

As the results shown in Figure 4.14 (chapter 4) % Inhibition of GOx/MnO_2/SPCE on the repeatability (n = 10) induced by 100 $\mu g.L^{-1}$ mercury are presented in the Table B.8.

Table B.8 The inhibition degree of GOx/MnO_2/SPCE induced by 100 $\mu g.L^{-1}$ mercury

Number		Current (μA) *	% Inhibition
I_0		0.596	-
I	1	0.570	4.48
	2	0.572	4.14
	3	0.571	4.31
	4	0.569	4.65
	5	0.571	4.31
	6	0.570	4.48
	7	0.571	4.31
	8	0.571	4.31
	9	0.570	4.48
	10	0.569	4.65
Mean ± SD (n=10)		0.570 ± 0.001	4.41 ± 0.16
%RSD		0.17	3.67

*Current (μA) is current of catalytic reaction (μA) – current of background (μA)

B.2.6 Regeneration of GOx/MnO_2/SPCE with EDTA

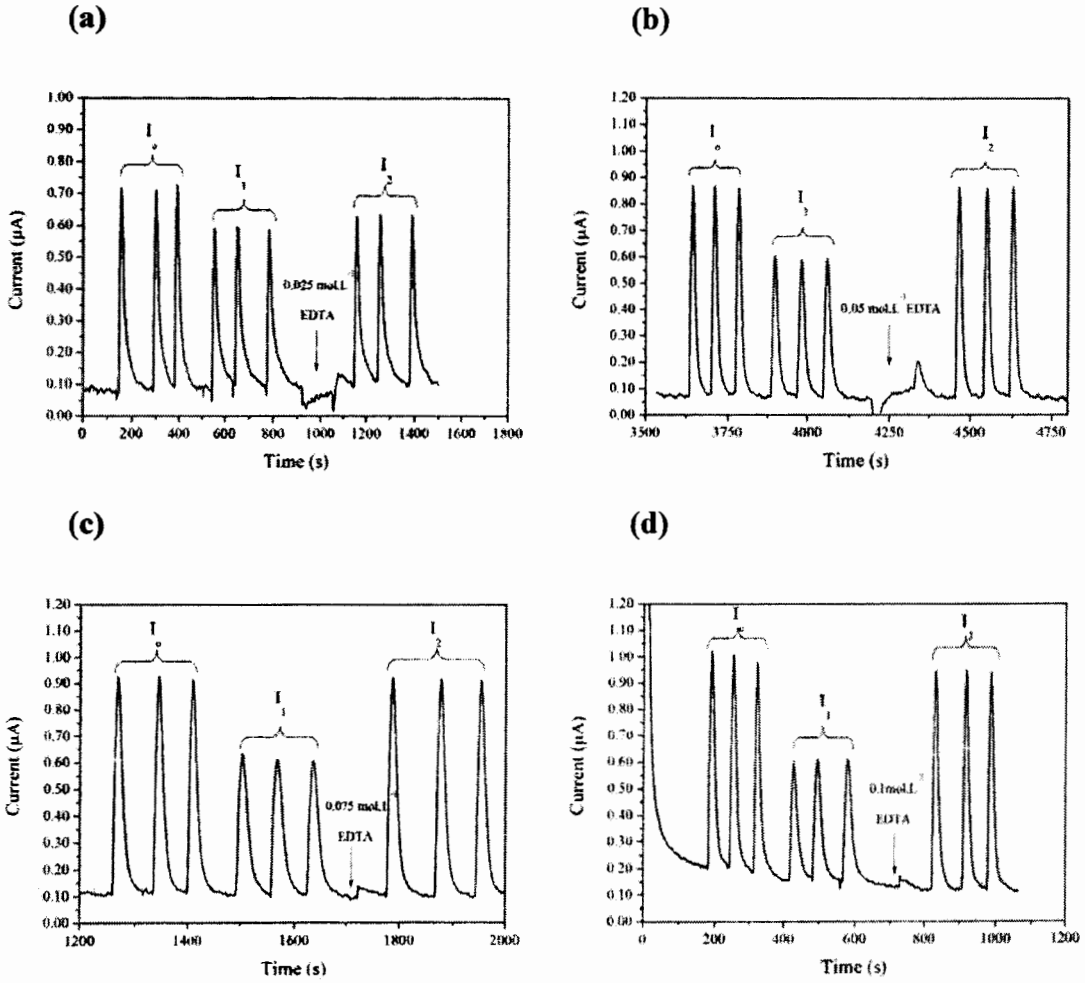

Figure B.12 Current responses of GOx/MnO_2/SPCE on the regeneration with EDTA; (a) 0.025 mol.L^{-1}, (b) 0.050 mol.L^{-1}, (c) 0.075 mol.L^{-1} and (d) 0.10 mol.L^{-1} where I_0 is current before inhibition, I_1 is current after inhibition and I_2 is current after regeneration.

As the results shown in Figure 4.17 (chapter 4) % regeneration of GOx/MnO_2/SPCE on the various EDTA concentrations (Figure B.12) are presented in the Table B-2.4.

Table B.9 The regeneration degree of GOx/MnO_2/SPCE on the concentration of EDTA

EDTA ($mol.L^{-1}$)	% Regeneration *			
	1	2	3	(Mean ± SD); (n=3)
0.025	90.38	87.34	89.56	89.09 ± 1.57
0.050	95.93	97.79	98.85	97.52 ± 1.48
0.075	98.92	96.59	99.77	98.43 ± 1.65
0.100	98.99	96.96	99.92	98.62 ± 1.51

*Regeneration= $\left(\frac{I_2}{I_0}\right)$ x 100 where I_2 is current after regeneration

I_0 is current before inhibition

B.3 Stability

As the results shown in Figure 4.18 (chapter 4) current responses of GOx/MnO_2/SPCE on its stability are presented in Table B.10.

Table B.10 The current of GOx/MnO_2/SPCE on the stability

Time (Days)	Current (μA)* Mean ± SD
1	0.499 ± 0.005
2	0.494 ± 0.008
3	0.479 ± 0.015
4	0.476 ± 0.010
5	0.466 ± 0.010
6	0.453 ± 0.006
7	0.446 ± 0.003
8	0.442 ± 0.018
9	0.436 ± 0.006
10	0.428 ± 0.006
11	0.403 ± 0.021
12	0.382 ± 0.025
13	0.386 ± 0.006
14	0.379 ± 0.007
21	0.311 ± 0.011

*Current (μA) is current of catalytic reaction (μA) – current of background (μA)

B.4 Interferences

As the results shown in Figure 4.19 (a) (chapter 4) current responses of GOx/MnO_2/SPCE on the interferences (Figure B.13 and B.14) are presented in the Table B.11.

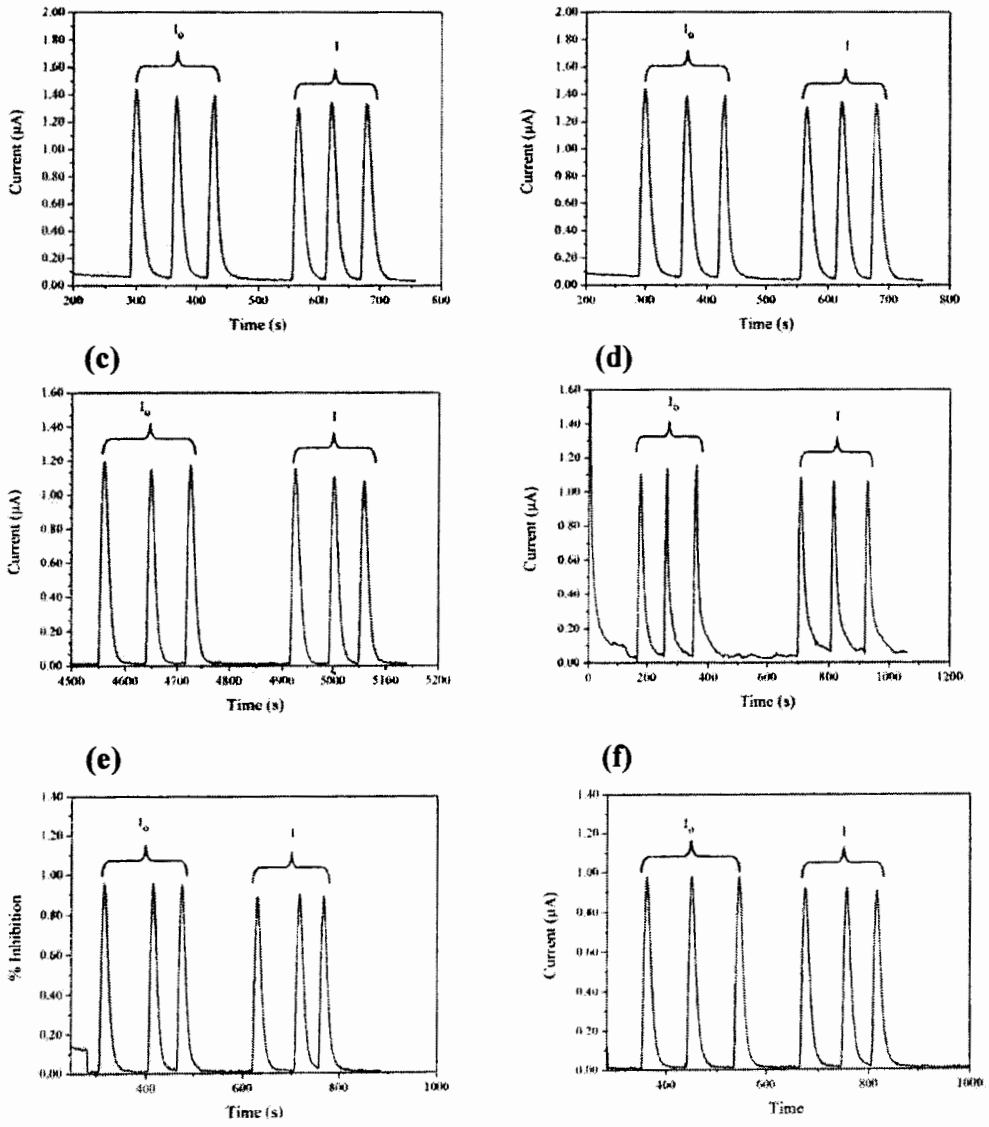

Figure B.13 Current responses of GOx/MnO_2/SPCE on the study of interferences with metal ions (a) Hg (II), (b) Fe (III), (c) Mn (II), (d) Cr (VI), (e) Cr (III) and (f) Zn (II), I_0 is current before inhibition and I is current after inhibition.

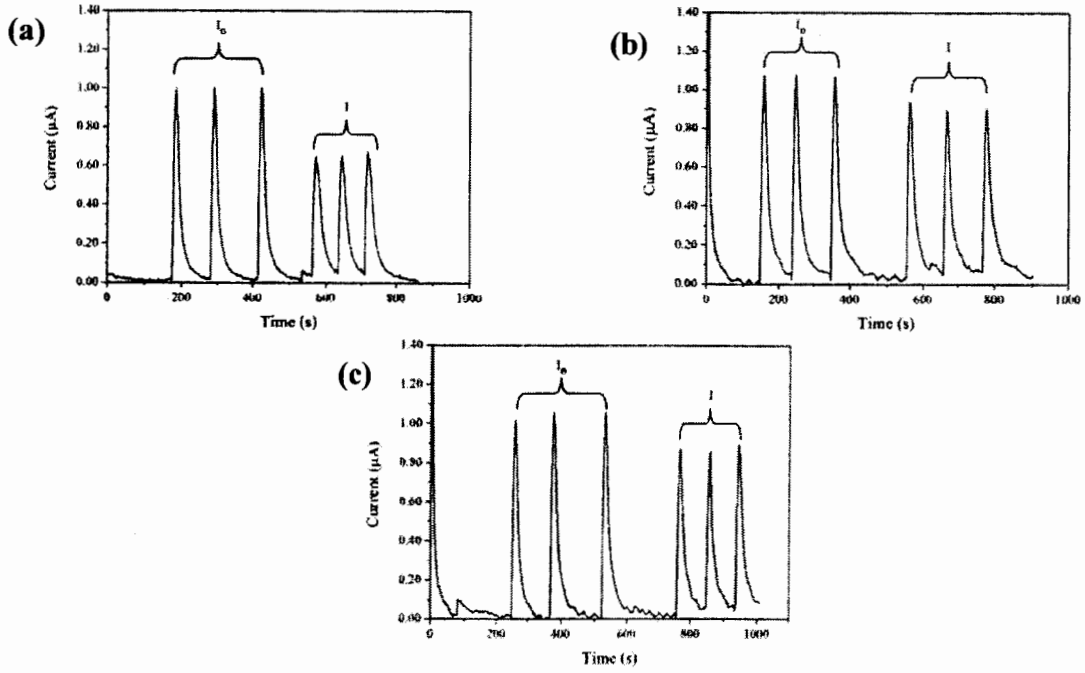

Figure B.14 Current responses of GOx/MnO_2/SPCE on the study of interferences with metal ions (a) Pb (II), (b) Cd (II) and (c) Cu (II), I_0 is current before inhibition and I is current after inhibition.

Table B.11 % inhibition of GOx/MnO_2/SPCE on the study of interferences (10 $mg.L^{-1}$)

Metal ions	% Inhibition
Hg (II)	3.84 ± 0.26
Fe (III	3.86 ± 0.21
Mn (II)	3.16 ± 0.27
Cr (VI)	3.17 ± 0.67
Cr (III)	3.84 ± 0.52
Zn (II)	3.85 ± 0.06
Pb (II)	31.53 ± 5.30
Cd (II)	19.65 ± 4.89
Cu (II)	21.22 ± 5.80

As the results shown in Figure 4.19 (b) (chapter 4) current responses of GOx/MnO_2/SPCE on the interferences (Figure B.15) are presented in the Table B.12.

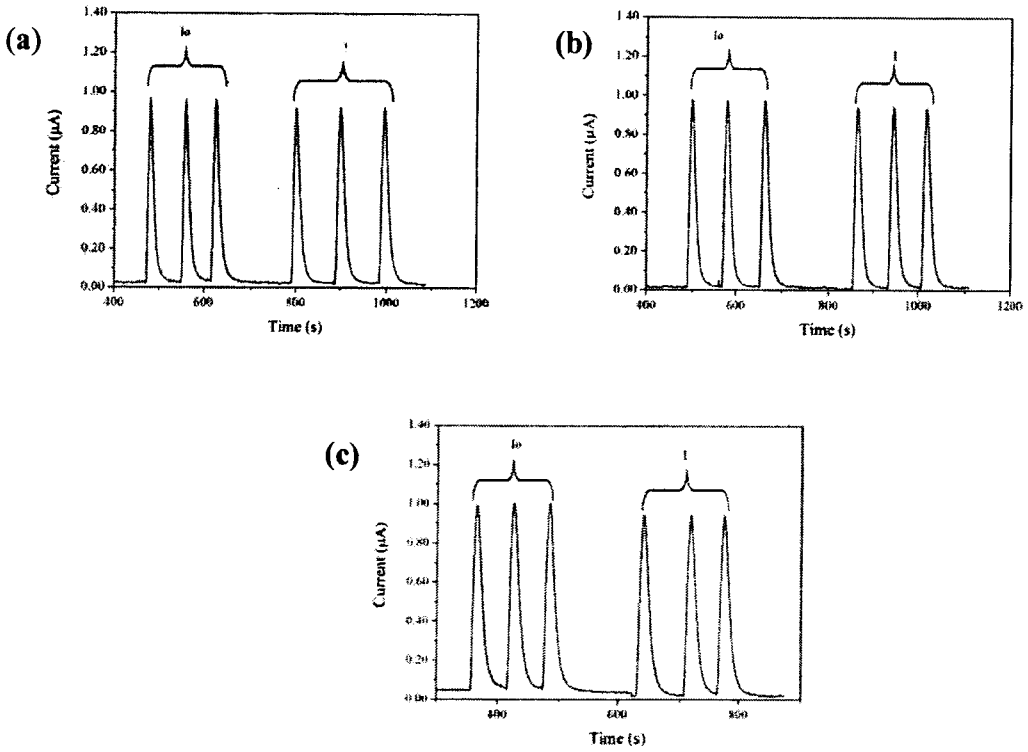

Figure B.15 Current responses of GOx/MnO_2/SPCE on the study of interferences with metal ions (a) Pb (II), (b) Cd (II) and (c) Cu (II) (1 mg.L^{-1}), I_0 is current before inhibition and I is current after inhibition.

Table B.12 The current of GOx/MnO_2/SPCE on the study of interferences (1 mg.L^{-1})

Metal ions	% Inhibition
Pb (II)	3.84 ± 0.26
Cd (II)	3.86 ± 0.21
Cu (II)	3.16 ± 0.27

B.5 Enzyme kinetics

The direct Michaelis-Menten and double-reciprocal Lineweaver-Burk were studied in the section 4.6 (chapter 4). The obtained currents are presented in Table B.13.

Table B.13 The current of GOx/MnO_2/SPCE on Michaelis-Menten and Lineweaver-burk plot

Glucose concentration ($mmol.L^{-1}$)	Current (μA)*	1/Glucose concentration $(mmol.L^{-1})^{-1}$	1/Current (μA^{-1})	Current (μA) * inhibited with 1 $mg.L^{-1}$ mercury	1/Current (μA^{-1}) inhibited with 1 $mg.L^{-1}$ mercury
0.20	0.20	5.00	5.04	0.11	8.98
0.40	0.30	2.50	3.38	0.17	5.91
0.60	0.31	1.67	3.23	0.17	5.69
0.80	0.42	1.25	2.38	0.20	5.00
1.00	0.60	1.00	1.68	0.34	2.91
2.00	0.91	0.50	1.10	0.57	1.75
3.00	1.35	0.33	0.74	0.73	1.38
4.00	1.58	0.25	0.63	0.85	1.18
5.00	2.00	0.20	0.50	1.12	0.89
6.00	2.43	0.17	0.41	1.33	0.75
8.00	2.74	0.12	0.37	1.58	0.63
10.00	3.18	0.10	0.31	2.14	0.47
12.00	3.59	0.08	0.28	2.50	0.40
14.00	3.97	0.07	0.25	2.70	0.37
16.00	4.17	0.06	0.24	2.69	0.37
18.00	4.27	0.06	0.23	2.67	0.38
20.00	4.40	0.05	0.23	2.59	0.39

B.6 Application of the biosensor to the determination of mercury in samples

B.6.1 Application to the certified reference material (DORM-2)

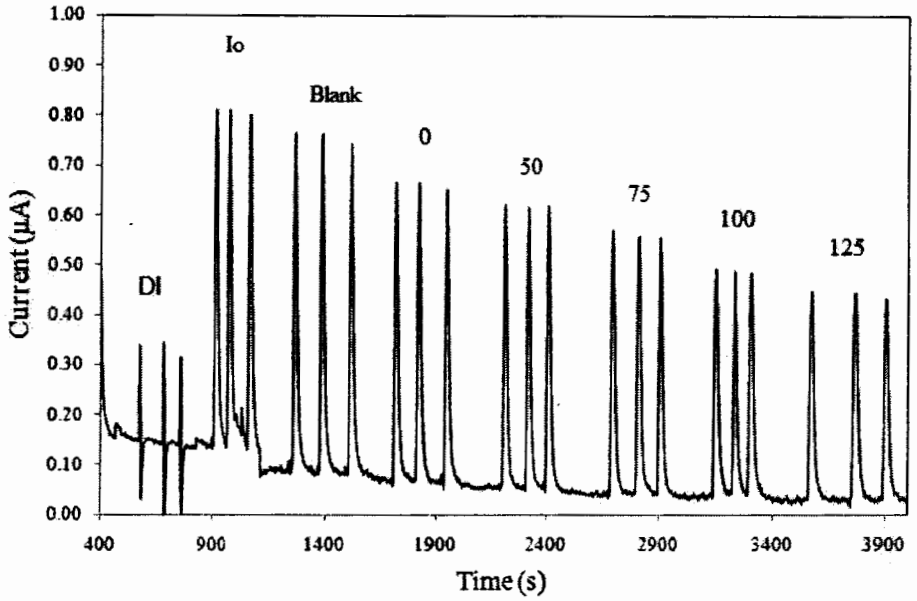

Figure B.16 The FIA grams of the standard addition for mercury determination in certified reference material (DORM-2)

As the result (Figure B.16), % inhibition of GOx/MnO_2/SPCE calculated by the standard addition method are presented in Table B.14.

Table B.14 The inhibition degree of GOx/MnO_2/SPCE on the standard addition method for determination of mercury in DORM-2 sample

Concentration of mercury ($\mu g.L^{-1}$)	% Inhibition
0	4.14 ± 0.61
50	9.71 ± 1.06
75	11.97 ± 1.05
100	15.10 ± 1.79
125	18.09 ± 1.80

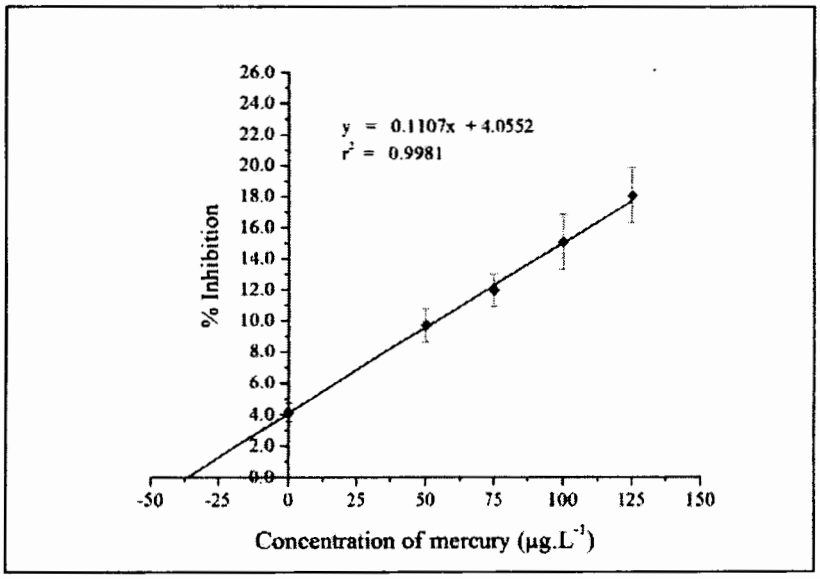

Figure B.17 The standard addition graph for mercury determination in DORM-2

Results from Table B.14 were plotted as the standard addition graph to determine mercury in DORM-2. The graph in Figure B.17 presents the linear regression of $y = 0.1107x + 4.0552$, $r^2 = 0.9981$.

Linear least squares regression analysis gives a slope = 0.1107 and the y - intercept = 4.0552

In the graphical method of standard additions the concentration of mercuric ion from the DORM-2 in the measured solution is equal to the absolute value of the x - intercept.

The x - intercept is equal to the y - intercept divided by the slope

$$x = \frac{4.0552}{0.1107}$$

$$x = 36.63\ \mu g.\ L^{-1}$$

Calculation of mercury in the total DORM-2 was studied. The DORM-2 (0.4020 g) was digested and diluted into 10.00 mL volumetric flask. Continually, 1.00 mL of the prepared solution was diluted into 5.00 mL.

From equation $C_1V_1 = C_2V_2$

$$(36.63\ \mu g.\ L^{-1})x(5.00\ mL) = C_2x(1.00\ mL)$$

$$C_2 = 183.15\ \mu g.\ L^{-1}$$

where C_1 is the concentration ($\mu g.L^{-1}$) of mercury after dilution

C_2 is the concentration ($\mu g.L^{-1}$) of mercury before dilution

V_1 is the volume of solution (mL) after dilution

V_2 is the volume of solution (mL) before dilution

Calculated mercury in DORM-2 certified reference sample

If 1000 mL of a solution contains 183.15 µg mercury

So 10 mL of a solution contains $= \frac{183.15\ \mu g\ x\ 10\ mL}{1000\ mL}$ mercury

$= 1.83\ \mu g$ mercury

If 0.4020 g of a fish tissue contains 1.83 µg mercury

So 1000 g of a fish tissue contains $= \frac{1.83\ \mu g\ x\ 1000\ g}{0.4020\ g}$ mercury

$= 4.55\ mg.\ Kg^{-1}$ mercury

As the results the linear regressions of three replications are presented in Table B.15.

Table B.15 The linear regression for determination of mercury and mercury in certified reference material (DORM-2) (three replications)

	Linear regression (y = mx + c)	r^2	Mercury in sample ($mg.Kg^{-1}$)
1	y = 0.1107x + 4.0552	0.9981	4.55
2	y = 0.1354x + 5.0142	0.9869	4.61
3	y = 0.1302X + 4.6904	0.9937	4.48

B.6.2 Application to local natural water

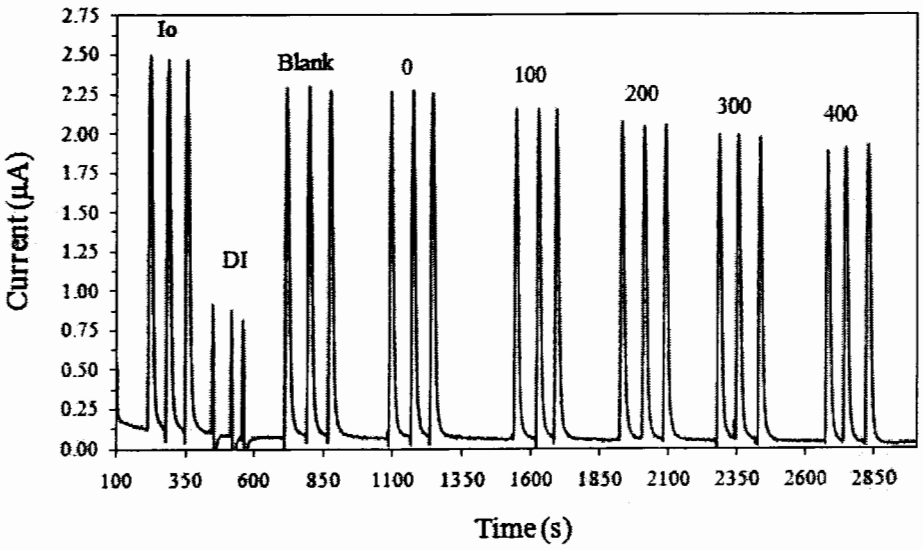

Figure B.18 The FIA gram of standard addition for mercury determination in local natural water

As the result (Figure B.18), % inhibition of GOx/MnO_2/SPCE calculated by the standard addition method are presented in Table B.16.

Table B.16 The inhibition degree of GOx/MnO_2/SPCE on the standard addition method for determination of mercury in local natural water

Concentration of mercury ($\mu g.L^{-1}$)	% Inhibition
0	0.05 ± 0.02
100	6.42 ± 1.02
200	12.20 ± 1.20
300	17.18 ± 1.30
400	22.47 ± 0.80

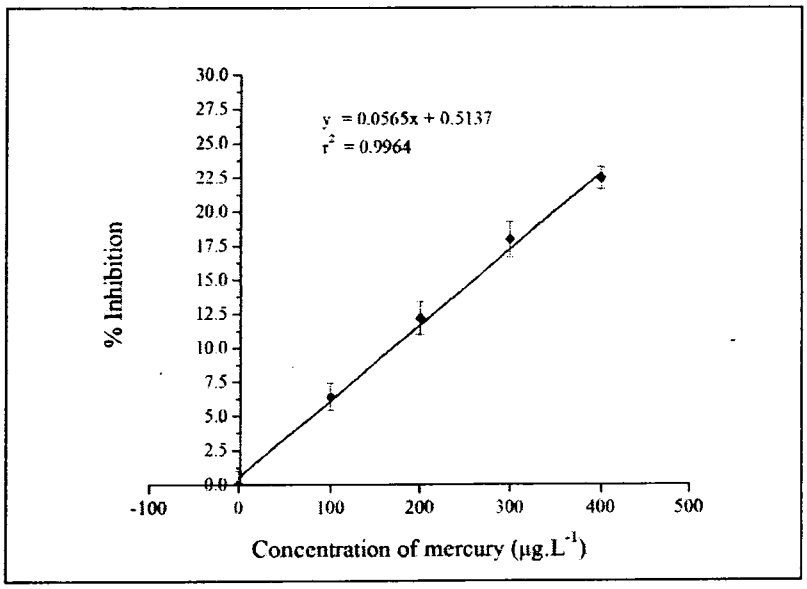

Figure B.19 The standard addition graph for mercury determination in local natural water

Results from Table B.16 were plotted as the standard addition graph to determine mercury in local natural water. The calibration graph in Figure B.19 presents linear regression of $y = 0.0565x + 0.5137$, $r^2 = 0.9964$.

As the results the linear regression graph of three replications is presented in Table B.17.

Table B.17 The linear regression for determination of mercury and mercury in local natural water (three replications)

	Linear regression (y = mx + c)	r^2	Mercury in sample ($mg.Kg^{-1}$)
1	y = 0.0560x + 0.5137	0.9964	ND.
2	y = 0.0454x + 0.0142	0.9869	ND.
3	y = 0.0397X + 0.6904	0.9937	ND.

B.6.3 Application to shrimp

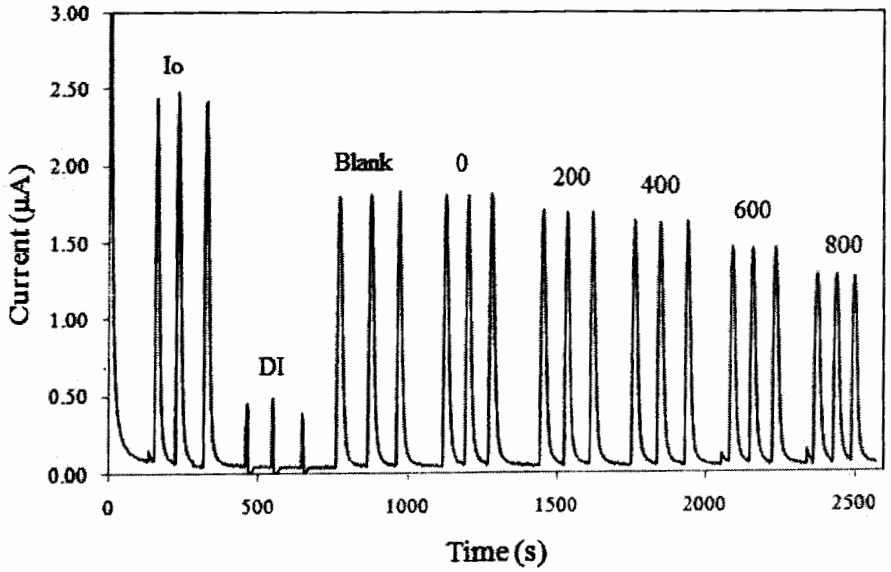

Figure B.20 The FIA gram of standard addition for mercury determination in shrimp

As the result (Figure B.20), % inhibition of GOx/MnO_2/SPCE calculated by the standard addition method are presented in Table B.18.

Table B.18 The inhibition degree of GOx/MnO_2/SPCE on the standard addition method for determination of mercury in shrimp sample

Concentration of mercury ($\mu g.L^{-1}$)	% Inhibition
0	0.01 ± 0.99
200	6.24 ± 1.45
400	9.36 ± 1.33
600	17.40 ± 1.77
800	26.10 ± 0.95

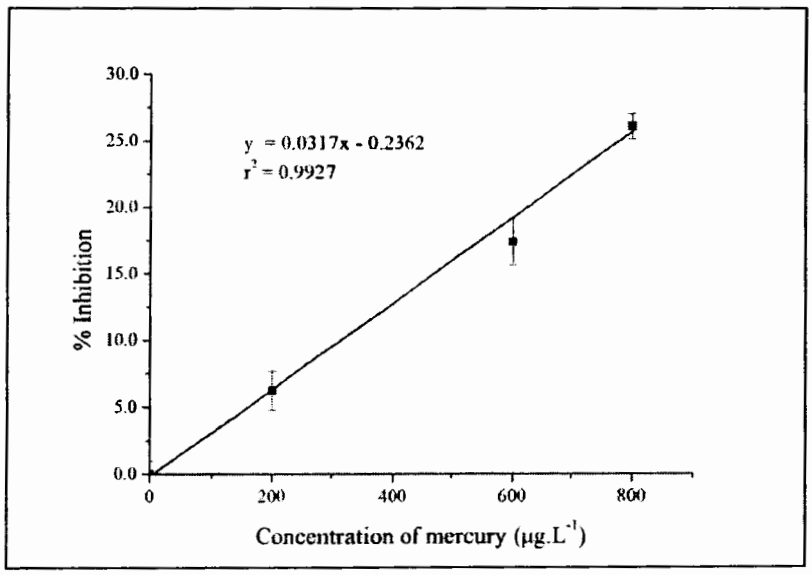

Figure B.21 The standard addition graph for mercury determination in shrimp sample

Results from Table B-6.5.18 were plotted as the standard addition graph for determination of mercury in shrimp. The calibration graph in Figure B.21 presents linear regression $y = 0.0317x - 0.2362$, $r^2 = 0.9927$.

As the result the linear regressions of three replications are presented in Table B.19.

Table B.19 The linear regression for determination of mercury and mercury in shrimp samples (three replications)

	Linear regression (y = mx + c)	r^2	Mercury in sample ($mg.Kg^{-1}$)
1	y = 0.0317x - 0.2361	0.9927	ND.
2	y = 0.0451x + 0.0397	0.9932	ND.
3	y = 0.0302x - 0.0904	0.9947	ND.

B.6.4 Application to mackerel

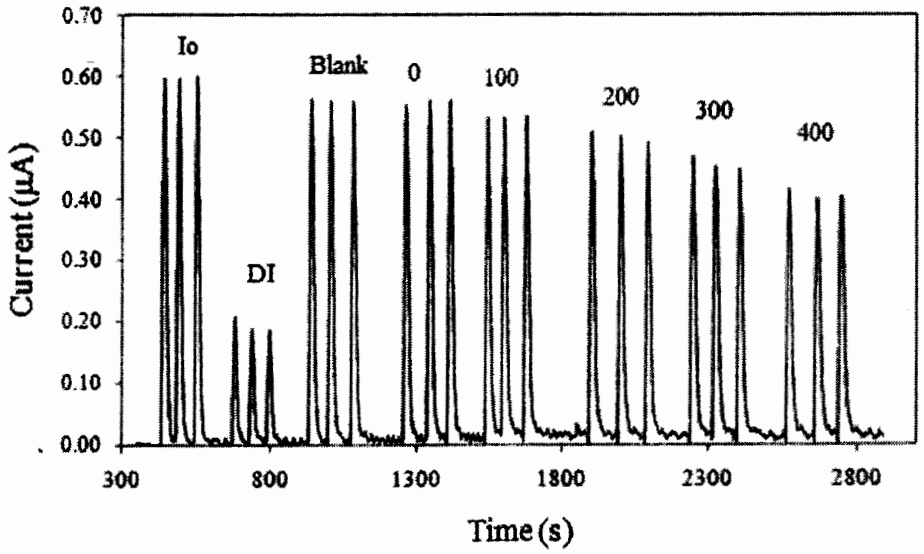

Figure B.22 The FIA gram of standard addition for mercury determination in mackerel sample

As the result (Figure B.22), % inhibition of GOx/MnO_2/SPCE calculated by the standard addition method are presented in Table B.20.

Table B.20 The inhibition degree of GOx/MnO_2/SPCE on the standard addition method for determination of mercury in mackerel sample

Concentration of mercury ($\mu g.L^{-1}$)	% Inhibition
0	0.57 ± 0.05
100	9.62 ± 3.06
200	18.30 ± 2.49
300	25.52 ± 2.69
400	31.88 ± 3.09

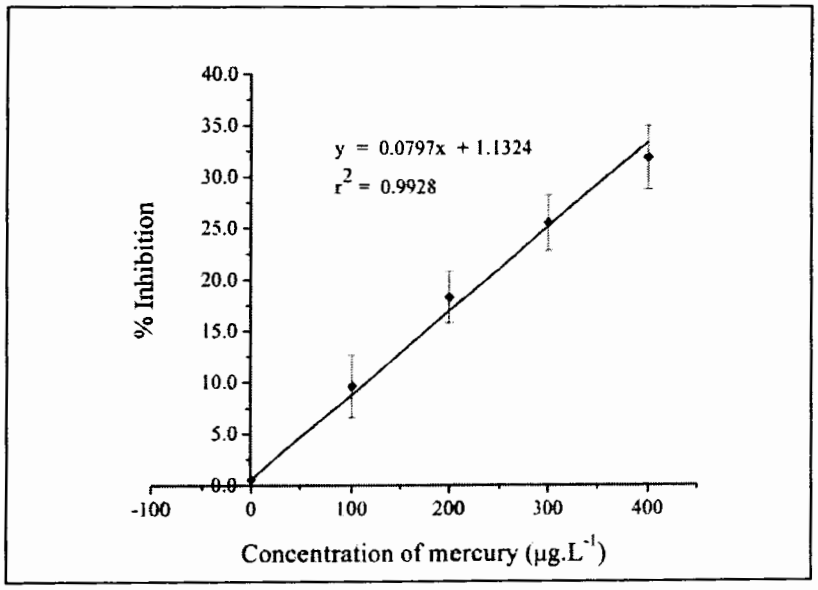

Figure B.23 The standard addition graph for mercury determination in mackerel sample

Result from Table B.20 were plotted as the standard addition graph for determination of mercury in mackerel. The calibration graph in Figure B.23 presents linear regression of $y = 0.0797x + 1.1324$, $r^2 = 0.9928$.

As the results the linear regressions of three replications are presented in Table B.21.

Table B.21 The linear regression for determination of mercury and mercury in mackerel samples(three replications)

	Linear regression (y = mx + c)	r^2	Mercury in sample ($mg.Kg^{-1}$)
1	y = 0.0797x + 1.1324	0.9928	ND.
2	y = 0.0644x + 0.7401	0.9880	ND.
3	y = 0.0524x + 0.2321	0.9912	ND.

B.6.5 Application to spiked water

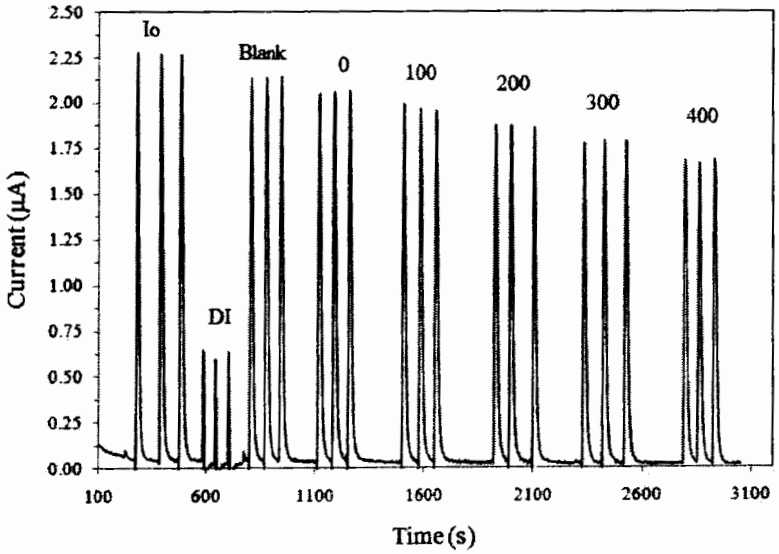

Figure B.24 The FIA gram of standard addition for mercury determination in spiked water

As the result (Figure B.24), % inhibition of GOx/MnO_2/SPCE calculated by the standard addition method are presented in Table B.22.

Table B.22 The inhibitiondegree of GOx/MnO_2/SPCE on the standard addition method for determination of mercury in spiked water sample

Concentration of mercury ($\mu g.L^{-1}$)	% Inhibition
0	6.42 ± 0.34
100	10.63 ± 0.62
200	16.25 ± 0.64
300	21.67 ± 0.71
400	28.75 ± 0.41

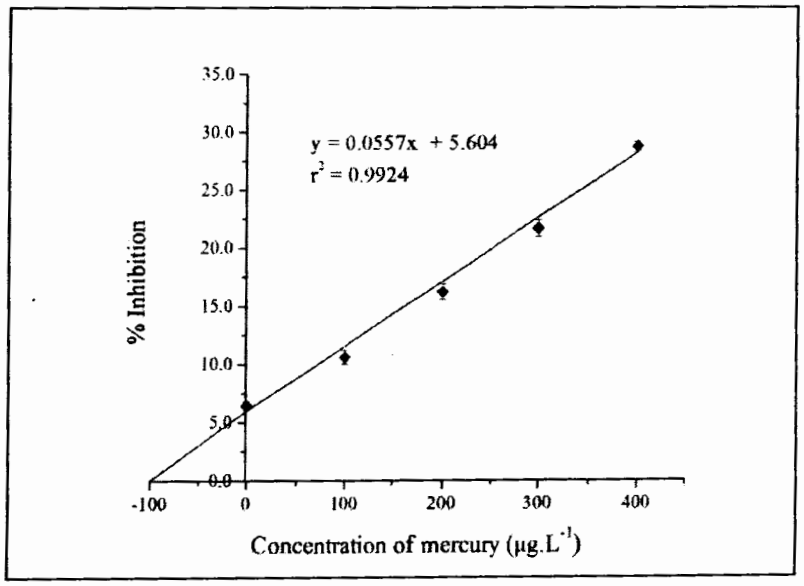

Figure B.25 The standard addition graph for mercury determination in spiked water sample

Results from Table B.22 were plotted as the standard addition graph for determination of mercury in spiked water. The calibration graph in Figure B.25 presents linear regression of $y = 0.0557x + 5.6040$, $r^2 = 0.9924$.

As the results the linear regressions of three replications are presented in Table B.23.

Table B.23 The linear regression for determination of mercury and mercury in spiked water (three replications)

	Linear regression (y = mx + c)	r^2	Mercury in sample ($mg.Kg^{-1}$)
1	y = 0.0557x + 5.6040	0.9924	1.94
2	y = 0.0470x + 5.1940	0.9956	2.21
3	y = 0.0285x + 2.6505	0.9990	1.86

B.6.6 Application to spiked shrimp sample

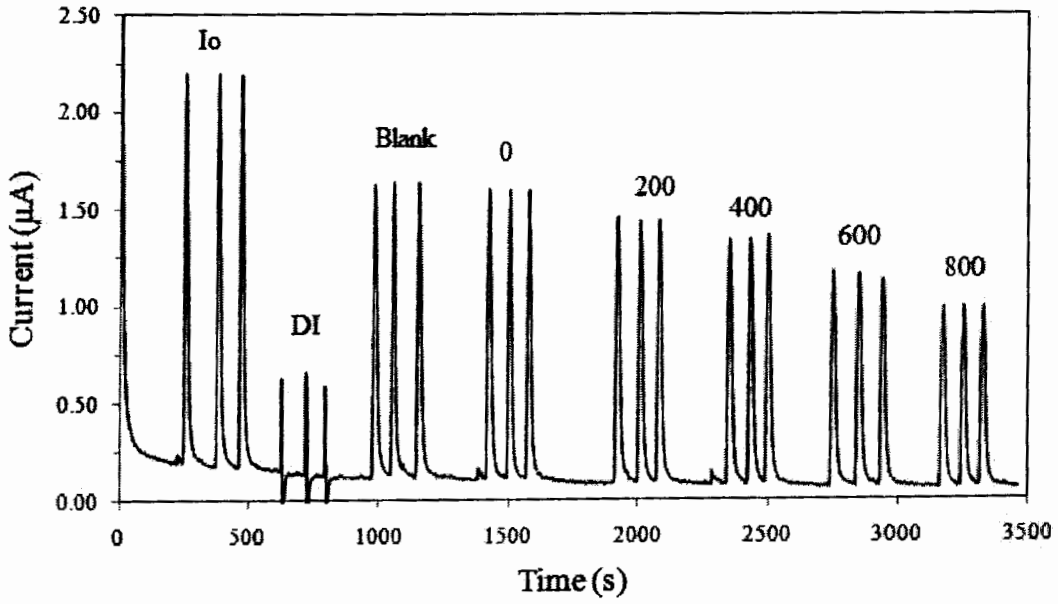

Figure B.26 The FIA gram of standard addition for mercury determination in spiked shrimp sample

As the result (Figure B.26), % inhibition of GOx/MnO_2/SPCE calculated by the standard addition method are presented in Table B.24.

Table B.24 The inhibition degree of GOx/MnO_2/SPCE on the standard addition method for determination of mercury in spiked shrimp sample

Concentration of mercury ($\mu g.L^{-1}$)	% Inhibition
0	2.87 ± 1.08
200	8.99 ± 1.59
400	15.19 ± 1.01
600	26.96 ± 1.67
800	35.26 ± 0.99

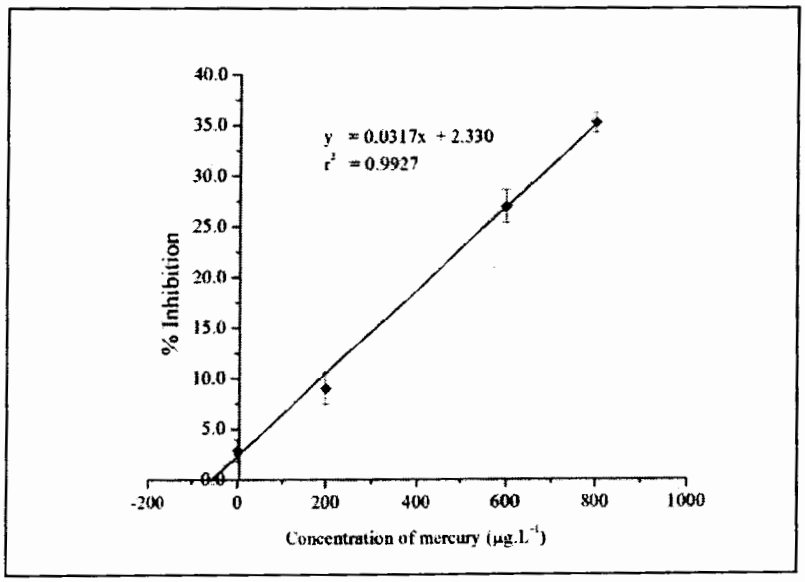

Figure B.27 The standard addition graph for mercury determination in spiked shrimp sample

Results from Table B.24 were plotted as the standard addition graph for determination of mercury in spiked shrimp that shows calibration graph in Figure B.27 with linear regression $y = 0.0317x + 2.330$, $r^2 = 0.9927$

As the results the linear regression graph of three replications are presented in Table B.25.

Table B.25 The linear regression for determination of mercury and mercury in spiked shrimp (three replications)

Linear regression (y = mx + c)		r^2	Mercury in sample ($mg.Kg^{-1}$)
1	y = 0.0317x + 2.330	0.9927	1.90
2	y = 0.0414x + 2.7525	0.9964	2.01
3	y = 0.0358x + 1.9668	0.9952	1.80

B.6.7 Application to spiked mackerel

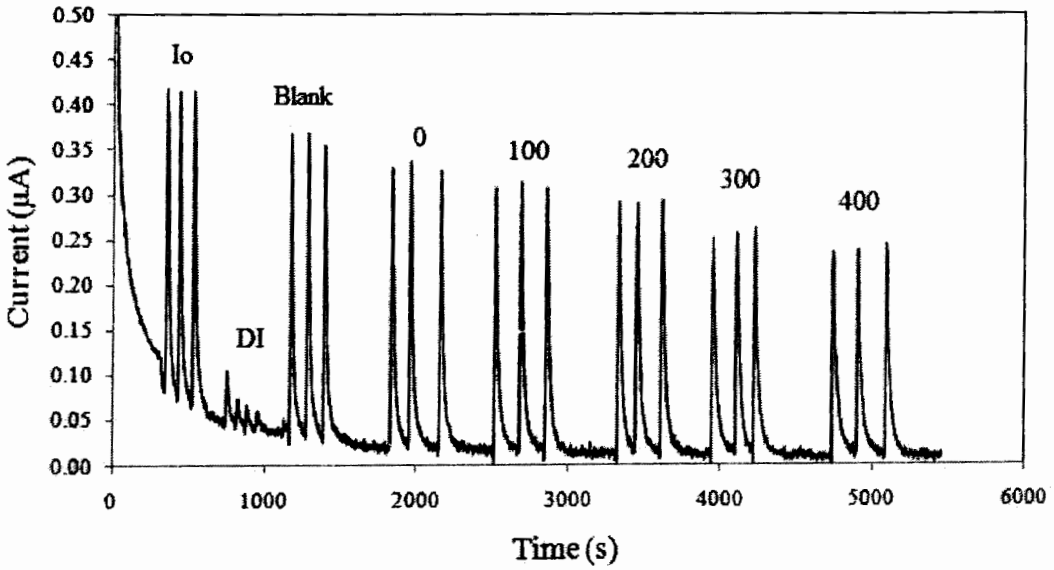

Figure B.28 The FIA gram of standard addition for mercury determination in spiked mackerel sample

As the result (Figure B.28), % inhibition of GOx/MnO_2/SPCE calculated by the standard addition method are presented in Table B.26.

Table B.26 The inhibition degree of GOx/MnO_2/SPCE on the standard addition method for determination of mercury in spiked mackerel sample

Concentration of mercury ($\mu g.L^{-1}$)	% Inhibition
0	8.76 ± 0.06
100	16.53 ± 1.48
200	25.62 ± 0.71
300	33.60 ± 0.63
400	43.62 ± 1.37

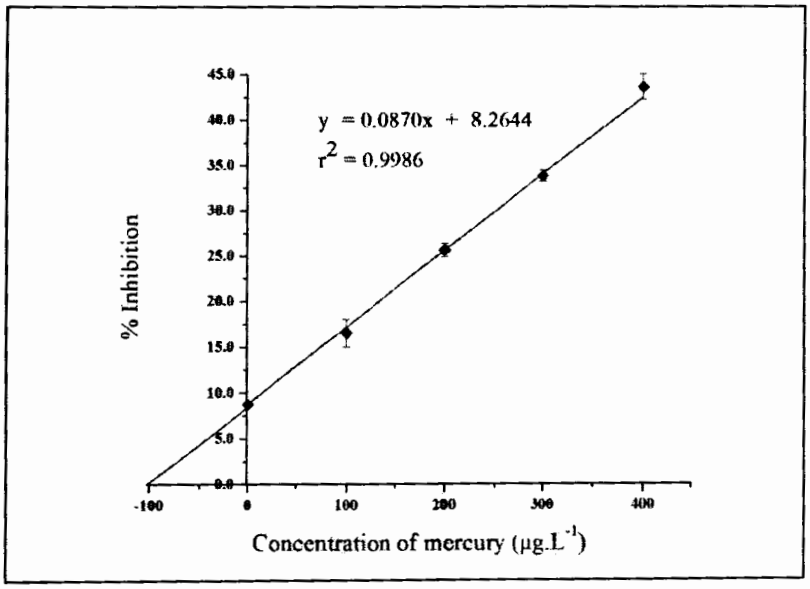

Figure B.29 The standard addition graph for mercury determination in spiked mackerel sample

Results from Table B.26 were plotted as the standard addition graph for determination of mercury in spiked mackerel. The calibration graph in Figure B.29 presents linear regression of $y = 0.0870x + 8.2644$, $r^2 = 0.9986$.

As the results the linear regressions of graph of three replications are presented in the Table B.27.

Table B.27 The linear regression for determination of mercury and mercury in spiked mackerel samples (three replications)

	Linear regression (y = mx + c)	r^2	Mercury in sample ($mg.Kg^{-1}$)
1	y = 0.0870x + 8.2644	0.9986	1.90
2	y = 0.0982x + 9.4135	0.9931	1.91
3	y = 0.0936x + 9.1172	0.9970	1.95

B.7 The paired t-test of mercury concentration by GOx/MnO_2/SPCE and CVAAS

Table B.28 The paired t-test of mercury concentration by GOx/MnO_2/SPCE and CVAAS at a confidence interval for 95% probability

Samples	t-test	
	$t_{observed}$	$t_{critical}$
DORM-2	2.55	4.30
Spiked water	3.24	4.30
Spiked shrimp	1.98	4.30
Spiked mackerel	2.12	4.30

CURRICULUM VITAE

NAME	Miss PiyanartSuebsanoh
BIRTH DATE	12 December 1988
BIRTE PLACE	Ubon Ratchathani Province, Thailand
EDUCATION	B. Sc. (Chemistry), Department of Chemistry, Faculty of Science, UbonRatchathani University, Thailand , 2007 - 2010 M. Sc. (Chemistry), Department of Chemistry, Faculty of Science, UbonRatchathani University, Thailand, 2010 - present
SCHOLARSHIPS	Center of Excellence for Innovation in Chemistry, (PERCH-CIC), 2010 - 2013 Faculty of Science, UbonRatchathani University, Ubon Ratchathani, Thailand, 2010 - 2013
PUBLICATION	Piyanart Suebsanoh, Juthamas Jitcharoen, Kurt Kalcher and Anchalee Samphao. "Indirect Method of Biosensor based on Flow Injection Analysis for Determination of Mercury". Proceeding of The 2nd Regional Symposium on Biosensors, Biodiagnostics and Biochips (ASEAN+ 2013), 11 - 13 December 2013, pages 24 - 27.
PRESENTATIONS	(1) Pure and Applied Chemistry International Conference 2013 (PACCON 2013), 23-25 January 2013. The Tide Resort, Bangsaen Beach, Chon Buri, Thailand, poster presentation. (2) International Congress for Innovation in Chemistry (PERCH-CIC Congress VII) 5-8 May 2013. JomtienPlam Beach Hotel & Resort, Pattaya, Thailand, poster presentation. (3) The 2nd Regional Symposium on Biosensors, Biodiagnostics and Biochips (ASEAN+ 2013), 11 - 13 December 2013, Mae FahLaung University, Chaing Rai, Thailand, poster presentation.